

UCSF

UC San Francisco Electronic Theses and Dissertations

Title

Transcriptional regulation of skeletal muscle development

Permalink

<https://escholarship.org/uc/item/25n7k0qh>

Author

Heidt, Analeah B

Publication Date

2006

Peer reviewed|Thesis/dissertation

Transcriptional Regulation of Skeletal Muscle Development

by

Analeah B. Heidt

DISSERTATION

Submitted in partial satisfaction of the requirements for the degree of

DOCTOR OF PHILOSOPHY

in

Biochemistry and Molecular Biology

in the

GRADUATE DIVISION

of the

UNIVERSITY OF CALIFORNIA, SAN FRANCISCO



Acknowledgements

There is no way to imagine graduate school in a place that is not the Black Lab. It is completely crazy, but full of the most amazing, intelligent, kind, helpful scientists one could imagine. I cannot begin to thank everyone sufficiently, but I would like to particularly thank Courtney Brown for being such a great collaborator and friend for the last few months. Her motivation and kindness are truly infectious and I really consider her an equal contributor to the skeletal muscle project. I would also like to thank Eric Ho for his invaluable help with my project. My experiments added a lot of extra hassle to his everyday job, and he was always happy to adjust to help me collect data.

The Black Lab has only become a spectacular workplace due to the incredible attention Brian pays to creating a good working environment. I give him the utmost credit for recognizing the importance of a group that can work together to synthesize ideas and approaches. The personality of the lab is a direct representation of Brian's enthusiasm and exuberance. I cannot thank Brian enough for teaching me essentially everything I know about being a scientist; and for only reminding me once in a while how terrible I was at the beginning. Brian prides himself on preparing his students for the science world, and I think he achieves that goal admirably.

Finishing graduate school is by no means an easy task, and without the support of my family I would never have been able to accomplish my goals. My parents are the two single greatest people on the planet. They have always supported my decisions and whims, and only occasionally suggested that I should have gone to culinary school. They

would have been proud of me regardless. I can never begin to repay my wonderful husband, Ian, for his unflinching support of this endeavor. Being married to a scientist is not always easy, and I can't apologize enough for my inability to estimate how long experiments will take. He has been simply wonderful through it all.

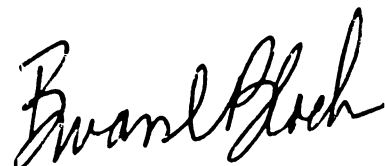
The majority of the 2nd chapter of this work and the accompanying figures were reprinted from *Genesis*, volume 42(1) by Analeah B. Heidt and Brian L. Black, Transgenic mice that express Cre recombinase under control of a skeletal muscle-specific promoter from *mef2c*, Pages No.28-32 Copyright 2005, with permission from John Wiley and Sons, Inc.

Abstract

Transcriptional regulation of skeletal muscle development

Analeah B. Heidt

The MyoD family of basic helix-loop-helix transcription factors has the remarkable ability to convert non-muscle cells into muscle in culture. The myogenic specificity inherent in these factors has been mapped to two amino acids in the basic domain of the proteins, an alanine and a threonine, which have been termed the myogenic code. Previous models suggest that the purpose of the myogenic code is to confer transcriptional activity to these proteins. Specifically, these models predict that a structural change in MyoD family members that have a mutated myogenic code disrupts interaction with co-activator proteins or prevents a conformational change that is necessary for inducing activation. Herein, I show that a significant requirement for the myogenic code is to optimize DNA binding interactions at critical muscle promoters. MyoD with a mutated myogenic code has a decreased capacity to bind to canonical E boxes, such as the established binding site in the skeletal muscle promoter of the *mef2c* gene. In addition, the myogenic code is required for binding to imperfect, non-canonical E boxes in the *myogenin* promoter. These DNA binding defects are due to a combination of a lower affinity and a defect in heterodimerization. These results indicate that the myogenic specificity inherent in MyoD is due, in part, to a role for the myogenic code in optimized DNA binding.



A critical MyoD target during skeletal muscle development is the *mef2c* gene. MEF2 transcription factors are known to be critical regulators of muscle differentiation. We sought to determine the function of MEF2C in skeletal muscle development and function. Mice lacking *mef2c* die at midgestation, too soon to analyze skeletal muscle development, we therefore used a conditional inactivation approach. Mice lacking MEF2C function in skeletal muscle have a decrease in overall body size, decreased exercise endurance and defects in mitochondrial morphology. In addition, these mice accumulate abnormal amounts of glycogen in their skeletal muscle. We hypothesize that MEF2C is a critical regulator of energy metabolism in skeletal muscle, and that an inefficiency of energy usage in skeletal muscle causes a negative energy balance in the organism, and therefore a smaller overall body size.

Table of Contents

Acknowledgments.....	iii
Abstract.....	v
List of Tables.....	viii
List of Figures.....	ix

Chapters:

1. General Introduction.....	1
2. Transgenic mice that express Cre recombinase under control of a skeletal muscle-specific promoter from <i>mef2c</i>	23
3. Conditional inactivation of <i>mef2c</i> in skeletal muscle causes an overall decrease in body size and disruption of energy metabolism during exercise.....	36
4. Determinants of myogenic specificity within MyoD are required for non-canonical E box binding.....	76
General Conclusions.....	103
Methods.....	107
References.....	135

List of Tables

Table 1. Sequence of RT-PCR primers used to measure levels of genes involved in glucose metabolism in <i>mef2c</i> skeletal muscle KO muscle.....	126
Table 2. Sequence of oligonucleotides used for EMSA analysis	132

List of Figures

Figure 2-1. Schematic representation of the skeletal muscle specific Cre transgene construct, <i>mef2c-73k-Cre</i>	33
Figure 2-2. The <i>mef2c-73k-Cre</i> transgene directs skeletal muscle specific expression of Cre during embryogenesis.....	33
Figure 2-3. The <i>mef2c-73k-Cre</i> transgene directs Cre expression exclusively in skeletal muscle and is active from early in muscle development.....	33
Figure 2-4. Cre expression from the <i>mef2c-73k-Cre</i> transgene is completely restricted to skeletal muscle and every muscle fiber exhibits Cre dependent recombination.....	34
Figure 2-5. The <i>mef2c-73k-Cre</i> transgene expresses Cre in every skeletal muscle fiber.....	34
Figure 2-6. Schematic representation of the skeletal muscle specific Cre transgene construct, MYO1565-Cre.....	35
Figure 2-7. The MYO1565-Cre transgene directs mainly skeletal muscle specific expression of Cre during embryogenesis.....	35
Figure 2-8. The MYO1565-Cre transgene directs Cre expression in skeletal muscle and is active from early in muscle development.....	35
Figure 3-1. Schematic representation of the crosses used to generate skeletal muscle specific knockout mice.....	61
Figure 3-2. Mice lacking <i>mef2c</i> in skeletal muscle are viable.....	61
Figure 3-3. <i>mef2c</i> in skeletal muscle is required for normal overall body growth...62	

Figure 3-4. Characterization of the muscle fibers in mice lacking <i>mef2c</i> in skeletal muscle.....	66
Figure 3-5. 73k-<i>mef2c</i> is conserved between the mouse and human genomes.....	67
Figure 3-6. Mice lacking <i>mef2c</i> in skeletal muscle have a decrease in type I fibers.....	68
Figure 3-7. Male mice lacking <i>mef2c</i> in skeletal muscle run less in a voluntary exercise assay.....	69
Figure 3-8. <i>mef2c</i> is critical for maintaining normal mitochondrial morphology during exercise.....	70
Figure 3-9. Mice lacking <i>mef2c</i> develop glycogen deposits in the soleus muscle following exercise.....	71
Figure 3-10. A conserved non-coding sequence near the PYGM gene, which encodes the muscle isoform of glycogen phosphorylase, contains a conserved MEF2 binding site.....	72
Figure 3-11. A conserved non-coding sequence in the first intron of the gene encoding the alpha 2 catalytic subunit of AMP activated protein kinase (PRKAA2) contains two MEF2 binding sites conserved in the mouse and opossum genomes.....	73
Figure 3-12. A model of MEF2C as a central regulator of energy metabolism and mitochondrial biogenesis.....	75
Figure 4-1. The myogenic code is necessary for maximal transcriptional activation of the <i>myogenin</i> promoter.....	96
Figure 4-2. Mutation of the myogenic code does not fundamentally disrupt the transcriptional activation domain of MyoD.....	97

Figure 4-3. The myogenic code of MyoD is critical for optimized DNA binding to a canonical E box.....98

Figure 4-4. The myogenic code is important for optimizing dimerization interactions between MyoD and E protein..... 99

Figure 4-5. Dimerization defects do not fully account for the transcriptional activation defect exhibited by myogenic code mutants..... 100

Figure 4-6. The myogenic code of MyoD is required for binding to non-canonical E boxes in the *myogenin* promoter..... 101

Figure 4-7. MyoD/E12 heterodimers form a tetrameric complex with Pbx/Meis heterodimers on juxtaposed binding sites in the *myogenin* promoter..... 102

Chapter 1: General Introduction

Members of the MEF2 family of transcription factors are widely expressed throughout the developing embryo, and are critical regulators of differentiation. In the mouse, *mef2* genes are among the earliest markers of the skeletal muscle lineage, and are known to be early and immediate targets of the muscle regulatory factor family of bHLH transcription factors, the master regulators of muscle development (Edmondson, Lyons et al. 1994; Wang, Valdez et al. 2001; Bergstrom, Penn et al. 2002; Dodou, Xu et al. 2003). The importance of MEF2 as a potentiator of differentiation is most clear in *Drosophila*, where inactivation of the single MEF2 family member, *D-mef2*, causes a block in the differentiation of all three muscle lineages (Lilly, Galewsky et al. 1994; Lilly, Zhao et al. 1995). In mice, the situation is more complex, as there are 4 members of this family, at least 3 of which are expressed in skeletal muscle at varying levels and times. In muscle cell lines, a truncated form of MEF2A that contains the DNA binding and dimerization domains but lacks a transcriptional activation domain acts as a dominant negative and inhibits myogenesis (Ornatsky, Andreucci et al. 1997).

MEF2 proteins contain a MADS (MCM1, agamous, deficiens, serum response factor) DNA binding domain that recognizes an AT rich consensus binding site, YTA(A/T)₄TAR, that is present near E boxes in the promoters of many skeletal muscle genes (Gossett, Kelvin et al. 1989; Andres, Cervera et al. 1995; Fickett 1996; Black and Olson 1998). MEF2 and MyoD are known to physically interact and can synergistically activate transcription of transfected reporters (Molkentin, Black et al. 1995; Naidu,

Ludolph et al. 1995). In the developing embryo, *mef2c* expression is first detected in the rostral somites at 9.0 dpc (Edmondson, Lyons et al. 1994; Wang, Valdez et al. 2001; Dodou, Xu et al. 2003). One day later, *mef2a* transcripts can be seen in caudal somites that do not yet express *mef2c* (Edmondson, Lyons et al. 1994). *Mef2d* is also expressed in the myotome from 9.5 dpc (Edmondson, Lyons et al. 1994). Although the timing of expression of these three factors is similar, there appears to be a spatial distinction between the expression patterns, as *mef2c* is in the periphery of the somite, while *mef2a* and *mef2d* are expressed at the highest levels in the center (Edmondson, Lyons et al. 1994). This difference in pattern suggests that these different family members may be marking distinct lineages in the developing myotome. *Mef2c* null mice die at midgestation due to cardiac insufficiency; these mice exhibit drastic morphogenetic defects including hearts to undergo looping morphogenesis and a disorganized vasculature (Lin, Schwarz et al. 1997; Lin, Lu et al. 1998; Bi, Drake et al. 1999). Mice lacking *mef2a* survive to birth, but most die perinatally from cardiac defects, which are probably due to mitochondrial deficiency (Naya, Black et al. 2002). The result of *mef2d* inactivation has yet to be reported, therefore the requirement and redundancy between these three MEF2 family members in skeletal muscle is unclear. *Mef2b* is the most divergent mammalian MEF2 family member and is also expressed early in the myogenic lineages, particularly in cells that migrate to become the head and limb musculature (Molkentin, Firulli et al. 1996).

While the role of MEF2 proteins in muscle differentiation is well established, it is likely that MEF2 factors may function in other aspects of muscle function as well. The MEF2

family of proteins is known to interact with numerous signaling pathways, providing a target by which different signals may regulate the entire array of muscle gene expression both pre- and post-natally (Lu, Chang et al. 2000; McKinsey, Zhang et al. 2001). There are many ways in which MEF2 proteins are regulated leading to the ability to function as either a repressor or activator of transcription (Ornatsky, Cox et al. 1999; Youn, Chatila et al. 2000; McKinsey, Zhang et al. 2001; Cox, Du et al. 2003; Kang, Gocke et al. 2006). The nature of MEF2 function is tightly regulated both by post-translational modification and by interaction with chromatin remodeling factors (McKinsey, Zhang et al. 2000; McKinsey, Zhang et al. 2000; McKinsey, Zhang et al. 2001). The phosphorylation state of MEF2 proteins dictates whether the protein interacts with a repressor of activation, histone deacetylase (HDAC), or a potentiator of activation, histone acetyltransferase (HAT) complex (McKinsey, Zhang et al. 2000; McKinsey, Zhang et al. 2000; McKinsey, Zhang et al. 2001). Co-activator and co-repressor proteins also utilize HDAC function to regulate MEF2 transcriptional activity; PC4 binds to MEF2 and displaces HDAC4, while MITR binds to the MADS/MEF2 domain of MEF2 family members and recruits class II HDACs (Sparrow, Miska et al. 1999; Micheli, Leonardi et al. 2005).

There is an additional level of regulation on the function of MEF2 transcriptional activity based on the nuclear localization of Class II HDACs. Both HDAC5 and HDAC7 are located in the nucleus in undifferentiated myoblasts, but are exported from the nucleus concurrent with the start of differentiation (McKinsey, Zhang et al. 2000; Dressel, Bailey et al. 2001). When unphosphorylated, these HDACs are localized to the nucleus, where they bind to MEF2 and form a repressive complex (Miska, Karlsson et al. 1999;

Lemercier, Verdel et al. 2000). Upon phosphorylation by CaMK, class II HDACs are exported from the nucleus by 14-3-3 proteins, freeing MEF2 to interact with co-activator proteins (McKinsey, Zhang et al. 2000). Other kinases that are necessary for myoblast differentiation, such as Mirk kinase, utilize a similar strategy to reduce nuclear accumulations of class II HDACs in differentiating cells (Deng, Ewton et al. 2003; Deng, Ewton et al. 2005).

Free from HDACs, MEF2 proteins are further modified both post translationally and through interaction with additional proteins to activate transcription. Although the effect of the interaction between MEF2 proteins and the coactivator protein p300 on chromatin and transcriptional activation is not entirely clear, it is known that p300 acetylates MEF2 proteins, improving both the DNA binding and activation properties of the protein (Sartorelli, Huang et al. 1997). Indeed, a non-acetyltable form of MEF2 functions as a dominant negative inhibitor of myogenesis in the C2C12 myoblast cell line (Ma, Chan et al. 2005). The activator form of MEF2 benefits from an interaction with GRIP-1, a potent co-activator (Chen, Dowhan et al. 2000). This is another interaction that is tightly regulated at the boundary between proliferation and differentiation in myogenic lineages. Smad3, a transcription factor activated by the TGF-beta signaling cascade, interacts with MEF2C and displaces GRIP-1 making MEF2C a less potent activator (Quinn, Yang et al. 2001; Liu, Kang et al. 2004). Disrupting the interaction between MEF2C and GRIP-1 is also one method by which the cyclinD/cdk4 complex functions to keep myoblasts in a proliferative state (Lazaro, Bailey et al. 2002).

It is clear that MEF2 functions in postnatal muscle to regulate fiber type (Wu, Naya et al. 2000; Calvo, Vullhorst et al. 2001; Parsons, Millay et al. 2004; Oh, Rybkin et al. 2005). Skeletal muscle fibers can be divided into two different metabolic classes, type I and type II fibers. These fibers have distinct transcriptional programs and utilize differing forms of structural genes such as myosin heavy chain (MyHC) and troponin (Schiaffino and Reggiani 1994). Type I, or slow twitch, fibers have a higher number of mitochondria per fiber and use mainly oxidative metabolism (Pette and Staron 2000). Type II, or fast twitch, fibers are further subdivided into three categories with decreasing similarity to type I fibers, A>X>B, with type IIB fibers having the most glycolytic metabolism. The different fiber types exist due to differences in the rate of input nerve firing, which directly affects the intracellular calcium concentration (Streeter, Gergely et al. 1973; Williams, Salmons et al. 1986). As calcium levels increase in a cell and are sustained, calcineurin, a calcium dependent phosphatase becomes activated (Olson and Williams 2000). Expression of a constitutively active form of calcineurin *in vivo* induces the formation of slow fibers in the absence of repeated stimulation and contraction (Naya, Black et al. 2002). Sufficient to induce slow fibers, calcineurin is also necessary for this process as mice that lack functional calcineurin have defects in fiber type switching (Parsons, Millay et al. 2004). MEF2 has repeatedly been shown to regulate fiber type in a calcineurin-dependent manner and to be an important regulator of the fast to slow fiber type transition (Liu, Liu et al. 1997; Wu, Naya et al. 2000; Michael, Wu et al. 2001). MEF2 transcriptional activity is further modified by calcineurin, as it is known to dephosphorylate and thereby induce nuclear translocation of NFATc1, a transcription factor

that functions synergistically as a coactivator of MEF2 to induce fiber type switching and hypertrophy (Beals, Clipstone et al. 1997; Chin, Olson et al. 1998; Wu, Naya et al. 2000).

MEF2 is also known to function in a positively reinforcing network with PGC-1 α , an important regulator of mitochondrial biogenesis and slow twitch fiber formation (Wu, Puigserver et al. 1999; Lin, Wu et al. 2002). PGC-1 α is a direct transcriptional target of MEF2, and the MEF2 site in the PGC-1 α promoter is critical for contractile activity-induced activation (Akimoto, Ribar et al. 2004). Following initial activation, PGC-1 α cooperates and directly interacts with MEF2C to further upregulate its own expression in addition to numerous other genes important for slow fiber formation (Michael, Wu et al. 2001). Both MEF2 and PGC-1 α are thought to be activated by p38 mediated phosphorylation, an additional level of coregulation that further supports that synergistic relationship between these proteins (Zhao, New et al. 1999; Akimoto, Pohnert et al. 2005).

The importance of MEF2 activity in the response of a muscle fiber to repeated stimulation is further highlighted by a mouse myotonic disease model that mimics endurance exercise due to nerve hyperactivity. These mice have increased levels of MEF2 activity, although it is not entirely clear if this is solely a response to increases in intracellular calcium, or if stressed fibers activate the p38 kinase pathway, thereby phosphorylating and activating MEF2 (Michael, Wu et al. 2001). In either case, MEF2 is an important protein in the induction of the slow fiber type. Strikingly, the same is true for fast muscle fibers. Type IIA, IIX and IIB all express different isoforms of MyHC.

Each of these genes contains a conserved MEF2 site that has been shown to be important for proper regulation of MyHC expression in fast fibers. Interestingly, the affinity MEF2 has for these sites correlates with the degree of glycolytic metabolism exhibited by a fiber; the site in MyHC IIB is the highest affinity site, while that in MyHC IIA is the lowest (Allen, Weber et al. 2005).

Skeletal muscle is the major site in the body that uptakes glucose in response to insulin. One of the major regulators of glucose transport in muscle is GLUT4, a glucose transporter that is trafficked to the plasma membrane in response to insulin to import glucose into muscle cells. GLUT4 levels are higher in oxidative than in glycolytic muscle, likely due to an increased need for energy utilization in slow twitch fibers (Kern, Tapscott et al. 1990). GLUT4 is rapidly induced upon exercise in a calcium and MEF2 dependent manner (Holloszy and Hansen 1996; Thai, Guruswamy et al. 1998; Mora, Yang et al. 2001; Moreno, Serrano et al. 2003; Silva, Giannocco et al. 2005). The mechanisms for upregulation seem to be multi-faceted, as both calcineurin and CaMK have been shown to mediate the increase (Ryder, Kawano et al. 1999; Ojuka, Jones et al. 2002). These two kinases are also known to activate MEF2 transcriptional activity, yet it is not clear if MEF2 activation is the only mechanism by which GLUT4 is upregulated. Mice lacking GLUT4 exhibit decreased insulin tolerance, but nearly normal glucose tolerance, suggesting that additional glucose transporter proteins compensate for the loss of GLUT4 (Katz, Stenbit et al. 1995; Charron, Katz et al. 1999). Mice that are null for Glut4 only in skeletal muscle, strikingly, have an increase in muscle glycogen despite decreased glucose transport (Kim, Peroni et al. 2005). This discrepancy is likely the

result of an increase in glycogen synthase activity and a decrease in glycogen phosphorylase activity.

As a regulator of PGC-1 α and GLUT4, MEF2 plays a role in the regulation of overall body metabolism and energy usage in skeletal muscle. The precise contribution of MEF2 deficiency to muscle disease is unclear. Mutations in genes that regulate glycogen storage often result in a disease state. For example, mice lacking alpha-glucosidase have an increase in lysosomal glycogen storage, which interrupts normal sarcomere function and force generation (Hesselink, Gorselink et al. 2002). MEF2 is known to activate transcription of *Srpk3*, a serine arginine protein kinase that is important for normal muscle integrity (Nakagawa, Arnold et al. 2005). Mice lacking this kinase have a severe, type II fiber-specific myopathy that is characterized by numerous centrally nucleated fibers. Determining additional targets of MEF2 in skeletal muscle may serve to further the understanding of muscle disease.

In this thesis, I describe a conditional inactivation approach to remove MEF2C function from skeletal muscle, utilizing a transgenic mouse that drives Cre recombinase under the control of a skeletal muscle specific promoter and enhancer from the *mef2c* gene itself. Generation of a new transgenic Cre expressing line was necessary, as previous skeletal muscle Cre lines, such as SM- α -actin-, Cardiac- α -actin- and MCK-Cre, also express Cre in cardiac muscle during development (Kahn, Bruning et al. 2000; Miwa, Koyama et al. 2000). Because of the requirement for MEF2C function in the developing heart, as evidenced by the lack of looping in null embryos, we sought to develop a tool that would

allow excision of a conditional allele solely in skeletal muscle (Heidt and Black 2005) (Chapter 2). Using mice that were transgenic for this skeletal muscle specific Cre, in combination with a conditional allele of *mef2c* with LoxP sites flanking the majority of the MADS and MEF2 domains of the gene (Vong, Ragusa et al. 2005), we show that *mef2c* is required for proper muscle development and function (Chapter 3). This includes establishment of proper fiber type and the ability of mice to respond appropriately to voluntary exercise. In addition, disruption of *mef2c* function in skeletal muscle results in defective glycogen storage and mitochondrial morphology, and *mef2c* skeletal muscle conditional knockout mice have an overall deficit in body size, suggesting that skeletal muscle dictates body size through cell non-autonomous mechanisms.

Due to the role for *mef2c* in skeletal muscle development and function, we were also interested in investigating the mechanism by which this gene is activated during the differentiation process. Numerous previous studies have shown that *mef2c* is an immediate early target of the MyoD family of transcription factors (MRFs) (Wang, Valdez et al. 2001; Dodou, Xu et al. 2003). In addition to being targets of MRF activation, MEF2 proteins are important for the propagation of the myogenic transcriptional program, as they function as coactivators for MRFs to activate differentiation genes and to positively reinforce expression of the MRF genes themselves (Edmondson, Cheng et al. 1992; Cheng, Wallace et al. 1993; Yee and Rigby 1993; Molkenin, Black et al. 1995; Naidu, Ludolph et al. 1995; Black and Olson 1998). Due to the critical role that MEF2 factors play in the propagation of the skeletal muscle transcriptional program, we were interested in studying the mechanism by which *mef2*

and other critical genes that control muscle differentiation are upregulated in the course of skeletal muscle development. We specifically focused on the ability of MyoD to bind to the promoters of these genes, as a critical step leading to differentiation.

The MRF family of transcription factors was discovered due to the amazing capacity to induce the muscle transcriptional program in non-muscle cells (Pinney, Pearson-White et al. 1988; Tapscott, Davis et al. 1988; Edmondson and Olson 1989; Rhodes and Konieczny 1989; Braun and Arnold 1991; Weintraub, Dwarki et al. 1991). MyoD, Myf5, Myogenin, and Mrf4 are members of the much larger family of bHLH transcription factors. bHLH proteins bind to a consensus DNA sequence known as an E box, which contains the CANNTG motif (Lassar, Buskin et al. 1989; Murre, McCaw et al. 1989). Although weakly capable of binding to DNA as homodimers, MRFs form a higher affinity complex when heterodimerized with E proteins, which are ubiquitous, non-myogenic members of the bHLH family (Murre, McCaw et al. 1989; Brennan and Olson 1990; Braun and Arnold 1991; Chakraborty, Brennan et al. 1991; Hu, Olson et al. 1992). Dimerization occurs through interaction of the HLH domains and is a necessary step prior to DNA binding (Spinner, Liu et al. 2002). Recognition of DNA and subsequent binding is mediated through the basic domain (Davis, Cheng et al. 1990; Voronova and Baltimore 1990). DNA binding is a critical step in activation the myogenic program, as it is thought that during activation of the myogenic program in cultured cells, MyoD binds directly to 20% of the approximately 3,000 genes that alter their expression in response to MyoD (Bergstrom, Penn et al. 2002).

The requirement for dimerization prior to DNA binding provides a conspicuous point at which proteins can negatively regulate bHLH protein activation. Id family proteins contain an HLH domain, but lack a basic domain and have a higher affinity for E protein than does MyoD. By sequestering E protein from heterodimerizing with MyoD, Id is able to inhibit myogenesis (Benzra, Davis et al. 1990; Benzra, Davis et al. 1990). At the onset of differentiation, Id proteins are degraded, freeing the sequestered pool of E protein for use by MyoD to activate transcription (Jen, Weintraub et al. 1992).

Sequestration of E protein is also one of the mechanisms by which M-Twist can inhibit myogenesis when expressed ectopically in the myotome (Hebrok, Wertz et al. 1994; Spicer, Rhee et al. 1996). Interaction with MyoD is also a strategy used to inhibit heterodimerization, as Smad3, a transcription factor upregulated by TGF-beta signaling, inhibits myogenesis by binding to the HLH domain of MyoD (Liu, Black et al. 2001). MyoR and Mist-1 are additional bHLH proteins that bind to MRF proteins; these heterodimers remain competent to bind E boxes, yet are unable to activate transcription (Lemerrier, To et al. 1998; Lu, Webb et al. 1999). The importance of dimerization is further highlighted by the observation that a forced heterodimer of MyoD and E47 is refractory to inhibition by both Id and TGF-beta (Neuhold and Wold 1993).

DNA binding of the MRF family of transcription factors is also inhibited both directly and indirectly by I-mfa, another inhibitor of myogenesis (Chen, Kraut et al. 1996). This protein is thought to reduce the DNA binding activity of MRF/E protein heterodimers and to mask the nuclear localization sequences (NLS) of the MRF, leading to a decrease in nuclear localization. There are two NLS domains in MyoD, one each in the basic

domain and helix 1, each of which can function independently as an NLS (Vandromme, Cavadore et al. 1995). Although it contains the NLS domains of MyoD, the bHLH does not have transcriptional activity on its own. Rather, this activity is contained in an amino-terminal acidic activation domain, which functions as such when tethered to the yeast GAL4 DNA binding domain (Weintraub, Davis et al. 1990; Weintraub, Dwarki et al. 1991). The other MRF family members also contain activation domains, although the structure of those molecules is somewhat different. The activation domain of Myf5 maps to the carboxy-terminal half of the protein, whereas myogenin has 2 activation domains, one in the C terminus and the other in the N terminus (Braun, Winter et al. 1990; Schwarz, Chakraborty et al. 1992). MRF4, the fourth member of the myogenic regulatory factor family, has a single activation domain in the N terminal domain of the protein (Mak, To et al. 1992)

The MRF family can be divided loosely into two classes, specification and differentiation, based on timing of expression, but also on the ability to induce chromatin remodeling in cultured cells. MyoD and Myf5 regulate specification of the hypaxial and epaxial lineages, respectively (Buckingham, Bajard et al. 2003; Kablar, Krastel et al. 2003). These proteins can substitute for one another in the developing embryo, however, since animals null for either gene individually have normal skeletal muscle at birth (Rudnicki, Schnegelsberg et al. 1993). The redundancy is not complete, as mice that lack MyoD have an increase in *myf5* transcript levels and a delay in the development of the hypaxial lineage (Rudnicki, Braun et al. 1992). Myf5 is expressed as early as 8.0dpc in the most rostral somites, whereas MyoD is not expressed until 10.5dpc in those same

regions (Wright 1992; Molkentin and Olson 1996; Summerbell, Ashby et al. 2000). The differentiation factors are expressed after *Myf5*, with *myogenin* expression initiating in the myotome at 8.5dpc, and *Mrf4* at 9.0dpc. This early wave of *Mrf4* expression does not persist and there is no accumulation of MRF4 in skeletal muscle until late fetal stages (Olson and Klein 1994). Mice that lack myogenin die at birth with a severe reduction of differentiated muscle, although they have the normal number of specified myoblasts, suggesting that myogenin is primarily important in myoblast differentiation (Hasty, Bradley et al. 1993; Nabeshima, Hanaoka et al. 1993). In addition, embryonic stem cells lacking myogenin fail to differentiate into muscle in culture, and the addition of exogenous MyoD is not sufficient to overcome this block in differentiation (Myer, Olson et al. 2001). Expression of an *Mrf4* transgene in *myogenin* null embryos or embryonic stem cells can rescue the phenotype to a varying degree, establishing a role for MRF4 as a differentiation factor (Zhu and Miller 1997; Sumariwalla and Klein 2001).

The division into specification and differentiation factors is not as simple as it first seems, however, as there are numerous examples of MRF proteins functioning in both categories. When knocked into the *myf5* locus, *myogenin*, thought of as a differentiation factor, is sufficient to drive some specification in a *Myod* null background, albeit it cannot fully replace *Myf5*, as these mice die at birth due to reduced muscle formation (Wang and Jaenisch 1997). MyoD clearly plays a part in differentiation, as a MyoD/MRF4 double null animal exhibits a similar phenotype to a myogenin null, suggesting that MyoD and MRF4 work together to induce skeletal muscle differentiation (Rawls, Valdez et al. 1998). MRF4 has until recently been thought of as a differentiation

factor, however, new results using multiple alleles of *myf5* that affect *Mrf4* expression to varying degrees show that it can also function as a specification factor (Kassar-Duchossoy, Gayraud-Morel et al. 2004). The rules are further stretched when primary myoblasts are cultured and induced to differentiate, as muscle progenitors from mice lacking myogenin alone or MyoD plus MRF4 form myofibers in culture, suggesting that the genetic results do not reveal the absolute requirements for differentiation (Nabeshima, Hanaoka et al. 1993; Rawls, Morris et al. 1995; Rawls, Valdez et al. 1998).

Each of the MRF family members binds to the same consensus sequence, an E box, and heterodimerizes with the same class of E proteins. The manner in which specificity between family members is achieved remains unclear. CASTing experiments were used to select for optimal binding sites with slightly different specificities, yet these are not sufficient to predict which MRF protein will bind to a particular E box *in vivo* (Blackwell and Weintraub 1990; Braun and Arnold 1991; Wright, Binder et al. 1991; Blackwell, Huang et al. 1993; Kunne, Meierhans et al. 1996). In C2C12 cells, chromatin immunoprecipitation (ChIP) analysis of the acetylcholine receptor subunit genes found that all four MRF proteins were bound to each gene analyzed, and detection of binding correlated with the expression level of a particular MRF (Liu, Spinner et al. 2000). In contrast, MRF selectivity is exhibited by the murine sarcoma virus v-ski transgene, a viral gene that causes hypertrophy in type IIB fibers. As MyoD is expressed preferentially over myogenin in type II fibers, it was suspected that MyoD would have higher binding affinity to the E boxes present in the LTR than would myogenin (Hughes, Koishi et al. 1997). Indeed, MyoD binds with higher affinity and exhibits more

cooperativity than myogenin on this viral promoter (Czernik, Peterson et al. 1996). The activation of a particular gene by MRFs is likely to be a combination of the intrinsic affinity a regulatory E box has for the MRF family members and simply the availability of particular MRFs due to variation in expression pattern and timing. This model is supported by work in *Xenopus* that shows each MRF to have a targeted subset of genes, but that these genes can be activated less efficiently by other members of the family (Chanoine, Della Gaspera et al. 2004).

Binding of an MRF/E protein heterodimer to DNA is not sufficient to initiate transcriptional activation, as it is known that these complexes are targeted by histone deacetylase (HDAC) complexes, which can transform the dimers into transcriptional repressors. In proliferating myoblasts, class I HDACs are known to interact with MyoD and inhibit the initiation of myogenesis (Mal, Sturniolo et al. 2001; Puri, Iezzi et al. 2001). The recruitment of HDACs to muscle gene promoters is further reinforced by the fact that the bHLH domain of MyoD also interacts with N-CoR, a co-repressor that is known to be another interacting partner for HDAC1 (Bailey, Downes et al. 1999). In differentiated myotubes, the interaction between MyoD and HDAC1 cannot be detected. Instead, MyoD is associated with PCAF, a protein with histone acetyltransferase (HAT) activity (Mal and Harter 2003). This handoff of HDAC1 for PCAF acts as a switch that turns MyoD into an activator that recruits chromatin remodeling activity to muscle specific genes (Gerber, Klesert et al. 1997; Puri, Sartorelli et al. 1997; Sartorelli, Puri et al. 1999).

The importance of chromatin modification and remodeling has been further substantiated by numerous examples of interactions these proteins make with both histone acetylase (HAT) and ATP-dependent chromatin remodeling complexes. It is known that p300 and CBP, which have HAT activity, can potentiate the activity of MyoD on plasmid reporters, and acetylation of the MyoD protein increases DNA binding and activation (Sartorelli, Huang et al. 1997; Poleskaya, Duquet et al. 2000). At endogenous muscle genes, p300 is located in a complex with MyoD that is bridged by PCAF and the acetylation activity of this complex is critical for myogenesis (Eckner, Ewen et al. 1994; Puri, Sartorelli et al. 1997). In addition to acetylating MyoD, the PCAF complex is likely to acetylate histones in the vicinity of E boxes leading to a more permissive chromatin state for activation of muscle genes. Indeed, hyperacetylation of histone H3 is correlated with gene activation in cells transfected with MyoD (Bergstrom, Penn et al. 2002).

Activation of transcription by MyoD is also known to be dependent on the ATP-dependent chromatin remodeling activity of the SWI/SNF complex. Dominant negative BRG1, the catalytic ATPase subunit of the SWI/SNF complex, inhibits the ability of MyoD to induce myogenesis by reducing the activation of one-third of MyoD induced genes (de la Serna, Carlson et al. 2001; de la Serna, Ohkawa et al. 2005). Direct inhibition of MyoD is the simplest model to explain the effect of the dominant negative BRG1, as MyoD has been shown to interact with BRG1 in differentiating cells (de la Serna, Ohkawa et al. 2005). p38, a differentiation-induced kinase, promotes differentiation in part by targeting SWI/SNF complexes to muscle specific loci, through

phosphorylation of BAF60 and recruitment of p38 directly to the chromatin of muscle genes (Simone, Forcales et al. 2004).

The chromatin remodeling ability of MyoD was mapped to two regions of the protein, a cysteine –histidine rich domain and an amphipathic alpha-helix in the carboxyl terminus, both of which are conserved in Myf5 (Gerber, Klesert et al. 1997). Swapping experiments have shown that the alpha-helical region is the critical specification region of the MyoD protein, as the Cys-His region of myogenin can functionally substitute for the analogous region in MyoD (Bergstrom and Tapscott 2001). In MyoD, the amphipathic alpha helix functions to allow for activation of skeletal muscle genes in chromatin, however, in myogenin, the analogous region functions only as a transcriptional activation domain on plasmid reporters. It is interesting to note that these two regions, which are certainly necessary for the full robustness of myogenesis, are distinct from the bHLH domain. The bHLH domain is the only region of MyoD required to induce myogenic conversion, which suggests that the minimal information necessary for the specificity of inducing the muscle transcriptional program is included in the bHLH domain (Molkentin, Black et al. 1995).

Herein, I present work that is aimed at determining the critical event in activation of the muscle program by MyoD, and therefore focuses on the role of the bHLH domain in initiating myogenesis (Chapter 4). Previous deletional analyses of MyoD showed that the bHLH domain was both necessary and sufficient to induce myogenesis, suggesting that the minimal components necessary for inducing the muscle transcriptional program

UCSF LIBRARY

reside in the bHLH domain (Tapscott, Davis et al. 1988; Murre, McCaw et al. 1989; Weintraub, Dwarki et al. 1991; Molkentin, Black et al. 1995). Careful analysis of the four muscle regulatory factors (MyoD, Myf5, Myogenin and Mrf4) showed that the characteristic shared by this family, and absent from other bHLH families, is two amino acids in the basic domain (Davis, Cheng et al. 1990; Brennan, Chakraborty et al. 1991; Weintraub, Dwarki et al. 1991). These two amino acids, an alanine and threonine, serve as an essential myogenic determinant and were termed the myogenic code, as mutation of these amino acids renders the MyoD family non-myogenic (Weintraub, Dwarki et al. 1991). Furthermore, these amino acids, when in the context of a bHLH protein, were also shown to be sufficient to induce myogenesis, as substitution of the myogenic code into E12 renders the protein myogenic (Davis and Weintraub 1992).

The function of the myogenic code is not clear, since in the crystal structure of MyoD bound to DNA, these two amino acids are buried in a helix of the molecule making no DNA base-pair contacts. Likewise, these residues are not accessible to make considerable protein-protein interactions (Ma, Rould et al. 1994). It is known that the basic domain forms an alpha helix upon DNA binding, and that affinity of a basic domain for DNA depends on the stability of the formed helix (Meierhan, el-Ariss et al. 1995; Kunne and Allemann 1997). Artificial stabilizing of the MyoD basic DNA binding helix by fusion to a disulfide stabilized peptide from apamin creates a molecule that has a higher affinity for the E box sequence (Turner, Cureton et al. 2004). In addition, the basic domain is critical for determining the DNA binding specificity of a bHLH protein, as swapping the basic domain of E2A for that of another bHLH protein, Twist, yields a

protein with the Twist binding specificity (Kophengnavong, Michnowicz et al. 2000). Similarly, replacing one amino acid of the neuronal bHLH protein MASH-1 and lengthening the alpha helix by one turn gives the protein MRF binding specificity (Dezan, Meierhans et al. 1999). Thus, the conformation of the basic domain is critical for achieving optimal DNA binding.

The crystal structure of the MyoD bHLH domain has suggested that, in addition to being part of the basic DNA binding helix, the myogenic code amino acids influence the position of an arginine residue at the amino-terminal end of the basic domain (Ma, Rould et al. 1994). In MyoD, the alanine and threonine of the myogenic code allow a pocket to form into which the arginine residue is buried. Non-myogenic bHLH proteins generally have a histidine or an asparagine in place of the alanine, and these larger amino acids prevent the arginine from remaining inside the pocket. Thus, the myogenic code mutants are likely to display the arginine in a way that is not present in wild type MyoD. While the arginine is displaced in these mutants, this does not explain the entirety of the defect, as a screen to identify second site suppressor mutations at this position was not able to reconstitute myogenic ability (Huang, Weintraub et al. 1998).

The displacement of the arginine in myogenic code mutants may be one part of an overall change in conformation that could affect both the DNA binding characteristics of the protein and other necessary protein-protein contacts. MyoD with a substitution of an asparagine for the alanine of the myogenic code exhibits altered sensitivity to a protease when bound to DNA, suggesting altered accessibility of the recognition site (Huang,

Weintraub et al. 1998). It has been suggested previously that binding of MyoD to a high affinity binding site may result in a conformational change that facilitates transcription (Bengal, Flores et al. 1994). It is plausible that intramolecular interactions between the amino- and carboxy- terminal portions of the protein are critical, as both contain activation domains that function together to activate genes important for muscle cell differentiation (Ishibashi, Perry et al. 2005). In addition to changes in intramolecular interactions, it is certainly possible that an altered conformation would disrupt interactions with other proteins. One of the original hypotheses regarding the function of MyoD suggested that a “recognition factor” was required for myogenic conversion of non-myogenic cells (Weintraub, Dwarki et al. 1991). This idea was developed due to the fact that MyoD-E12basic, MyoD with a substitution of the basic domain with that of E12, can only activate transcription in certain cell types, suggesting that these cells contain a factor that allows MyoD-E12basic to function as an activator. Although the identity of such a “recognition factor” remains to be determined, it is possible that disruption of the conformation of MyoD would reduce the affinity for this necessary interacting partner.

More recent results that aim to define the function of the myogenic code have focused mainly on the activation exhibited by MyoD compared to myogenic code mutants.

MyoD-E12basic is non-myogenic, however it exhibits similar, albeit diminished, affinity for a muscle gene E box (Weintraub, Dwarki et al. 1991). MyoD-E12basic has also been shown to activate transcription of a reporter plasmid containing multimerized E boxes and to synergize with MEF2, a common co-activator partner for the MRF family of transcription factors (Black, Molkentin et al. 1998). It has been proposed that the

discrepancy between the ability exhibited by myogenic code mutants to activate a plasmid reporter and to activate the myogenic program is due to a conformational change that prevents the proper display of an activation domain necessary to activate genes in chromatin (Black, Molkentin et al. 1998; Huang, Weintraub et al. 1998).

The activation and DNA binding deficits in myogenic code mutants do not appear sufficient to account for the fact that the myogenic capacity of MyoD is completely eradicated when the myogenic code is mutated. Over expression of mutant protein should be able to drive the equilibrium between free and bound MyoD to the bound state and induce myogenesis, if binding to a consensus E box was the limiting step. Thus, the regulation of myogenesis may be more subtle, as recent work has shown that MRF factors recognize and bind to imperfect binding sites in order to fully activate the *myogenin* promoter (Berkes, Bergstrom et al. 2004). As it is clear that there is a mutually reinforcing network that exists between bHLH proteins in the MyoD family, *myogenin* is not only an immediate early target of MyoD, but is a critical member in the positively reinforcing loop that enacts the muscle transcriptional program (Braun, Bober et al. 1989; Thayer, Tapscott et al. 1989). The *myogenin* promoter contains a binding site for the HOX-TALE family members Pbx/Meis, and this heterodimer is resident at the promoter in repressive chromatin prior to differentiation (de la Serna, Ohkawa et al. 2005). This heterodimer is adjacent to two overlapping non-canonical E boxes for which MyoD has low affinity. According to the model, the presence of Pbx/Meis allows MyoD/E protein heterodimers to recognize these sites and form a quaternary complex, stabilizing the MRF protein at the site necessary to induce transcription (Berkes, Bergstrom et al. 2004).

WEST LIBRARY
MAR 07 2007

I show herein that the myogenic code of MyoD is required for binding to non-canonical E boxes and for interaction with Pbx/Meis heterodimers at the *myogenin* promoter (Chapter 4). This is likely to be a critical requirement for MyoD to activate the muscle transcriptional program in non-muscle cells and provides a likely explanation for the requirement of the myogenic code in the induction of myogenesis.

UNIVERSITY OF
MICHIGAN

Chapter 2: Transgenic mice that express Cre recombinase under control of a skeletal muscle-specific promoter from *mef2c*

I. Summary

Genes expressed in skeletal muscle are often required in other tissues. This is particularly the case for cardiac and smooth muscle, both contractile tissues that share numerous characteristics with skeletal muscle, such that targeted inactivation can lead to embryonic lethality prior to a requirement for gene function in skeletal muscle. Thus, it is essential that conditional inactivation approaches are developed to disrupt genes specifically in skeletal muscle. Several Cre mouse lines have been established previously using promoters from genes that are expressed in both cardiac and skeletal muscle, including *muscle creatine kinase* (MCK), *human smooth muscle alpha-actin* and *cardiac alpha-actin* (Wang, Wilhelmsson et al. 1999; Miwa, Koyama et al. 2000). An additional skeletal muscle Cre line has been generated by homologous recombination of Cre into the *myosin light chain (mlc) 1f* locus, but Cre expression in this line is restricted to fast fibers and is activated relatively late in development (Bothe, Haspel et al. 2000; Jiang, Song et al. 2002). The transgenic lines described herein express Cre throughout skeletal muscle, including fast and slow fibers, as well as muscle of hypaxial and epaxial origins. One line utilizes a highly conserved promoter from the *mef2c* gene that lies 71 kb upstream of the first translated exon. In addition, we developed a transgenic line that expressed Cre under control of the proximal *myogenin* promoter. These early skeletal

muscle specific Cre lines will be useful tools to define the function of genes specifically in skeletal muscle.

II. Analysis of *mef2c*-73k-Cre transgenic mice

In order to circumvent the problem that arises due to the similarity between muscle types, we sought to establish an exclusively skeletal muscle-specific Cre transgenic mouse line. Our goal was to generate a line in which Cre expression was abundant throughout skeletal muscle, including fast and slow fibers, as well as muscles of hypaxial and epaxial origins and in which Cre was expressed from the earliest stages of skeletal muscle development.

Previous studies have identified a highly conserved promoter from the mouse *mef2c* gene that lies 71 kb upstream of the first translated exon and is sufficient to direct expression exclusively to skeletal muscle (Wang, Valdez et al. 2001; Dodou, Xu et al. 2003). The activity of this promoter fragment is first detected at 8.75 dpc, consistent with the earliest expression of *mef2c* in the developing myotome (Edmondson, Lyons et al. 1994). The early activation of this promoter from *mef2c*, combined with its highly restricted activity, suggested that it might serve as an ideal tool to direct Cre expression exclusively to skeletal muscle. Therefore, we cloned the Cre cDNA under the control of the *mef2c* skeletal muscle promoter and used this construct, designated *mef2c*-73k-Cre, to generate transgenic mice (Fig. 2-1).

Eight Cre transgene-positive founders were crossed to ROSA26R Cre-dependent *lacZ* reporter mice (Soriano 1999) and screened for β -galactosidase activity at 11.5 dpc. Five of

the eight *mef2c*-73k-Cre lines induced recombination at the ROSA26 locus exclusively in skeletal muscle. The remaining three transgene-positive lines displayed no detectable expression of β -galactosidase when crossed to ROSA26R reporter mice (data not shown). Among the five transgenic lines that demonstrated Cre activity at 11.5 dpc, three displayed robust excision at the ROSA26 locus (Fig. 2-2). The expression of Cre by all three of these independent transgenic lines was restricted exclusively to skeletal muscle, consistent with the previously described activity of this *mef2c* promoter element (Wang, Valdez et al. 2001; Dodou, Xu et al. 2003).

To determine the expression pattern of Cre directed by the *mef2c* skeletal muscle promoter in more detail, we examined β -galactosidase activity in embryos and offspring from crosses of *mef2c*-73k-Cre with ROSA26R reporter mice (Fig. 2-3). β -galactosidase expression was evident by 9.0 dpc and X-gal staining could easily be detected in the somites by 9.5 dpc (Fig. 2-3a). β -galactosidase activity intensified until 11.5 dpc (Fig. 2-3b) and by 13.5 dpc, X-gal staining was obvious in every skeletal muscle in the embryo (Fig. 2-3c). β -galactosidase expression in neonatal mice could be observed robustly in every skeletal muscle in the animal and was not detected in any other tissues, even those of sclerotomal origin, including the bones of the limbs and ribs (Fig. 2-3d,e). Notably, β -galactosidase expression was never observed in the heart at any stage (Fig. 2-3f).

To define the activity of *mef2c* skeletal muscle promoter-directed Cre expression more precisely, transverse sections from Cre positive, ROSA26R transgenic embryos and neonatal muscles were examined by X-gal staining. Sections from transgenic embryos collected at

11.5 dpc showed expression in the myotomal component of the somites and in muscle cells in the limb buds (Fig. 2-4a). Expression was completely absent from all four chambers of the heart and from all of the smooth muscle in the embryo, including the smooth muscle cells in the trachea, esophagus and the vascular system. These results support the observation that the activity of this *mef2c* Cre transgene is completely restricted to skeletal muscle. By 13.5 dpc, *lacZ* expression marked all of the skeletal muscle fibers in the embryo, while nonmuscle tissues all remained unstained by X-gal (Fig. 2-4b). Similarly, sections of X-gal stained neonatal muscles showed that every muscle fiber in the animal was positive for β -galactosidase activity, including muscles of hypaxial (diaphragm) and epaxial (longissimus thoracis) origins (Fig. 2-4c, d).

To test directly the overlap of β -galactosidase activity in neonatal *mef2c-73k-Cre* Tg/0; ROSA26R Tg/+ mice, we compared the staining generated with an antibody against β -galactosidase to the staining of muscle cells by anti-skeletal muscle MyHC (MY-32) in transverse sections of neonatal limb muscles (Fig. 2-5). Anti-myosin stained every muscle fiber in the neonatal limb as expected (Fig. 2-5a), and anti- β -galactosidase also stained every muscle fiber in the animal, including those in the limb (Fig. 2-5b). Importantly, no nonmuscle cells were stained by the anti- β -galactosidase antibody, which was consistent with the X-gal staining results and indicated that Cre had not been expressed outside the skeletal muscle lineage (Fig. 2-5c). These results further demonstrate that *mef2c-73k-Cre* directs Cre expression throughout skeletal muscle during development and that expression is completely restricted to the skeletal muscle lineage.

The expression of Cre directed by the *mef2c* promoter was observed in both hypaxial and epaxial muscles and is not restricted to any specific fiber type. This is an important distinction from a previously described Cre transgenic line in which Cre expression directed from the *mlc* locus is restricted during development to fast fibers (Bothe, Haspel et al. 2000). In addition, the Cre transgene described here is active from very early in skeletal muscle development (Fig. 2-3). This is also in contrast to other previously described muscle Cre lines, which are activated later in skeletal muscle development than the *mef2c* promoter. Indeed, the *mck* and *mlc* promoters are direct transcriptional targets of MEF2 in skeletal muscle, indicating that they are activated after significant accumulation of MEF2 proteins in the myotome (Gossett, Kelvin et al. 1989; Amacher, Buskin et al. 1993; McGrew, Bogdanova et al. 1996; Rao, Donoghue et al. 1996; Ferrari, Molinari et al. 1997). By contrast, we have shown previously that the *mef2c* skeletal muscle promoter is activated directly by MyoD and other myogenic bHLH family members and is not subject to autoregulation by MEF2 factors (Dodou, Xu et al. 2003).

III. Analysis of MYO1565-Cre transgenic mice

In a similar strategy to that employed with the *mef2c* 73k enhancer, we generated transgenic mice that expressed Cre recombinase under control of the proximal promoter of the *myogenin* gene. The activity of the *myogenin* promoter (nucleotides -1565 to +17) is first detected at 8.5 dpc in the most rostral somites and is an early and critical target of specification factors in developing skeletal muscle (Ott, Bober et al. 1991; Edmondson,

Cheng et al. 1992; Edmondson, Lyons et al. 1994). This line might have an advantage over the *mef2c*-73k-Cre since the *myogenin* promoter is active approximately 0.25 days earlier in skeletal muscle development, but maintains highly restricted skeletal muscle activity. This suggested that it might serve as an additional and complementary tool to direct Cre expression exclusively to skeletal muscle. Therefore, we cloned the Cre cDNA under the control of the *myogenin* skeletal muscle promoter and used this construct, designated MYO1565-Cre, to generate transgenic mice (Fig. 2-6).

Three Cre transgene-positive founders were crossed to ROSA26R Cre-dependent *lacZ* reporter mice (Soriano 1999) and screened for β -galactosidase activity at 11.5 dpc. All of the three MYO1565-Cre lines induced recombination at the ROSA26 locus in skeletal muscle with additional superficial ectopic expression in the head (Fig. 2-7). To determine the expression pattern of Cre directed by the MYO1565 skeletal muscle promoter in more detail, we examined β -galactosidase activity in embryos and offspring from crosses of MYO1565-Cre with ROSA26R reporter mice (Fig. 2-8). β -galactosidase expression was evident by 9.0 dpc and X-gal staining was robust in the somites by 9.5 dpc, with the beginning of expression in migrating muscles (Fig. 2-8a). β -galactosidase activity intensified and continued throughout embryonic development (data not shown). In neonatal animals every skeletal muscle exhibited X-gal staining including those of the hindlimb (Fig. 2-8b) and diaphragm (Fig. 2-8c). The ectopic expression observed in the embryo contributed to staining in a few cells in the heart with no obvious pattern (Fig. 2-8d) and a distinct three-spot expression pattern in the hindbrain (Fig. 2-8e). We chose line 641A as the established MYO1565-Cre

UNIVERSITY OF CALIFORNIA

transgenic line, as this line had the highest ratio of skeletal muscle to ectopic expression (Fig. 2-7).

IV. Potential uses for skeletal muscle specific Cre transgenic mice

Several transcription factors have been implicated in skeletal muscle development, but play essential roles elsewhere in the embryo at early developmental times, making it difficult to determine the function of these genes in skeletal muscle using conventional targeting approaches. For example, the transcription factor GATA2, a member of the GATA family of zinc finger transcription factors, has been implicated strongly in postnatal skeletal muscle function (Musaro, McCullagh et al. 2001), but mice lacking *Gata2* exhibit embryonic lethality prior to 11.5 dpc due to hematopoietic defects (Tsai, Keller et al. 1994). Similarly, members of the MEF2 family of transcription factors play key roles in the differentiation of multiple cell types (Black and Olson 1998). Conventional targeted inactivation of the *mef2c* gene results in early embryonic lethality due to severe cardiovascular defects making it impossible to address the genetic function of *mef2c* in skeletal muscle (Lin, Srivastava et al. 1997; Lin, Lu et al. 1998; Bi, Drake et al. 1999). The *mef2c*-73k-Cre and MYO1565-Cre lines described here should be useful for early skeletal muscle-specific inactivation of these and other genes that are important in the heart or elsewhere during development.

V. Figure Legends

UNIVERSITY OF MICHIGAN LIBRARY

Figure 2-1. Schematic representation of the skeletal muscle specific Cre transgene construct, *mef2c-73k-Cre*. A 954 bp highly conserved promoter from the mouse *mef2c* gene, was cloned upstream of the Cre cDNA and a splice and polyadenylation sequence from SV40 and used to generate transgenic mice.

Figure 2-2. The *mef2c-73k-Cre* transgene directs skeletal muscle specific expression of Cre during embryogenesis. Three independent transgenic founder lines, 44K (a), 441G (b) and 453G (c) were crossed to ROSA26R Cre-dependent *lacZ* reporter mice and embryos were collected and X-gal stained at 11.5 dpc. Cre induced recombination in the hypaxial (hyp) and epaxial (ep) lineages, and also in the developing muscle of the face (arrowhead).

Figure 2-3. The *mef2c-73k-Cre* transgene directs Cre expression exclusively in skeletal muscle and is active from early in muscle development. Whole mount X-gal stained embryos resulting from crossing Cre-positive transgenic mice from line 441G to ROSA26R Cre-dependent *lacZ* reporter mice are shown at 9.5 dpc (a), 11.5 dpc (b), 13.5 dpc (c), exhibiting a strictly skeletal muscle specific pattern with no staining ever witnessed in the heart (hrt), or any other tissue. Tissues collected from neonatal mice also exhibit Cre dependent recombination exclusively in skeletal muscle, including the hindlimb (d) and intercostal muscles (e). No recombination was observed in the heart (f).

Figure 2-4. Cre expression from the *mef2c-73k-Cre* transgene is completely restricted to skeletal muscle and every muscle fiber exhibits Cre dependent recombination. Transverse

sections through the developing embryo at 11.5 dpc (a) and 13.5 dpc (b) show that β -galactosidase activity due to Cre dependent recombination in ROSA26R reporter mice, occurs in the myotome (myo), intercostals (ic) and body wall muscles (BW), but not in the smooth muscle of the trachea (Tr), esophagus (Es), or the vasculature. Expression was not observed in the cardiac muscle in the four chambers of the heart. Additionally, staining was not observed in the neural tube (NT), dorsal root ganglia (DRG) or sclerotome-derived tissue of the ribs (rib). Sections through neonatal muscles of hypaxial (c, diaphragm) and epaxial (d, longissimus thoracis) origins show Cre-induced recombination in every skeletal muscle fiber, indicating that the *mef2c-73k-Cre* transgene is expressed in every skeletal muscle progenitor population. Arrowhead marks the limb bud and the scale bar is equal to 100 μ m. RA, right atrium; RV, right ventricle; LA, left atrium; LV, left ventricle; da, dorsal aorta; cv, cardinal vein.

Figure 2-5. The *mef2c-73k-Cre* transgene expresses Cre in every skeletal muscle fiber. (a) The expression of myosin heavy chain (MyHC) in neonatal limb skeletal muscle was compared to the expression of the β -galactosidase (b). The merged image (c) shows that every MyHC-positive fiber is also positive for β -galactosidase protein produced from Cre-dependent recombination at the ROSA26R locus.

Figure 2-6. Schematic representation of the skeletal muscle specific Cre transgene construct, MYO1565-Cre. A 1565 bp highly conserved promoter from the mouse *myogenin* gene was cloned upstream of the Cre cDNA and a splice and polyadenylation sequence from SV40 and used to generate transgenic mice.

Figure 2-7. The MYO1565-Cre transgene directs mainly skeletal muscle specific expression of Cre during embryogenesis. Three independent transgenic founder lines, 641A (a), 220T (b) and 218T (c) were crossed to ROSA26R Cre-dependent *lacZ* reporter mice and embryos were collected and X-gal stained at 11.5 dpc. Cre induced recombination in the hypaxial (hyp) and epaxial (ep) lineages, and also in the developing muscle of the face (arrowhead).

Figure 2-8. The MYO1565-Cre transgene directs Cre expression in skeletal muscle and is active from early in muscle development. In addition, there is minimal ectopic expression in non-muscle tissues. Whole mount X-gal stained embryos resulting from crossing Cre-positive transgenic mice from line 641A to ROSA26R Cre-dependent *lacZ* reporter mice are shown at 9.5 dpc (a) exhibiting strong skeletal muscle specific staining. Tissues collected from neonatal mice also exhibit Cre dependent recombination strongly in skeletal muscle, including the hindlimb (b) and diaphragm (c). Minimal and sporadic recombination was observed in the heart (d). A reproducible pattern of expression was observed in the hindbrain (e).

AMNH
LIBRARY

Figure 2-1



Figure 2-2

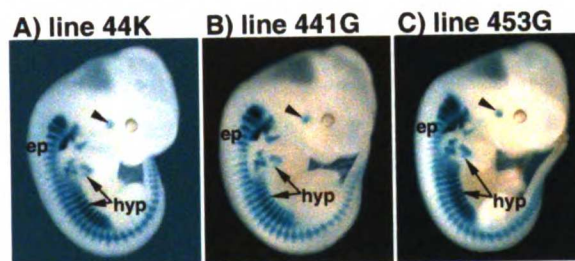


Figure 2-3

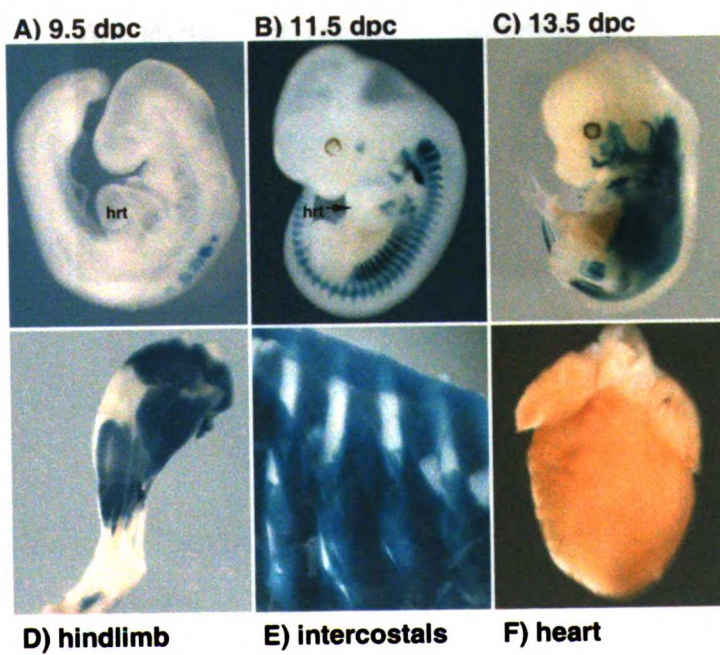


Figure 2-4

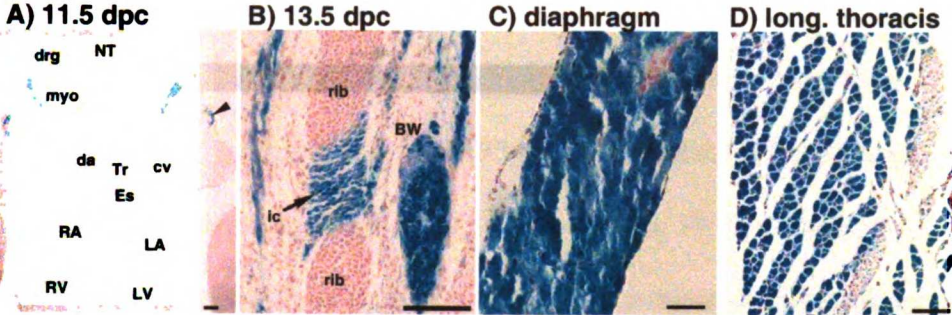


Figure 2-5

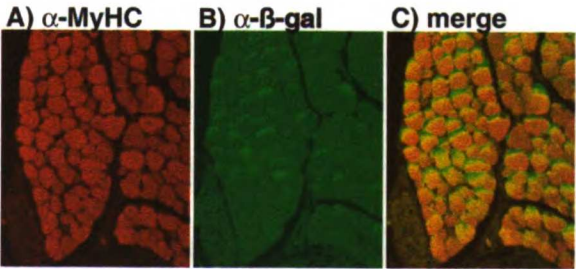


Figure 2-6



Figure 2-7

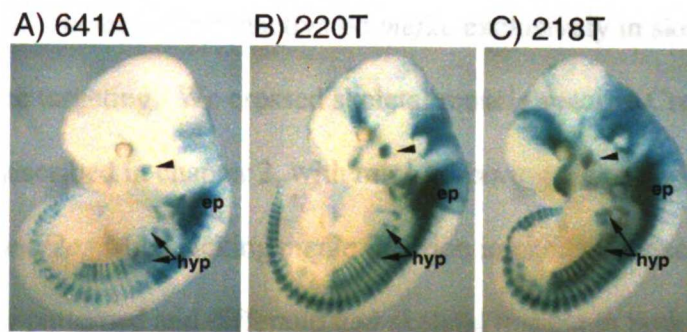
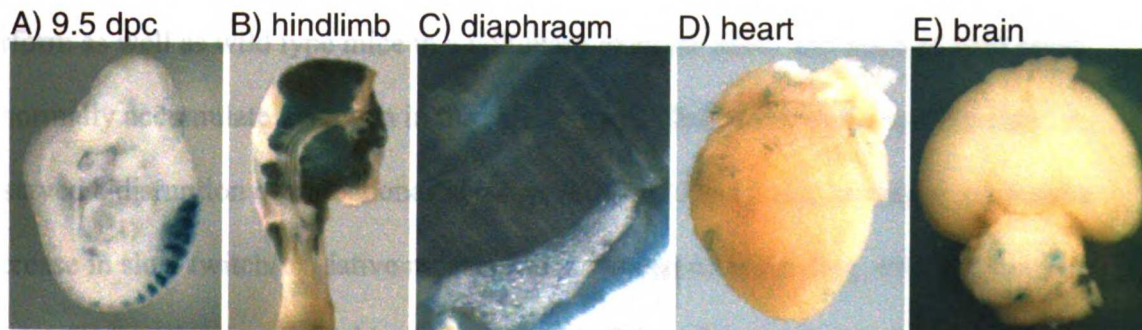


Figure 2-8



UCST LIBRARY

Chapter 3: Conditional inactivation of *mef2c* in skeletal muscle causes an overall decrease in body size and disruption of energy metabolism during exercise

I. Summary

Based on the critical role of MEF2 transcription factors in the development of myoblasts in culture and in *Drosophila*, we hypothesized that MEF2 would be a critical regulator of skeletal muscle differentiation in the mouse embryo (Lilly, Zhao et al. 1995; Ornatsky, Andreucci et al. 1997). The role of *mef2c* in skeletal muscle development and physiology has not been determined, as mice lacking *mef2c* die at midgestation (Lin, Lu et al. 1998; Bi, Drake et al. 1999). Therefore, we inactivated *mef2c* exclusively in skeletal muscle using conditional gene targeting. We crossed skeletal muscle specific Cre expressing transgenic mice, as described in chapter 2, with mice harboring a Cre-dependent conditional allele of *mef2c*. Mice lacking *mef2c* function in skeletal muscle are viable and develop normally patterned and differentiated skeletal muscle in both the hypaxial and epaxial lineages. However, these skeletal muscle knockout mice are smaller than their wild type littermates and this is not due solely to a decrease in skeletal muscle mass. Tibia length in adult mice is significantly reduced in conditional knockout mice indicating an overall decrease in body size. In addition, male knockout mice do not perform as well as wild type mice in a voluntary exercise assay and mice of both sexes abnormally accumulate glycogen in the soleus muscle following exercise. We also observed a disruption of mitochondrial morphology in conditional knockout mice and a decrease in slow twitch/oxidative muscle fibers. Based on these data, we hypothesize that *mef2c* function is required in skeletal muscle for, under situations of increased energy

demand, the proper relay of signals to the machinery that increases mitochondrial number and/or function.

II. Results

Mice lacking *mef2c* in skeletal muscle are viable, but are smaller than wild type littermates

The explicit role of *mef2c* in skeletal muscle has remained elusive, as embryos lacking *mef2c* die at midgestation with morphogenetic defects in the cardiovascular system (Lin, Schwarz et al. 1997; Bi, Drake et al. 1999). MEF2 family members have been implicated as important regulators of the differentiation of skeletal muscle both in cultured myoblasts and in *Drosophila* (Lilly, Zhao et al. 1995; Ornatsky, Andreucci et al. 1997). We generated skeletal muscle-specific Cre transgenic mice (Chapter 2) to utilize in combination with a Cre-dependent conditional allele of *mef2c* to inactivate *mef2c* in skeletal muscle (Vong, Ragusa et al. 2005). We generated three distinct Cre lines of varying timing of expression and intensity. Two lines 44K and 453G were derived from an injection of the *mef2c*-73k-Cre transgene, and 453G is the stronger of the two lines, as indicated by earlier expression of *lacZ* when crossed to ROSA26R reporter mice. A third line, 641A, was generated using the MYO1565-Cre transgene, which is expressed approximately 0.25 days earlier than *mef2c*-73k. As outlined in Figure 3-1, the crossing scheme to generate skeletal muscle-specific mice required crossing the skeletal muscle specific Cre lines into a heterozygous *mef2c* background (Cre Tg/0; *mef2c* +/-) (Lin, Schwarz et al. 1997). Male mice of this genotype were then crossed to female mice that

were homozygous for a conditional allele of *mef2c*, denoted by flox/flox. The result of these crosses was as expected for skeletal muscle specific knockout mice generated with either of the *mef2c*-73k-Cre transgenic lines at normal Mendelian frequencies (Fig. 3-2A, B). The number of litters generated using Line 641A is substantially fewer, and thus, the offspring do not yet exhibit Mendelian ratios (Fig. 3-2C, * $p < 0.05$). This deviation from the normal distribution is not solely due to a decrease in knockout offspring and therefore does not indicate that knockout mice exhibit any lethality. More litters are necessary to define the inheritance patterns with this line.

Mice lacking *mef2c* function in skeletal muscle did not exhibit any overt defects in patterning or differentiation. They were, however, smaller than wild type mice generated in the same litters. The degree and timing of significant size discrepancy varied with Cre line, but generally mice were noticeably smaller by weaning and continued to be smaller into adulthood (Fig. 3-3). Line 44K, the weakest of the lines used, male conditional knockouts were significantly smaller than wild type at 7 days post birth (Fig. 3-3A, P7), continuing until weaning at P21. Female conditional knockout mice generated with Line 44K did not exhibit a size discrepancy during early postnatal development (Fig. 3-3B), but tibia length at 8 weeks of age was significantly smaller for these animals (Fig. 3-3G). Skeletal muscle-specific *mef2c* knockout mice generated with Cre Line 453G exhibited slightly different patterns of body size in early development. Male mice were not significantly smaller until 14 days after birth (Fig. 3-3D, P14) and remained smaller at P28. Female conditional knockout mice generated with this stronger Cre line were also smaller than their wild type littermates between 10 days after birth (P10) and weaning at

P21 (Fig. 3-3E). It is unclear if these measured size differences are present at birth, as litter size has a dramatic effect on the size of both wild type and knockout mice at birth. The size differences become evident after mice have time to normalize from the effects of litter size and before the increase in body weight variability during early adulthood. In any case, tibia length of all knockout mice, regardless of line, is significantly smaller than wild type mice at 8 weeks of age, suggesting that growth is limited when *mef2c* is absent from skeletal muscle. Although we did not generate enough animals to achieve significant differences, conditional knockout mice generated with Line 641A were always at least 20% smaller than wild type-sex matched littermates (unpublished observation). It is critical to mention that the variability in the observed phenotypes may be due to the fact that all experiments were done on an outbred mouse background. Also, the nature of Cre dependent conditional alleles suggests that the recombination will not be complete and our conditional knockouts do not fully lack MEF2C function fully, but rather, harbor a hypomorphic allele. This is an especially important consideration in skeletal muscle, as the syncytial nature of the tissue allows one nucleus to compensate for another.

Having established the decrease in overall body size in mice lacking *mef2c* in skeletal muscle, we were interested in determining the degree to which a decrease in skeletal muscle contributed to this decrease. Gross analysis of neonate knockout mice did not indicate a substantial reduction in mass or alteration in the patterning of skeletal muscle (data not shown). We therefore analyzed individual muscle fibers, with the hypothesis that fiber number or area could be substantially altered in the absence of a gross change

in muscle appearance. Male knockout mice were generated using *mef2c-73k-Cre* line 453G, and the soleus muscle was dissected and sectioned to allow for staining with wheat germ agglutinin to visualize membranes. The number of individual fibers counted in a section across the entire soleus muscle did not indicate any difference between conditional knockout and wild type muscle (Fig. 3-4A). In addition, measurement of cross sectional area showed no significant decrease between conditional knockout mice and their wild type littermates (Fig. 3-4B). While there was no difference in fiber number, it is still a distinct possibility that an altered numbers of cells contribute to these fibers, and further studies are ongoing to determine if the number of nuclei in knockout fibers is altered.

Regulation of body size has long been known to be regulated by IGF-1 (Stewart and Rotwein 1996). Interestingly, IGF-1 is known to influence MEF2 activity by increasing the activity of the phosphatase calcineurin, which de-phosphorylates MEF2 and makes it a more potent activator (Michael, Wu et al. 2001; Musaro, McCullagh et al. 2001). In addition, calcineurin is known to dephosphorylate the NF-AT family of transcription factors, which are critical for regulating skeletal muscle hypertrophy (Musaro, McCullagh et al. 2001). Therefore, we determined if, in addition to the known interface between IGF-1 signaling and post-translational modifications of MEF2, activated NF-AT regulated the transcription of *mef2c*. We noted that the sequence of the *mef2c* 73k skeletal muscle specific enhancer has a conserved, consensus binding site for the NF-AT class of proteins (Fig. 3-5A), so we tested the ability of this site to bind NF-ATc1, the NF-AT isoform expressed in skeletal muscle by EMSA (Fig. 3-5B). Oligonucleotides

representing the NF-AT site in the *mef2c* 73k enhancer competed for binding to NF-ATc1 protein with the validated NF-AT site from the IL-4 gene (Fig. 3-5B, Lane 5). This binding was specific, as a mutant version of the oligonucleotide did not compete (Fig. 3-5B, Lane 6). In addition, the *mef2c* 73k NF-AT binding site was bound directly and specifically by NF-ATc1 (Fig. 3-5B, Lane 8-12). We are currently completing experiments designed to test the functional relevance of this binding site for *mef2c* expression during development, hypertrophy and muscle regeneration in transgenic mice.

***mef2c* is critical for normal energy metabolism in skeletal muscle**

Having established that skeletal muscle develops seemingly normally in mice with hypomorphic *mef2c*, we next tested the role of *mef2c* in regulating muscle function and metabolism. Skeletal muscle is a highly adaptive tissue, and in muscles that are subjected to repeated contraction, numerous changes occur to allow the muscle to produce energy for prolonged periods of excitation. These changes correlate with a particular fiber type, and type I/oxidative fibers are the most prominent in muscles that undergo endurance exercise (Fitts and Widrick 1996). These fibers have a higher number of mitochondria than type II fibers and utilize mainly oxidative metabolism (Howald 1982). Type II fibers (type IIA, B and X) are critical in muscles that undergo less frequent bursts of contraction and have a more glycolytic metabolism (Pette 2002). Fiber type switching, from type II to type I fibers following prolonged exercise, is known to be regulated by MEF2 family members (Chin, Olson et al. 1998; Wu, Naya et al. 2000). Therefore, we measured the percentage of type I muscle fibers in the soleus muscle of wild type and skeletal muscle specific *mef2c* knockout mice (Fig. 3-6). The soleus muscle is one of the

UNIVERSITY OF MICHIGAN LIBRARY

few muscles in mice with a large proportion of type I fibers (Rafael, Townsend et al. 2000; Stockdale, Nikovits et al. 2002). Staining sections of soleus muscle with MY32, an antibody that recognizes all fast type fibers, showed a significantly higher number of stained fibers in skeletal muscle knockout mice than in wild type littermates (Fig 3-6A). Quantitation of this staining pattern indicated that mice lacking *mef2c* in skeletal muscle have a significant decrease in the percentage of type I fibers in the soleus muscle: 24% compared to 33% in wild type soleus muscle (Fig3-6B).

Based on the decrease in slow twitch muscle fibers in *mef2c* skeletal muscle conditional knockout mice, we hypothesized that *mef2c* may be critical for performance in a voluntary exercise assay. Wild type and knockout mice generated with *mef2c-73k-Cre* were allowed access to a running wheel for 10 days. The duration and distance run by each mouse was recorded each morning for the final 7 days. Female conditional knockout mice did not exhibit a statistically significant decrease in any of the parameters measured (Fig. 3-7). Male knockout mice, however, showed a significant decrease in the distance run per 12 hour night (Fig. 3-7A, $p=0.02$). This decrease seems to be, at least in part, due to a decrease in the duration of running. The number of minutes run by male knockout mice (Fig. 3-7B) was not significantly reduced, but did show a trend toward reduction. These data support our hypothesis that a decrease in slow muscle fibers leads to mice that lack endurance, and therefore run for less time. It remains to be determined if time run will explain the entirety of the deficit in distance run, or if another component, such as speed, contributes to the deficit.

Running is a complicated behavior that requires multiple aspects of skeletal muscle structure and physiology to function properly for maximal performance. In order to determine whether a structural defect exists in mice lacking *mef2c* in skeletal muscle we analyzed cellular architecture of the soleus muscle post-exercise using electron microscopy (Fig. 3-8). Electron micrographs of post exercise muscle indicated two distinct phenotypes in conditional knockout mice. The first was an altered morphology of mitochondria, with a distended appearance and a disruption of the internal cristae structure (Fig. 3-8B). Wild type muscles processed in parallel did not exhibit this altered morphology (Fig. 3-8A), indicating that this disruption was not due to a fixation artifact. In addition, mitochondria in wild type muscle aligned directly between myofibrils, while knockout organization seemed disorganized, with less linear groupings of mitochondria. In addition to alterations in mitochondrial morphology, in some skeletal muscle specific knockout animals we also witnessed the presence of large vacuolar inclusion bodies in the soleus muscle (Fig. 3-9B). These vacuoles were scattered throughout the muscle and contained a granular material that was most consistent with glycogen deposits (Fig. 3-9B, black arrow). To determine the scale of these inclusion bodies more closely, we stained muscle sections with toluidine blue to analyze general histology (Fig. 3-9C,D). The inclusion bodies were readily visible by light microscopy (Fig. 3-9D, black arrowhead). To confirm our hypothesis that these vacuoles were filled with glycogen, we exercised additional mice and used periodic acid/Schiff's base (PAS) to stain frozen sections of the soleus muscle (Fig. 3-9B). 60% of post-exercise knockout mice had substantial accumulation of glycogen in the soleus muscle (Fig. 3-9F, black arrowhead), and these large, darkly staining regions were never seen in wild type muscle

(Fig. 3-9E). We hypothesized that this increase in glycogen content might be due to a decrease in the exercise induced glucose transporter GLUT4, a known MEF2 target (Holmes and Dohm 2004; Zorzano, Palacin et al. 2005). Mice lacking GLUT4 in skeletal muscle also show increases in glycogen storage due to multiple adaptations in the function of enzymes that are critical for the formation of glycogen (Stenbit, Tsao et al. 1997; Kim, Peroni et al. 2005). The levels of *Glut4* transcript, however, were not decreased in *mef2c* skeletal muscle specific knockout mice, as measured by RT-PCR (data not shown).

We next undertook an informatic approach to identify conserved MEF2 binding sites near genes that are critical for glucose metabolism. We identified a conserved consensus MEF2 binding site 4 kb upstream of the promoter region of *muscle glycogen phosphorylase (PYGM)*, Fig. 3-10A), which is the enzyme that is critical for breakdown of glycogen back into utilizable glucose units (Sato, Imai et al. 1977; Sengers, Stadhouders et al. 1980). This sequence was capable of competing for MEF2C binding to the established MEF2 binding site from the *myogenin* gene (Fig. 3-10B, Lane 5). This was a specific interaction, as a mutant version of the oligonucleotide was not able to compete for MEF2C binding (Fig. 3-10B, Lane 6). The affinity of the binding site was slightly weaker than that of the established MEF2 binding site from the *Glut4* gene, as the *Glut4* site is able to compete fully with the MEF2 site from *myogenin* for binding (Fig. 3-10B, Lane 7). The MEF2 binding site from *PYGM* was also bound directly by MEF2C protein (Fig. 3-10B, Lane 11) and this interaction was also specific as competition with a wild type oligonucleotide representing the MEF2 binding site from the *myogenin* gene

UNIVERSITY OF TORONTO

could compete for binding (Fig. 3-10B, Lane 12), while a mutant version of this oligonucleotide could not (Fig. 3-10B, Lane 13). We are currently investigating the levels of numerous glycogen regulatory genes, including *PYGM*, in skeletal muscle specific knockouts of *mef2c*. We are using both candidate and unbiased microarray approaches to identify dysregulated genes.

Having established that mice lacking MEF2C in skeletal muscle exhibit numerous phenotypes that suggest an inability to regulate energy metabolism properly, we sought to identify the signals that impinge on MEF2C to allow a cell to adapt to an increased need for energy. Recent work has shown that a critical regulator of cellular metabolism in skeletal muscle is AMP activated protein kinase (Rutter, Da Silva Xavier et al. 2003). AMP kinase is phosphorylated by AMP kinase kinase when intracellular levels of AMP are increased as compared to ATP levels, signaling the need to produce more energy in the cell. Currently, we are completing experiments to test if MEF2C transcriptional activity is upregulated by AMP kinase through the p38 signaling cascade. In addition, we wanted to test the hypothesis that MEF2 might upregulate transcription of the gene encoding AMP kinase (*PRKKA2*) in a positive feedback loop. We identified a region of high conservation between the first and second exons of *PRKKA2* that was conserved not only between mouse and human, but also with the opossum, a marsupial mammal (Fig. 3-11A). Two perfectly consensus MEF2 binding sites were identified in this conserved region (Fig. 3-11A, expanded sequence). We tested the ability of these sites to bind MEF2C *in vitro* (Fig. 3-11B, kindly provided by Courtney Brown). Oligonucleotides representing the mouse sequence of the MEF2 sites and flanking

regions of MEF2 sites 1 and 2 from the *PRKKA2* first intron were both able to compete with the validated MEF2 binding site from the myogenin gene for binding to MEF2C (Fig. 3-11B, Lanes 5, 7). This binding was specific, as mutant versions of the oligonucleotides did not compete for MEF2C (Fig. 3-11B, Lanes 6, 8). In addition, these binding sites were bound directly by MEF2C *in vitro* (Fig. 3-11B, Lanes 10, 16). The ability of MEF2C to activate transcription of the catalytic subunit of AMP kinase through binding to these sites is currently being investigated. If these sites are indeed bound and activated by MEF2C, these data would be consistent with our model of MEF2C as a critical component in the regulation of energy metabolism and the adaptation of skeletal muscle to increased energy demand.

III. Discussion

The MEF2 family of transcription factors is known to play a critical role in the differentiation of numerous tissues including skeletal muscle (Black and Olson 1998). Numerous skeletal muscle genes, including structural and metabolic factors have been shown to be targets of MEF2 (Amacher, Buskin et al. 1993; Ferrari, Molinari et al. 1997; Puigserver 2005). In the current study, we set out to determine the role of *mef2c* in developing mammalian skeletal muscle. The requirement for *mef2c* in skeletal muscle development and function has not been identified previously, as mice lacking MEF2C die at midgestation with severe cardiovascular morphogenetic defects before significant development of skeletal muscle (Lin, Schwarz et al. 1997; Bi, Drake et al. 1999). Using

UNIVERSITY OF MICHIGAN LIBRARY

a conditional inactivation approach, we generated mice lacking MEF2C in skeletal muscle at normal Mendelian frequencies (Fig. 3-2). Although viable, these conditional knockout mice were smaller than wild type littermates (Fig. 3-3). In addition, we identified a disruption of mitochondrial morphology in the soleus muscle following exercise, suggesting that MEF2C is critical for establishment of the proper machinery for energy metabolism. Inefficient energy utilization was also manifested in the soleus muscle as an over accumulation of glycogen following exercise (Fig. 3-9). These data suggest that the lack of MEF2C in skeletal muscle causes an overall decrease in body size and an upregulation of glycogen storage in muscle as a compensatory mechanism under conditions of stress.

A disruption of mitochondrial function is not altogether surprising in the absence of a MEF2 transcription factor. MEF2 sites in the PGC-1 α promoter are known to be required for upregulation in response to exercise and PGC-1 α function is critical for mitochondrial biogenesis (Wu, Puigserver et al. 1999; Czubryt, McAnally et al. 2003). This decreased function is exacerbated since, in addition to being activated by MEF2, PGC-1 α is also a co-activator protein for MEF2 proteins (Handschin, Rhee et al. 2003). Mitochondrial biogenesis is a critical step in the postnatal switch from fast to slow muscle fibers. The decrease in fiber type switching in mice lacking MEF2C function in skeletal muscle suggests that PGC-1 α function may be disrupted; however, further studies are necessary to determine the levels of PGC-1 α both before and after exercise. Interestingly, we have often observed a degeneration of normal muscle architecture in skeletal muscle lacking MEF2C following exercise. This phenotype is strikingly similar

UNIVERSITY OF TORONTO

response in skeletal muscle that is not generating sufficient energy. The latter hypothesis is supported by a similar phenotype seen in *Glut4* skeletal muscle conditional knockout mice. These mice lack the insulin responsive glucose transporter and upregulate glycogen synthase activity to compensate for the decreased influx of glucose into muscle (Zisman, Peroni et al. 2000). An additional, but not mutually exclusive hypothesis, predicts that MEF2C may directly regulate genes necessary for proper glucose import and glycogen storage; indeed, the *Glut4* gene is known to be a target of the MEF2 family of transcription factors (Thai, Guruswamy et al. 1998).

It is still an open question as to which particular signaling pathways are responsible for the upregulation of MEF2C in response to increased energy demand. Recent work on skeletal muscle metabolism suggests that AMP activated protein kinase (AMP kinase) is a critical sensor of cellular AMP levels, and functions when AMP levels are high to turn on pathways that increase cellular ATP. There is evidence that AMP kinase activity leads to increased MEF2 DNA binding and transcriptional activation activities, although it is unclear if this through direct phosphorylation (Al-Khalili, Chibalin et al. 2004; Holmes, Sparling et al. 2005). We are currently testing the hypothesis that AMP kinase may activate MEF2 indirectly through the p38 MAP kinase pathway, an established modulator of MEF2 activity (Al-Khalili, Chibalin et al. 2004). Our model predicts that the combination of direct or indirect regulation by AMP kinase and the known upregulation of MEF2 activity by the phosphatase calcineurin in response to increased intracellular calcium levels position MEF2C as a critical regulator of energy metabolism in skeletal muscle (Fig. 3-12).

It is unclear to what degree the phenotype observed in mice lacking MEF2C in skeletal muscle is due to defects in development that are manifested in the adult as a metabolic disorder. MEF2C certainly functions in postnatal muscle, as switching from fast to slow fiber type is exclusively a postnatal event. We have not ruled out, however, that a basic defect in sarcomere integrity does not also contribute to the defects seen in conditional knockout mice due to inefficient force generation. In addition, it is interesting that the small body size phenotype is more severe in mice that are generated using MYO1565-Cre, which is expressed approximately 0.25 days earlier than *mef2c*-73k-Cre. The difference between these mice could be due to a requirement for MEF2C early in muscle development, or to increasing the percentage of life span that energy metabolism is dysregulated. Skeletal muscle development in embryos lacking *mef2c* in skeletal muscle develops with seemingly normal timing and patterns. No delay in the migration of muscle cells or expression of differentiation markers was observed at knockout embryos (data not shown). We are currently investigating the requirement for MEF2 proteins in skeletal muscle development by generating a conditional skeletal muscle knockout of *mef2c* in the background of a *mef2a* knockout. Mice with a targeted mutation of MEF2A die soon after birth due to the development of dilated cardiomyopathy, but have ostensibly normal skeletal muscle at this time (Naya, Black et al. 2002). The goal of generating the double knockout in skeletal muscle is to determine more closely the requirement for overall MEF2 function in developing skeletal muscle.

UNAT LIBRARY

The work herein supports the notion that MEF2 family members are necessary for the precise and highly coordinated regulation of genes necessary for many processes in the development of normal skeletal muscle. We hypothesize that MEF2C specifically regulates genes necessary for the function of mitochondria in skeletal muscle during and after exercise. A decrease in slow twitch fibers, increased glycogen storage and a decrease in overall body size are all consistent with the notion that mice lacking MEF2C in skeletal muscle use energy less efficiently than wild type mice. Examples such as this, of mutations in developmentally important transcription factors that lead to the disruption of normal physiology in the adult, may contribute to our understanding of the underlying mechanism of metabolic disorders.

IV. Figure Legends

Figure 3-1. Schematic representation of the crosses used to generate skeletal muscle specific knockout mice. Skeletal muscle-Cre refers to transgenic mice generated using the skeletal muscle specific enhancer from the *mef2c* or *myogenin* gene, as described in Chapter 2. *mef2c* +/- mice harbored one (-) allele of a targeted mutation of *mef2c* (TM1). Male *mef2c* heterozygous mice that were positive for a Cre transgene were crossed to female mice homozygous for the conditional allele of *mef2c* (flox/flox) to generate offspring, of which 25% will have conditionally inactivated *mef2c* in skeletal muscle. The Cre transgene was always introduced as a paternal allele, as there was a possibility of

NOT FOR PUBLICATION

maternal contribution of Cre recombinase to the oocyte or early embryo (unpublished observation).

Figure 3-2. Mice lacking *mef2c* in skeletal muscle are viable. These tables represent all mice generated using three independent Cre lines. Line 44K and Line 453G are two independent insertions events of the *mef2c*-73k-Cre, while Line 641A expresses Cre recombinase under control of the MYO1565 promoter. Alleles in the populations of mice from both *mef2c*-73k-Cre mice follow a Mendelian pattern of inheritance and skeletal muscle knockout mice represent $\frac{1}{4}$ of all offspring ($p>0.1$). Line 641A appears to deviate from Mendelian patterns of inheritance ($p<0.05$), but this pattern may return to expected Mendelian ratios with an increase in the number of litters pooled to generate this table. In any case, the altered pattern is not solely due to a decrease in conditional knockout mice, as heterozygous mice with Cre are also underrepresented.

Figure 3-3. *mef2c* in skeletal muscle is required for normal overall body growth. Mice lacking *mef2c* in skeletal muscle and their wild type littermates were weighed over the first four weeks after birth. A) Time course of male mice generated from line 44K (*mef2c*-73k-Cre). The numbers preceded by the letter P represent days post birth, with P1 starting the evening of the day of birth. Dark blue diamonds represent the average body weight of wild type male mice on a given day with standard deviation given as the black error bars. The light blue triangles represent the average body weight of skeletal muscle specific conditional *mef2c* knockout mice, with standard deviation given as the gray error bars. ** $p<0.008$. B) Time course of female mice generated from line 44K (*mef2c*-73k-

Cre). Averages of the body weight of wild type female mice are represented by purple diamonds, with the standard deviation represented by black error bars. Skeletal muscle specific *mef2c* knockout mice body weight averages are represented by pink triangles, with gray error bars indicating the standard deviation. C) p values representing the degree of statistical difference between knockout and wild type mice resulting from crosses generated using line 44K, as calculated using a t-test assuming equal variance. Variance was compared between both populations and this test was deemed appropriate (data not shown). D,E,F) Data is similar to those shown in A,B and C, however the transgenic Cre line used to generate the skeletal muscle specific knockout mice was line 453G (*mef2c*-73k-Cre). * p<0.02, **p<0.008. G) Table showing the number of animals averaged to generate the data seen in A-F. H) The tibia length of *mef2c* skeletal muscle specific knockout mice was measured at 8 weeks of age. Both male and female mice have statistically shorter tibia lengths, indicating smaller overall body size. The data are combined for lines 44K and 453G, as there was no statistical difference between mice generated with these lines (data not shown). ***p<0.0002.

Figure 3-4. Characterization of the muscle fibers in mice lacking *mef2c* in skeletal muscle. Mice used in this experiment were skeletal muscle specific knockouts generated with *mef2c*-73k-Cre line 453G and wild type littermates. All mice analyzed were male. The soleus muscle was sectioned and stained with wheat germ agglutinin conjugated to TRITC for membrane visualization. Sections were photographed for counting of the total number of fibers (A) and measurement of fiber area (B). There was no significant decrease in either fiber number or area in mice lacking *mef2c* in skeletal muscle.

Figure 3-5. (A) *mef2c-73k* is conserved between the mouse and human genomes. Depicted is an alignment of the 400 proximal nucleotides of the skeletal muscle promoter from the mouse and human genomes. The transcriptional start site is indicated with an arrowhead. The binding site for the MRF family of proteins, E2, has previously been shown to be a critical element for skeletal muscle specific expression of this fragment (Wang, Valdez et al. 2001; Dodou, Xu et al. 2003). The putative NF-AT binding site is outlined by a black box. (B) The Rel DNA binding domain of NF-ATc1 was used in EMSA analyses with double-stranded oligonucleotides representing the validated NF-ATc1 binding site from the IL-4 gene and the putative NF-ATc1 binding site from the *mef2c-73k* skeletal muscle enhancer. NF-ATc1 bound directly to the site from IL-4 (Lane 2) in a specific manner, as an unlabeled oligonucleotide representing the IL-4 binding site competed for binding (Lane 3), while a mutant version of this oligonucleotide did not (Lane 4). An unlabeled oligonucleotide representing the NF-ATc1 binding site from *mef2c-73k* was also able to compete for binding to NF-ATc1 (Lane 5), and this was specific, as a mutant version of this oligonucleotide did not compete (Lane 6). Radiolabeled oligonucleotides representing the *mef2c-73k* NF-ATc1 binding site were also bound directly by NF-ATc1 protein (Lane 8). This binding was specific as unlabeled oligonucleotides representing the NF-ATc1 site from IL-4 (Lane 9) or *mef2c-73k* (Lane 11) competed for binding, while mutant versions of these oligonucleotides did not (Lanes 10 and 12). Lanes 1 and 8 did not contain recombinant protein; however, a comparable amount of reticulocyte lysate was included, represented by a minus sign.

Figure 3-6. Mice lacking *mef2c* in skeletal muscle have a decrease in type I fibers. The soleus muscle was sectioned and stained with MY-32, an antibody that recognizes all fast type myosin isoforms. Non-staining fibers indicate a slow-twitch, type I myosin expressing fiber. The muscles pictured are from male mice generated from a cross that included *mef2c-73k-Cre* from line 453G, A) WT, B) Conditional knockout. C) Quantitation of the number of non-staining fibers, as shown in panels A and B, indicates that mice lacking *mef2c* in skeletal muscle have a 10% reduction in type I fibers in the soleus muscle. These data are pooled from both line 44K and like 453G, as there was no statistical difference between the knockouts generated with these two lines (data not shown). *** $p < 0.00002$

Figure 3-7. Male mice lacking *mef2c* in skeletal muscle run less in a voluntary exercise assay. Skeletal muscle specific *mef2c* knockout mice were allowed access to a running wheel continuously for 10 days. Each gray diamond represents the average value of distance run in (kilometers, A), time run (min, B) or speed (km/min, C) for a single mouse during the final 7 days of the recording period. Averages are indicated by a dash, with the statistical difference between groups indicated next to the average for the knockout group. p values were calculated using a t-test assuming equal variance, and significant differences to a 95% confidence interval are indicated by an asterik. Conditional knockout data represent mice from both groups, line 44K and line 453G, as no significant differences were found in any variable between these groups (data not shown).

Figure 3-8. *mef2c* is critical for maintaining normal mitochondrial morphology during exercise. Female mice lacking *mef2c* in skeletal muscle (line 453G) and wild type littermates were subjected to a voluntary running assay (See figure 3-7). Following 10 days of exercise, the soleus muscle was harvested and processed for electron microscopy. A) A wild type mouse exhibited normal muscle morphology following exercise with a repeating sarcomeric pattern and mitochondria lining up between myofibrils (white arrowhead). B) The knockout mouse exhibited alterations in mitochondrial morphology after exercise. The white arrowhead indicates mitochondria that are distended and have disrupted cristae.

Figure 3-9. Mice lacking *mef2c* develop glycogen deposits in the soleus muscle following exercise. Female mice lacking *mef2c* in skeletal muscle (line 453G) and wild type littermates were subjected to a voluntary running assay (See figure 3-7). Following 10 days of exercise, the soleus muscle was harvested and processed for electron microscopy. A) A wild type mouse exhibited normal muscle morphology following exercise with a repeating sarcomeric pattern and mitochondria lining up between myofibrils (white arrowhead). B) The knockout mouse exhibited large, granular inclusion bodies interrupting the sarcomeric pattern (black arrow). The morphology of these vacuolar bodies is most consistent with glycogen deposits. C,D) Toluidine blue stain for general histology of 1 μ m sections of post exercise soleus muscle. These muscles were harvested post exercise from female mice (line 453G) and treated with the same fixation protocol as for electron microscopy. The black arrowhead indicates large inclusion bodies that are believed to be glycogen. The black arrow indicates a centrally

located nucleus, another common feature of skeletal muscle that lacks *mef2c*. E,F) PAS stain for glycogen on sections of the soleus muscle post exercise. Male mice (line 453G) underwent a voluntary exercise assay for 10 days prior to harvesting muscle for PAS staining. The black arrowhead indicates large deposits of glycogen in the knockout muscle. Centrally located nuclei are also present in this muscle (black arrow) and this stain also allows visualization of hypertrophied endomysial connective tissue (asterisk).

Figure 3-10. A conserved non-coding sequence near the PYGM gene, which encodes the muscle isoform of glycogen phosphorylase, contains a conserved MEF2 binding site. (A) VISTA plot showing a schematic of the sequence upstream of the PYGM gene that is conserved between the mouse and human genomes. This plot was generated using the whole genome alignments on the website of Lawrence Berkeley National Laboratories (<http://genome.lbl.gov/VISTA>). All peaks represent a region of the genome that is conserved at greater than 70% between mouse and human. Blue shaded peaks represent annotated exon sequences, light green represents annotated UTR sequences and pink peaks are conserved non-coding sequences. The line drawn above the plot designated PYGM represents the genomic region for that gene, with the arrow indicating the orientation. The peak in the lower right of the plot is expanded to allow for sequence analysis. The top row of sequence represents the PYGM genomic region in the human genome, compared to the mouse genome on the bottom line. A box is drawn around a conserved and consensus MEF2 binding site (YTAWWWWTAR). (B) MEF2C was used in EMSA analyses with double-stranded oligonucleotides representing the validated MEF2 binding site from the *myogenin* gene and the putative MEF2 site from the mouse

PYGM gene. MEF2C is bound directly to the site from *myogenin* (Lane 2) in a specific manner, as an unlabeled oligonucleotide representing the *myogenin* binding site competed for binding (Lane 3), while a mutant version of this oligonucleotide did not (Lane 4). An unlabeled oligonucleotide representing the MEF2 binding site from PYGM also competed for binding to MEF2C (Lane 5), and this was specific, as a mutant version of this oligonucleotide did not compete (Lane 6). The conditions of the EMSA were also validated using competition with an unlabeled oligonucleotide representing the MEF2 binding site from the GLUT4 gene. A wild type version of this binding site competed for binding to MEF2C (Lane 7), while a mutant version did not (Lane 8). Radiolabeled oligonucleotides representing the PYGM MEF2 binding site were bound directly by MEF2C (Lane 11). This binding was specific as unlabeled oligonucleotides representing the MEF2 site from *myogenin* (Lane 12) or PYGM (Lane 14) competed for binding, while mutant versions of these oligonucleotides did not (Lanes 13 and 15). Lanes 1 and 10 do not contain recombinant protein, however, a comparable amount of reticulocyte lysate was included, represented by a minus sign; lysate-derived non-specific mobility shifts are present where indicated. Lane 9 does not contain lysate or radiolabeled probe.

Figure 3-11. A conserved non-coding sequence in the first intron of the gene encoding the alpha 2 catalytic subunit of AMP activated protein kinase (PRKKAA2) contains two MEF2 binding sites conserved in the mouse and opossum genomes. (A) VISTA plot showing a schematic of the sequence of the PRKKAA2 gene that is conserved between the mouse and human genomes (top comparison) and the mouse and opossum genomes (bottom comparison). This plot was generated as in Fig. 3-10, again with peaks

representing a region of the genome that is conserved at greater than 70% between species. The line drawn above the plot designated PRKKAA2 delineates the genomic region for that gene, with the arrow indicating the orientation. The peak circled in the lower comparison indicates the extent of the intronic sequence that is conserved to opossum. The mouse:human comparison that is comparable to the region conserved in opossum is expanded for sequence analysis visualization. The top row of sequence represents the PRKKAA2 intronic region in the human genome, compared to the mouse genome on the bottom line. A box is drawn around both conserved and consensus MEF2 binding sites (YTAWWWTAR). (B) MEF2C was used in EMSA analyses with double-stranded oligonucleotides representing the validated MEF2 binding site from the *myogenin* gene and the putative MEF2 sites from the mouse PRKKAA2 gene; these data were kindly provided by Courtney Brown. MEF2C bound directly to the site from *myogenin* (Lane 2) in a specific manner, as an unlabeled oligonucleotide representing the *myogenin* binding site competed for binding (Lane 3, M), while a mutant version of this oligonucleotide did not (Lane 4, mM). An unlabeled oligonucleotide representing the first MEF2 binding site from PRKKAA2 also competed for binding to MEF2C (Lane 5, 1), and this was specific, as a mutant version of this oligonucleotide did not compete (Lane 6, m1). The second site from the PRKKAA2 gene also competed for binding to MEF2C in a specific manner. A wild type version of the AMPK2 binding site competed for binding to MEF2C (Lane 7, 2), while a mutant version did not (Lane 8, m2). A radiolabeled oligonucleotide representing the first PRKKAA2 MEF2 binding site (AMPK1) was bound directly by MEF2C (Lane 10). This binding was specific as unlabeled oligonucleotides representing the MEF2 site from *myogenin* (Lane 11, M) or

AMPK1 itself (Lane 13, 1) competed for binding, while mutant versions of these oligonucleotides did not (Lanes 12, mM and 14, m1). Similarly, a radiolabeled oligonucleotide representing the second PRKKAA2 MEF2 binding site (AMPK2) was bound directly by MEF2C (Lane 16). This binding was specific as unlabeled oligonucleotides representing the MEF2 site from *myogenin* (Lane 17, M) or AMPK2 itself (Lane 19, 2) competed for binding, while mutant versions of these oligonucleotides did not (Lanes 18, mM and 20, m2). Lanes 1, 9 and 15 do not contain recombinant protein, however, an identical amount of un-programmed reticulocyte lysate was included, represented by a minus sign; lysate-derived non-specific mobility shifts are present where indicated.

Figure 3-12. A model of MEF2C as a central regulator of energy metabolism and mitochondrial biogenesis. MEF2C is known to upregulate transcription of PGC-1 α and GLUT4, both critical genes in regulating glucose uptake and energy generation. We hypothesize that signals of decreasing energy, such as increased AMP or increased intracellular calcium, signal for upregulation of MEF2C activity as a critical step in the pathway for increasing intracellular ATP.

11/11/11 10:11 AM

Figure 3-1

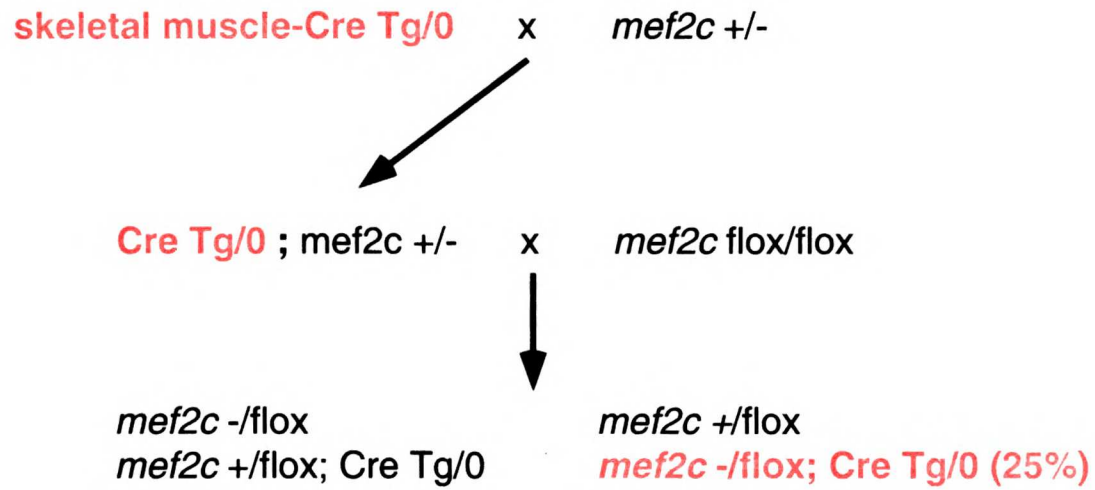
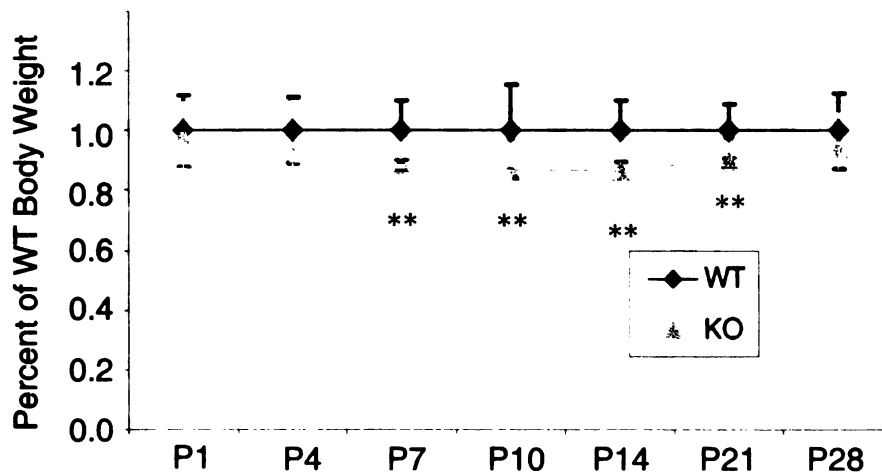


Figure 3-2

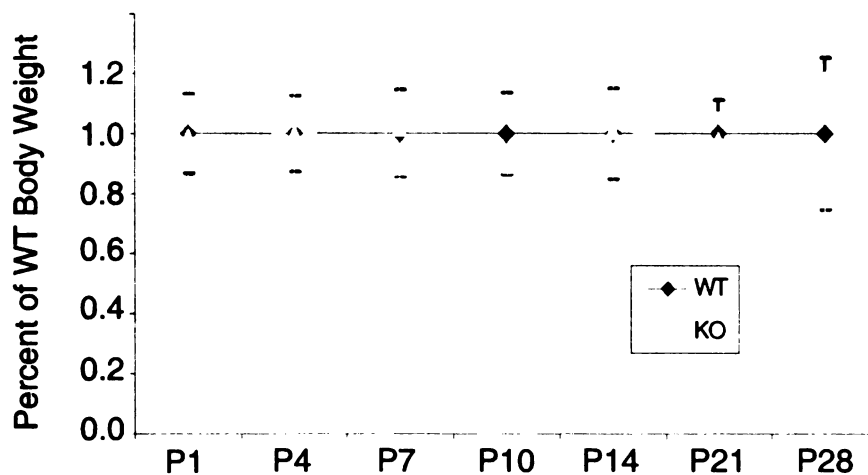
A) Line 44K			B) Line 453G			C) Line 641A		
	Cre	+		Cre	+		Cre	+
Flox/+	37	44	Flox/+	53	43	Flox/+	6	18
Flox/Tm	32	30	Flox/Tm	33	47	Flox/Tm	9	24
	p>0.1			p>0.1			p<0.05*	

Figure 3-3

A) Line 44K males



B) Line 44K females

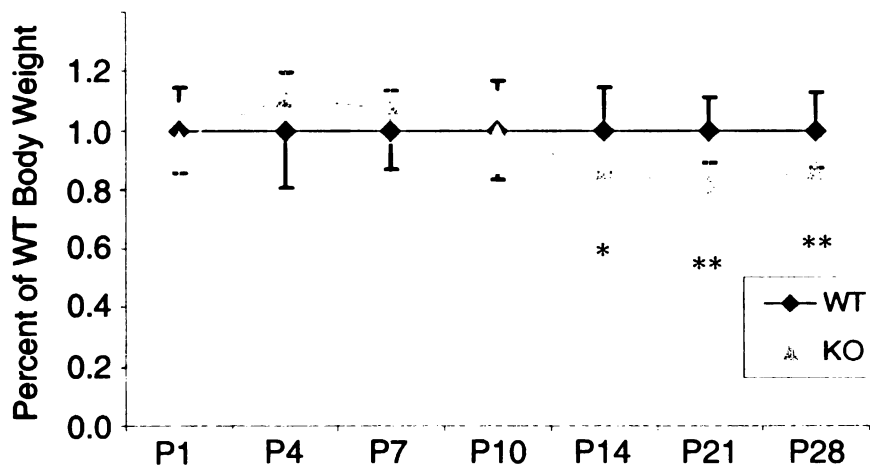


C)

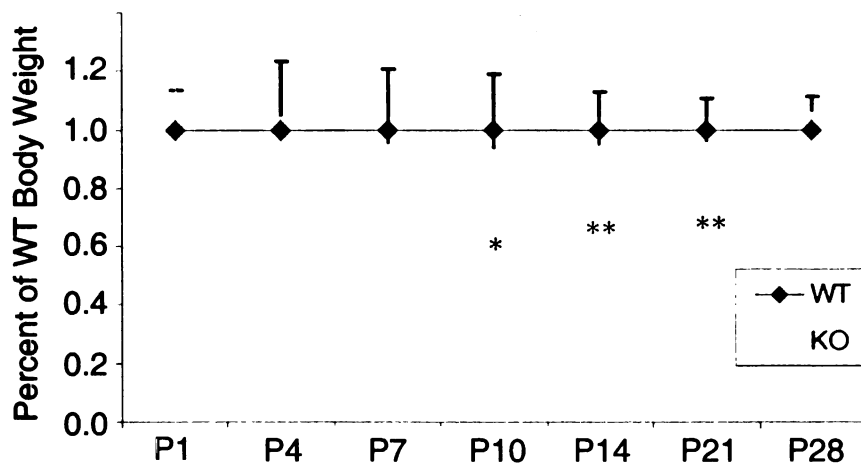
44K WT vs. KO	F	M
P1	0.84	0.66
P4	0.98	0.17
P7	0.77	0.0077
P10	0.32	0.0039
P14	0.87	0.0035
P21	0.65	0.0069
P28	0.15	0.18

Figure 3-3 (cont.)

D) Line 453G males



E) Line 453G females



F)

453G WT vs. KO	F	M
P1	0.23	0.49
P4	0.26	0.14
P7	0.054	0.22
P10	0.015	0.93
P14	0.007	0.014
P21	0.006	0.0014
P28	0.105	0.007

Figure 3-3 (cont.)

G) Number of animals for body weight data

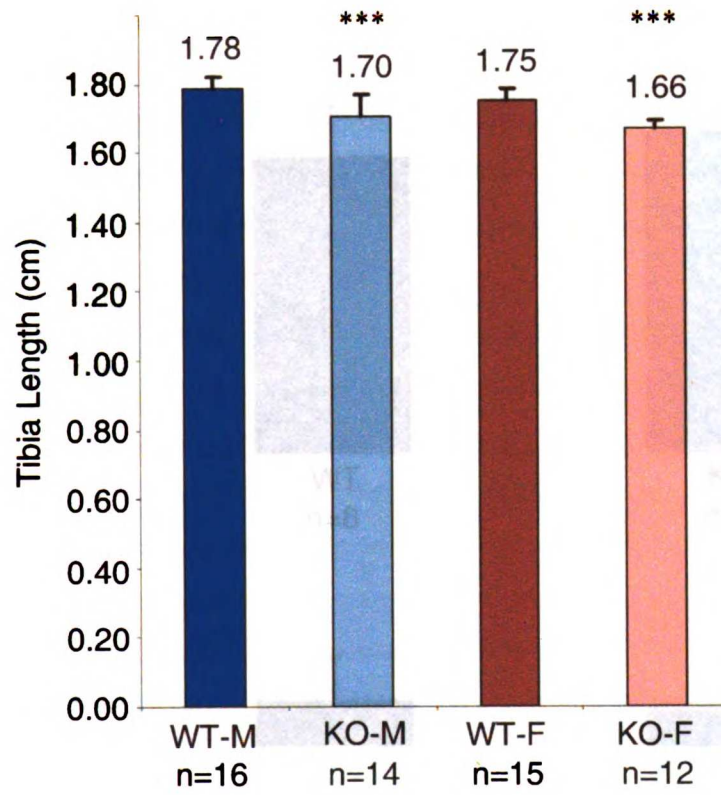
44K	P1	P4	P7	P10	P14	P21	P28
WT	16	13	12	14	16	14	15
KO	11	7	9	10	8	10	12
WT	22	15	15	19	16	16	16
KO	18	14	13	18	17	11	15

453G	P1	P4	P7	P10	P14	P21	P28
WT	16	13	10	12	13	14	16
KO	11	7	5	9	9	8	14
WT	19	15	13	18	18	17	19
KO	18	10	8	13	16	18	18

bioRxiv preprint doi: <https://doi.org/10.1101/201707>; this version posted July 11, 2017. The copyright holder for this preprint (which was not certified by peer review) is the author/funder, who has granted bioRxiv a license to display the preprint in perpetuity. It is made available under aCC-BY-NC-ND 4.0 International license.

Figure 3-3 (cont.)

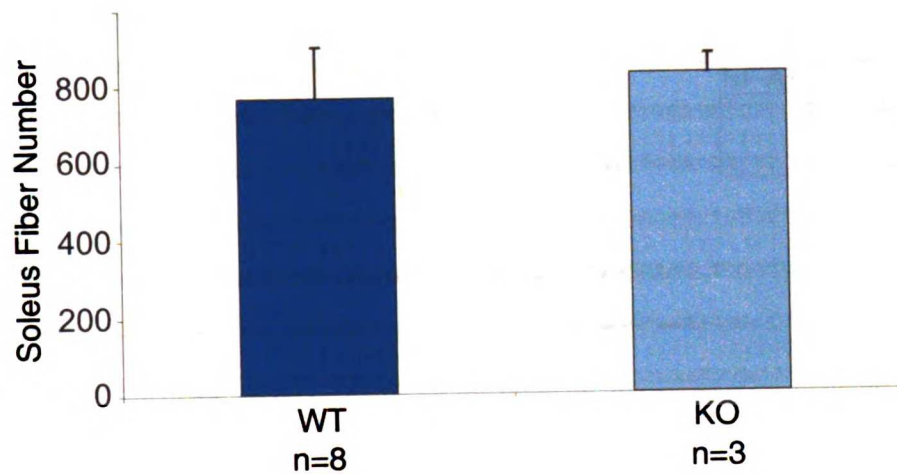
H)



11/17/17 10:00

Figure 3-4

A)



B)

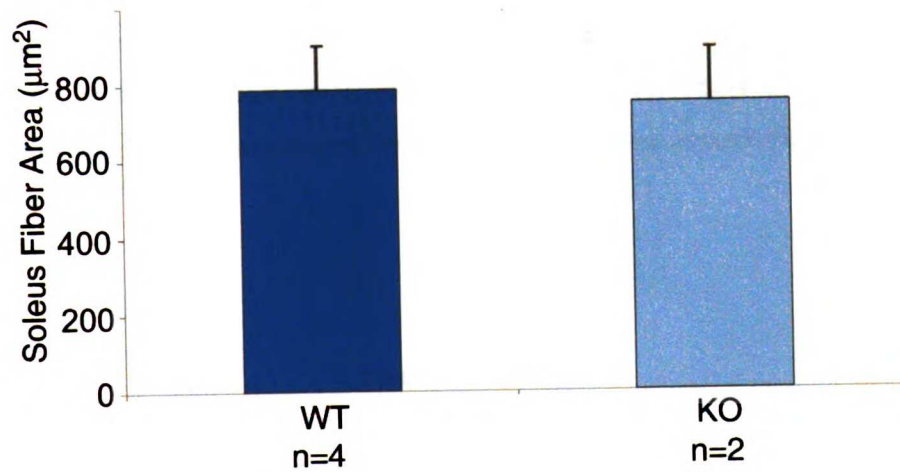


Figure 3-5

A) Sequence of the 73k-mef2c skeletal muscle enhancer

mouse GTAATTTTAAAGCCTG-TGTGAAATGAGGAACTTAACTTTTT-ATACCATATGAAAGCA
 |||||
human GTAATTTTAAATCTGCT-TGAAATGAGGAACTTA-CTTTTTTATACCATATGAAAGCA
 |||||
mouse ATTCATTTTTTAGGAATGATTTT-GGATAGACTTCCGATTGGATA|TTTTCCATTGGAAC
 |||||
human ATTCATTTTTTAGGAATGATTTTGGATAGACTTCCGATTGGATA|TTTTCCATTGGAAC
 |||||
mouse TAACAGTGTAGAGGCTGGG-GTGGGGAG---AG--A-GCAGTCTGTGTCTTTTGGCA
 |||||
human TAGCAGCATAGGGGTCGGGAGGGGGAGGGGAGGGAAGCAATTCTGTGTCTTTTGGCA
 |||||
mouse GCACTGACAAAGGTCTGGTTGTCAATGATACCTTTACAGCTAAATTTACTCCAGAGTGAC
 |||||
human GCACTGACAAAGGTCTGGTTGTCAAGTATACCTTTACAGCTAAATTTACTCCAGAGTGAC
 |||||
mouse ATGAA-|EAGGTGCACC-CTGGCCTGCCAGACACTTGTGCAGAGGGATCAGGCATCTCACC
 |||||
human A-GAAACAGGTGCACCTC-GGCCTGCCAGACACTTGTGCAGAGAGATCAGGCATCTCACC
 |||||
mouse GCTTGACGATCAAGGGGGCAAAGCTTCGGTCTCATAGAAAAGGAGAGGGAGGCGAGCGCA
 |||||
human GCTTGACGATCAAGGGGGCAAAGCCTTCGGTCTCATAGAAAAGGAGAGGGGCAAAGCGCA
 |||||
mouse GCCCAAACCTGGGGGGTTTCTCTTCAAAGCCAGCTGGTCTGGCTTTATTCTACAGGAATTT
 |||||
human GCCCAAACCTGGGGGGTTTCTCTTCAAAGCCAGCTGGTCTGGCTTTATTCTACAGGAATTT
 |||||

B)

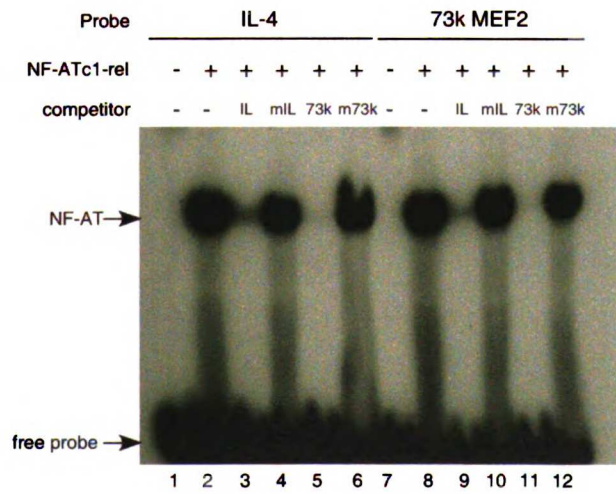
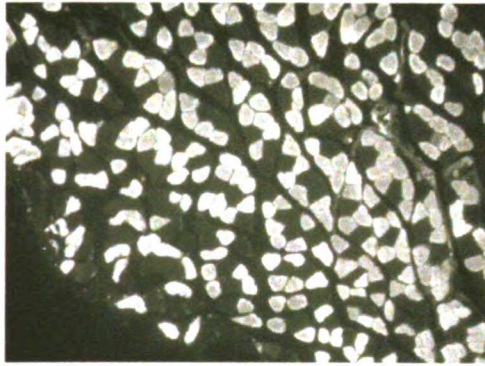
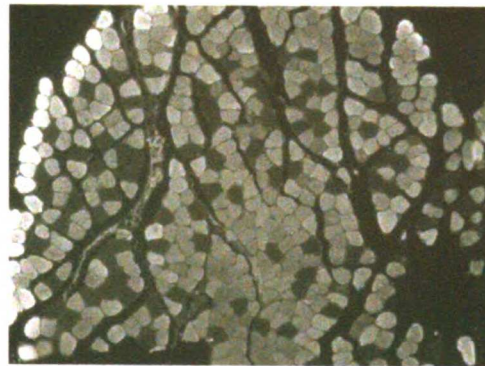


Figure 3-6

A) WT



B) KO



C)

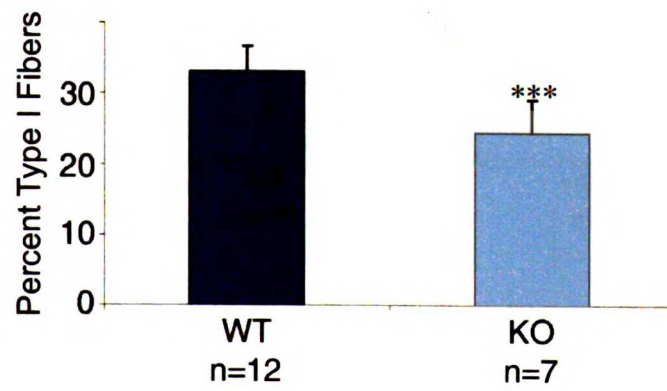
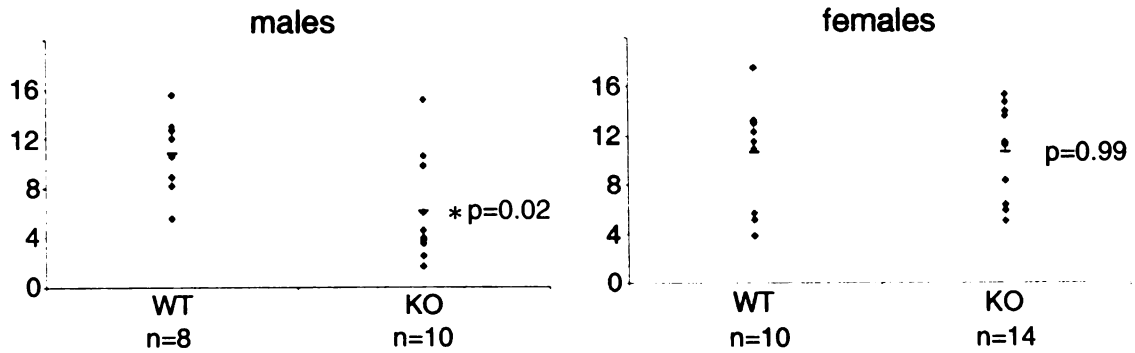
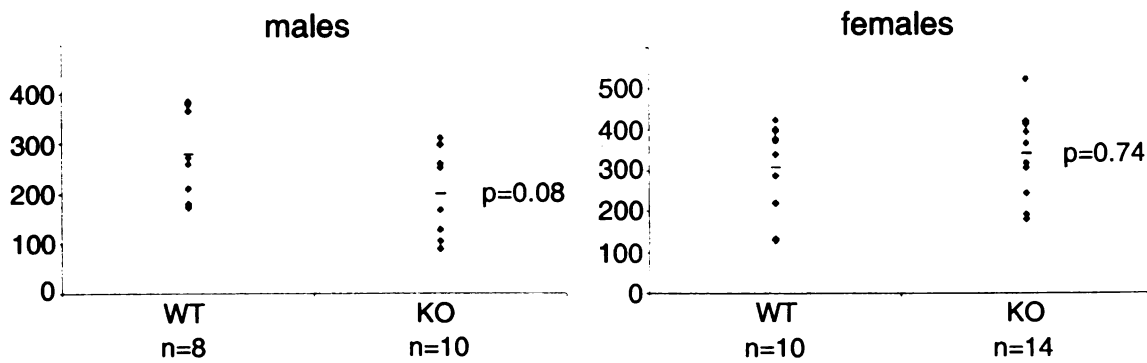


Figure 3-7

A) Distance (km)



B) Time (min)



C) Speed (km/min)

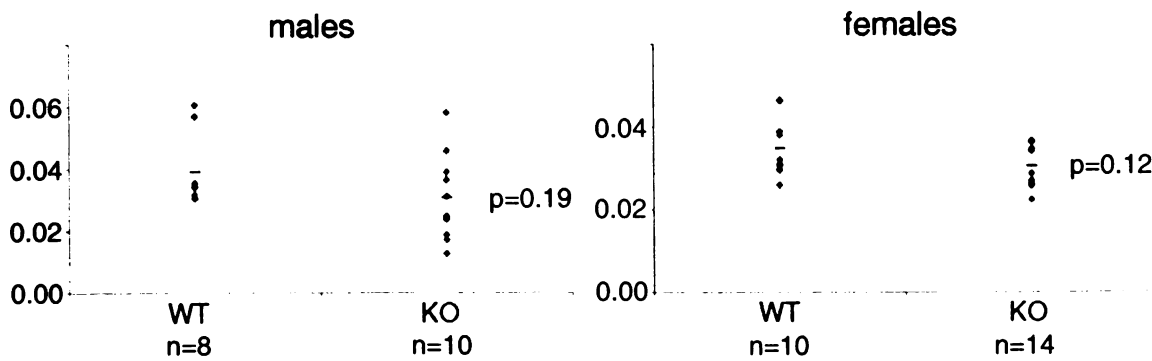


Figure 3-8

A) WT



B) KO



bioRxiv preprint doi: <https://doi.org/10.1101/100000>; this version posted October 1, 2016. The copyright holder for this preprint (which was not certified by peer review) is the author/funder, who has granted bioRxiv a license to display the preprint in perpetuity. It is made available under aCC-BY-NC-ND 4.0 International license.

Figure 3-9

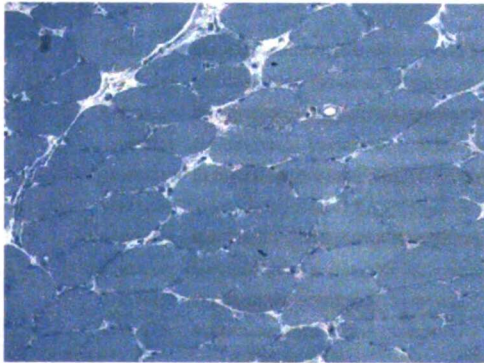
A) WT



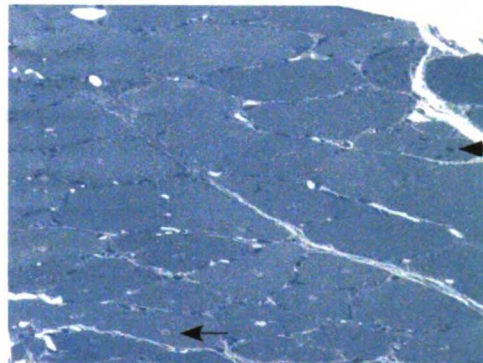
B) KO



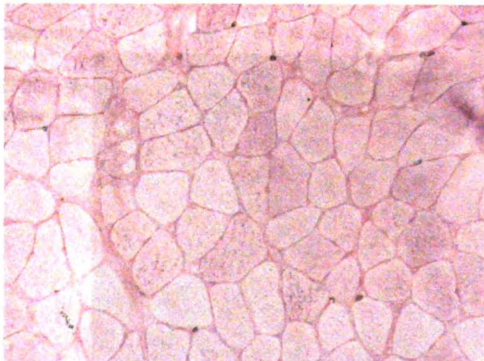
C) WT



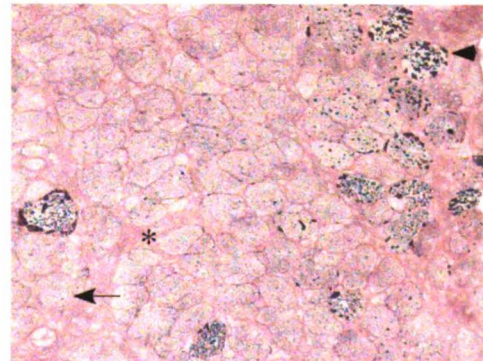
D) KO



E) WT



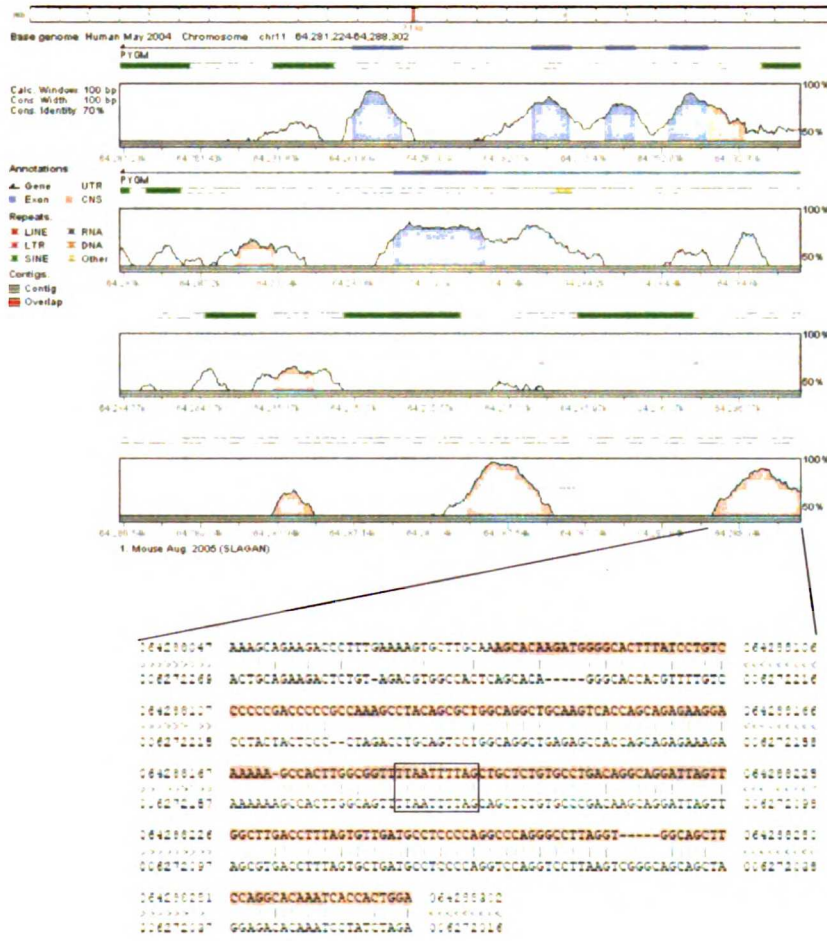
F) KO



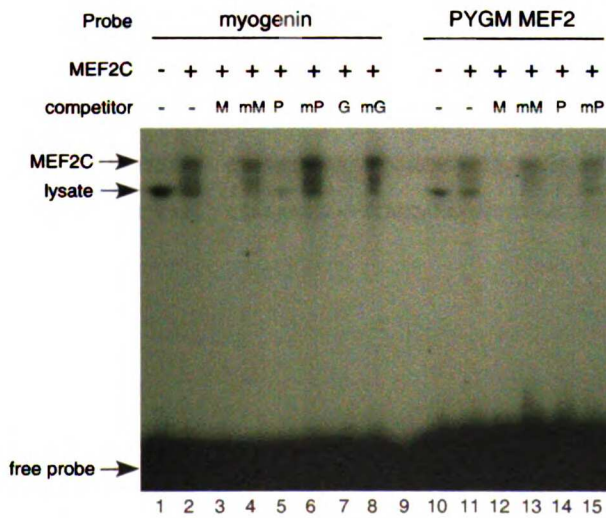
bioRxiv preprint doi: <https://doi.org/10.1101/187717>; this version posted November 14, 2017. The copyright holder for this preprint (which was not certified by peer review) is the author/funder, who has granted bioRxiv a license to display the preprint in perpetuity. It is made available under aCC-BY-NC-ND 4.0 International license.

Figure 3-10

A)



B)



www.ijerph.com

Figure 3-11

A)

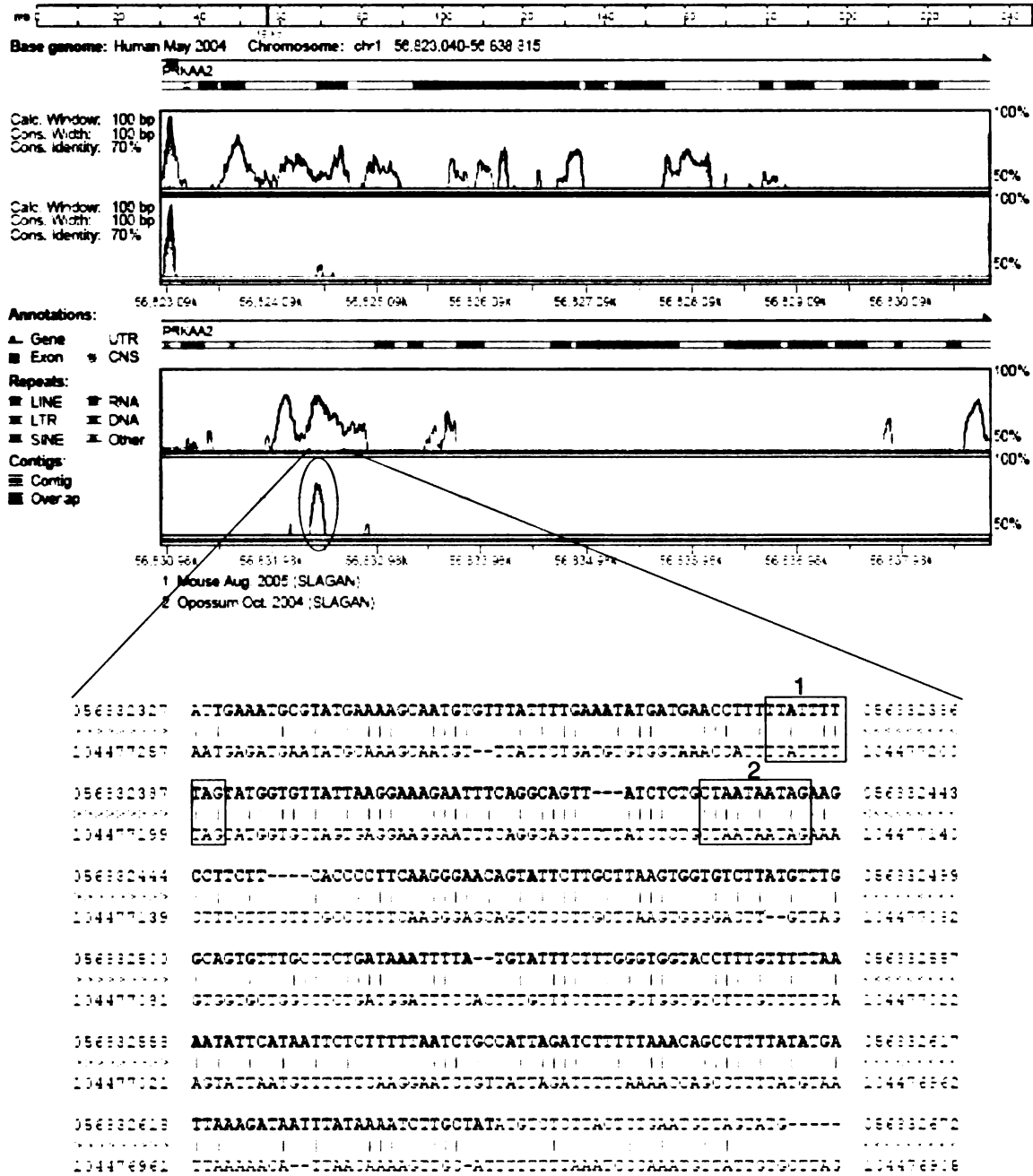
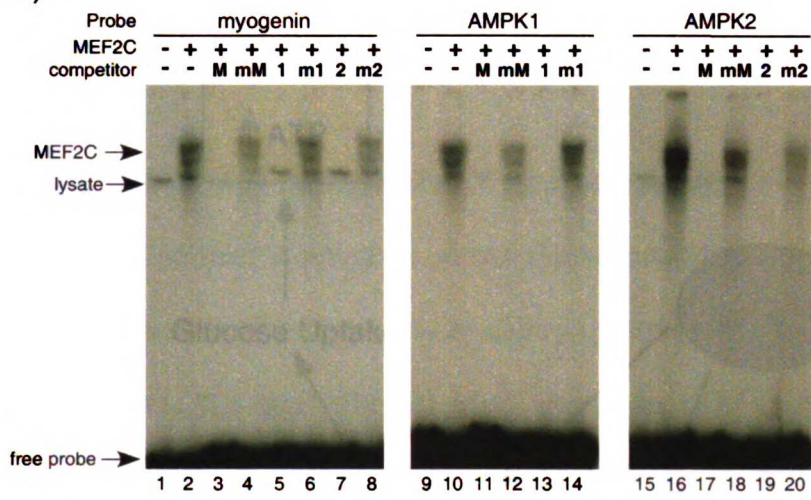


Figure 3-11 cont.

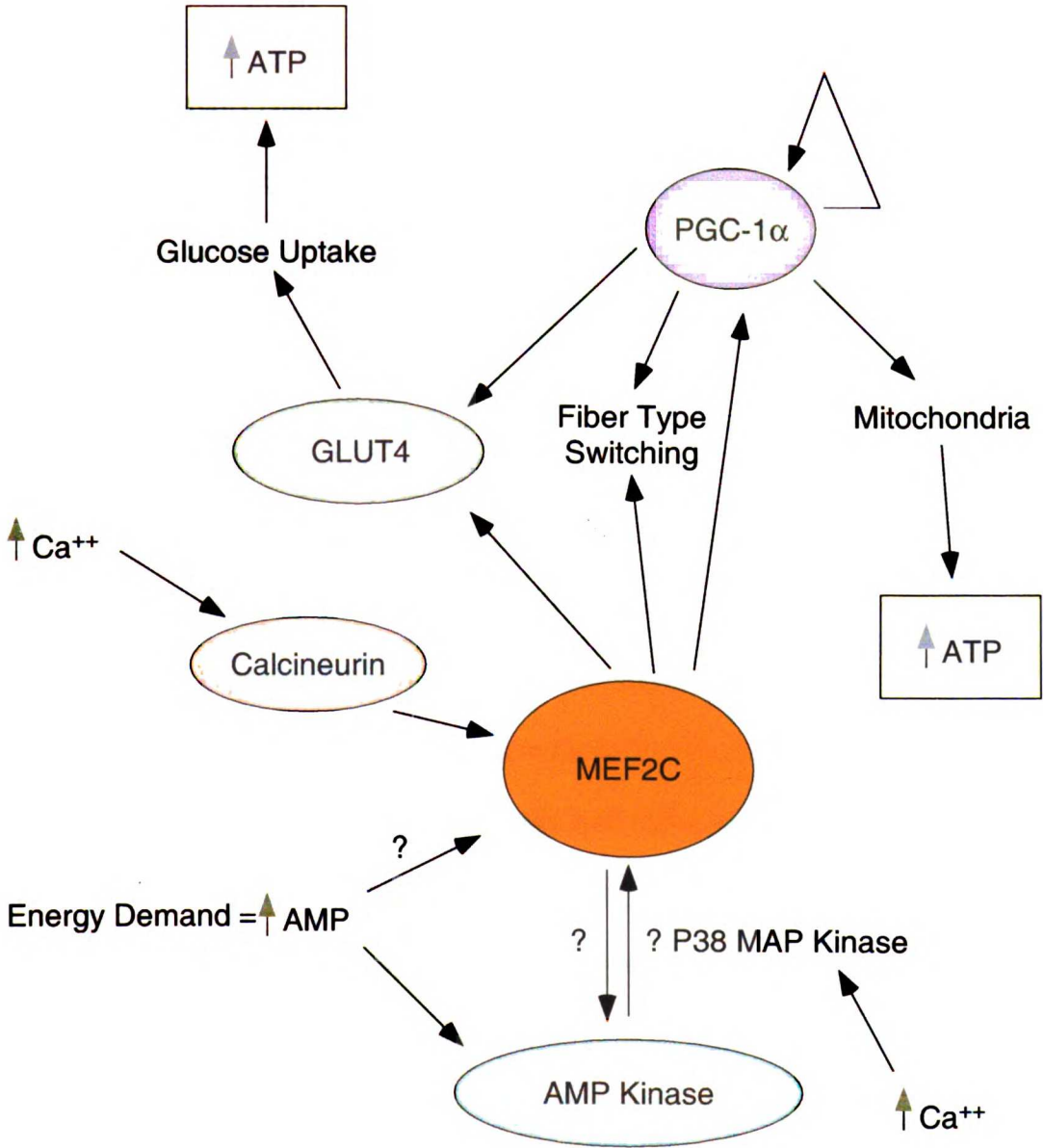
B)



Data for Figure 3-11B was generated by Courtney Brown

EMSA

Figure 3-12



11/11/11 10:00 AM

Chapter 4: Determinants of myogenic specificity within MyoD are required for non-canonical E box binding

I. Summary

Members of the MyoD family of muscle regulatory factors (MRFs) are basic helix-loop-helix (bHLH) proteins required for normal skeletal muscle specification and differentiation in the developing mouse embryo. Genetic studies have indicated that the four members of this family (MyoD, Myf5, myogenin, MRF4) play distinct but overlapping roles in the embryo (Sabourin and Rudnicki 2000; Buckingham, Bajard et al. 2003; Tajbakhsh 2003). In addition, MyoD family members share the ability to convert non-muscle cells into muscle cells in culture (Davis, Cheng et al. 1990; Olson 1990; Brennan, Chakraborty et al. 1991; Weintraub, Dwarki et al. 1991). The ability of each of the myogenic bHLH proteins to induce the muscle transcriptional program requires two amino acids, an alanine and threonine (AT), in the basic region of the DNA binding domain that have been designated the myogenic code (Brennan, Chakraborty et al. 1991; Davis and Weintraub 1992; Weintraub, Genetta et al. 1994). Activation of the myogenic program requires that MyoD be capable of locating the correct muscle genes in the complicated organization of the genome, and recent work has provided an interesting mechanism through which MyoD appears to bind initially to the *myogenin* promoter. Heterodimers of Pbx and Meis, two homeodomain containing transcription factors, were found to occupy the *myogenin* promoter in a repressive chromatin state (Berkes, Bergstrom et al. 2004; de la Serna, Ohkawa et al. 2005). The presence of bound Pbx/Meis allows MyoD/E12 heterodimers to bind an imperfect E box adjacent to the

Pbx/Meis binding site, presumably through interaction with the resident Pbx/Meis heterodimer. In studies presented in this chapter, I examined the requirement of the myogenic code for MyoD to bind to non-canonical E boxes in the *myogenin* promoter. I show that the myogenic code is critical for DNA binding and is required for MyoD to bind to the non-canonical E boxes in *myogenin*, even in the presence of bound Pbx/Meis. Furthermore, I show that mutation of the myogenic code does not affect the intrinsic transcriptional activation potential of MyoD, suggesting that a primary function of the myogenic code is for E box recognition and binding.

II. Results

The MyoD myogenic code is required for E box-independent activation of the *myogenin* promoter

Activation of the muscle transcriptional program by MyoD exquisitely depends on two amino acids in the basic domain, an alanine and threonine, referred to as the myogenic code. However, the precise requirement of the myogenic code for MyoD function has remained elusive. We tested the ability of MyoD and a myogenic code mutant of MyoD, referred to as MyoD(NN), to activate the *myogenin* promoter via E box-dependent and E box-independent mechanisms (Fig. 4-1). Wild type MyoD efficiently activated the *myogenin* promoter (Fig. 4-1B, Lane 5). MyoD also efficiently activated a mutant form of the *myogenin* promoter in which both canonical E boxes (E1 and E2) were mutated (Fig. 4-1B, Lane 8). These observations are consistent with the notion that activation of

myogenin by MyoD occurs via the non-canonical E boxes in the promoter (Fig. 4-1A) (Berkes, Bergstrom et al. 2004). MyoD(NN) also activated the *myogenin* promoter significantly (Fig. 4-1B, Lane 6) although less robustly than wild type MyoD (Fig. 4-1B, Lane 5). Thus, these data and data presented elsewhere (Weintraub, Dwarki et al. 1991; Black, Molkentin et al. 1998; Huang, Weintraub et al. 1998) clearly demonstrate that MyoD(NN) is less efficient at activating the *myogenin* promoter than wild type MyoD, but this mutant still exhibits significant activation of the reporter.

In contrast to wild type MyoD, the MyoD(NN) myogenic code mutant appeared to have little ability to activate the *myogenin* promoter in which the two non-canonical E boxes were mutated (Fig. 4-1B, Lane 9). This can be clearly seen when the abilities of MyoD and MyoD(NN) to activate the E box mutant *myogenin* promoter are expressed as a percentage of their abilities to activate the wild type promoter (Fig. 4-1C). Wild type MyoD activated the *myogenin* E box mutant reporter 64% as efficiently as it activated the wild type reporter (Fig. 4-1C, compare lanes 1 and 3). By contrast, the myogenic code mutant MyoD(NN) was only 23% as effective at activation of the mutant reporter (Fig. 4-1C, compare lanes 2 and 4). This defect in E box-independent activation, coupled with the overall defect in activation by MyoD(NN) results in a near complete failure to activate *myogenin* in a E box-independent fashion (Fig 4-1B, lane 9). Taken together, these data suggest that the myogenic code of MyoD is required for activation of the *myogenin* promoter via the non-canonical E boxes in the promoter.

The myogenic code of MyoD is required for efficient dimerization and DNA binding to canonical E boxes

The observation that myogenic code mutants are defective at inducing transcription of reporters containing the promoters of muscle genes has previously been proposed as the fundamental distinction between wild type and myogenic code mutant MRF proteins and as the reason why the myogenic code is required to induce the muscle transcriptional program (Black, Molkentin et al. 1998; Huang, Weintraub et al. 1998). Interestingly, while we observed a defect in transcriptional activation of *myogenin* by MyoD(NN), the degree of the discrepancy between MyoD(NN) and MyoD differed greatly depending on the presence or absence of canonical E boxes in the reporter (Fig. 4-1). Thus, we hypothesized that the defect in transcriptional activation may be secondary to a DNA binding defect since MyoD(NN) appeared to be incapable of activation via the non-canonical E boxes in *myogenin*. To test this notion, we examined the transcriptional activation potential of MyoD and MyoD(NN) when DNA binding by the bHLH domain was not required (Fig. 4-2). To generate MyoD proteins with identical DNA binding characteristics, we designed fusion proteins that would bind DNA via the yeast GAL4 DNA binding domain, rather than the MyoD basic domain. Co-transfection of these fusion proteins with a UAS-dependent reporter showed that the activation domain of MyoD(NN) induced transcription to equal levels as that induced by wild type MyoD when DNA binding by the basic domain was not a requirement for activation (Fig. 4-2). While this does not preclude the possibility that the myogenic code may be required for activation when bound to DNA through the basic domain, it does suggest that the

transcriptional activation domain is not fundamentally defective in the absence of an intact myogenic code.

Having established that the transcriptional activation defect observed in MyoD(NN) is not a fundamental deficit in the transcriptional activation potential of the protein, we tested the notion that the myogenic code may be required for efficient DNA binding by comparing the ability of MyoD and MyoD(NN) to bind to a canonical E box (Fig. 4-3). In order to compare binding affinities over a range of concentrations, we performed EMSA over a range of MyoD and MyoD(NN) concentrations in binding reactions that contained an excess of E12 protein (Fig. 4-3A). MyoD and MyoD(NN) each bound to the E box probe, but there was clearly less heterodimeric MRF/E12 complex formed when MyoD(NN) was included in the binding reaction (Fig. 4-3A, lanes 8-12), versus when MyoD was added (Fig. 4-3A, lanes 3-7). We quantified the binding of MyoD and MyoD(NN) to the canonical E box probe over a range of concentrations, which indicated there was approximately four to five-fold more wild type DNA bound species than mutant at any given concentration (Fig. 4-3B).

DNA binding by MyoD/E protein heterodimers requires two distinct steps. The proteins must dimerize and then the heterodimer must bind to the E box sequence. Therefore, we sought to determine whether the MyoD(NN) DNA binding defect observed in Fig. 4-3 was due all or in part to a requirement of the myogenic code for dimerization. To address this possibility, we utilized a mammalian two-hybrid system, which allowed for transcription of a GAL4-dependent reporter, pG5E1b-*luciferase*, in a dimerization

dependent manner. We fused the bHLH region of either wild type MyoD or MyoD(NN) to the GAL4 DBD. Since these fusion proteins lack the MyoD activation domains, they should have no ability to activate the reporter. However, if the bHLH fused to the GAL4 DBD heterodimerizes with another bHLH protein that contains an activation domain, the complex will then activate transcription and provide an indirect measurement of dimerization. The GAL4-dependent reporter exhibited no activity when co-transfected with the GAL4 DBD alone or with GAL4-MyoD bHLH or GAL4-MyoD(NN) DBD (Fig. 4-4, Lanes 1-3). Likewise, the reporter was not activated by E47-VP16 in the presence of the GAL4 DBD alone (Fig. 4-4, Lane 4). By contrast, co-transfection of GAL4-MyoD bHLH and E47-VP16 resulted in strong activation of the reporter due to MyoD-E47 dimerization (Fig. 4-4, lane 5). Mutation of the myogenic code resulted in approximately three-fold less transcriptional activation due to reduced dimerization with E47 (Fig. 4-4, Lane 6), suggesting that a defect in dimerization contributes, at least in part, to the diminished DNA binding of MyoD(NN).

The data presented in Fig. 4-4 suggest that the myogenic code is required for efficient dimerization between MyoD and its E protein partner. However, the relatively small change in dimerization efficiency seemed unlikely to account for the entire deficit in transcriptional activation by MyoD(NN) observed in Fig. 4-1, suggesting that the myogenic code may be required for DNA binding independent of dimerization. To overcome the dimerization defect in MyoD(NN), we used tethered heterodimers of either MyoD or MyoD(NN) and E47. These tethered dimers have the two bHLH partners covalently joined via a flexible linker, which drastically increases the local concentration

of E protein. The increase in local concentration of E protein and MyoD relative to each other is thought to make dimerization no longer rate limiting, and the wild type version of this molecule, MyoD~E47, is fully functional since it has been shown to be active in converting fibroblasts into skeletal muscle (Neuhold and Wold 1993). To test if dimerization is the critical requirement of the myogenic code, we co-transfected a reporter that contains four multimerized copies of an E box driving luciferase expression (4R-TK-*luciferase*) with expression vectors for the tethered dimers, MyoD~E47 or MyoD(NN)~E47 (Fig. 4-5A). MyoD~E47 activated the E-box dependent reporter as efficiently as untethered MyoD (Fig. 4-5A, compare Lanes 2 and 3). MyoD(NN) also activated the reporter, but less efficiently than wild type MyoD (Fig. 4-5A, compare Lanes 2 and 4), which is consistent with previous studies (Weintraub, Dwarki et al. 1991; Black, Molkentin et al. 1998; Huang, Weintraub et al. 1998). Importantly, we found that tethering MyoD(NN) to E47 resulted in a slight increase in transcriptional activation by MyoD(NN), but was unable to restore wild type levels of activation (Fig. 4-5A, Lane 5).

To determine if the transcriptional activation defect of the tethered MyoD(NN)~E47 was due to a deficiency in DNA binding, we examined the ability of the tethered heterodimers to bind to DNA over a range of concentrations (Fig. 4-5B). MyoD(NN)~E47 bound to a canonical E-box in a dose-dependent manner (Fig. 4-5B, Lanes 9-15), but the affinity was substantially lower than that of wild type MyoD tethered to E47 (Fig. 4-5B, Lanes 2-8).

To determine if the decrease in DNA binding observed in Figs. 4-3A and 4-5B was due to an increased rate of dissociation between the MyoD(NN)-E protein heterodimer and DNA, we examined the kinetics of MyoD(NN)~E47/E box dissociation compared to the

dissociation of wild type MyoD~E47 from the E box (Fig. 4-5C). Tethered heterodimers were incubated with radiolabeled oligonucleotides representing a canonical E box, followed by competition with unlabeled oligonucleotide for various amounts of time before loading the complex on a gel. MyoD~E47 bound robustly to the E box (Fig. 4-5C, Lane 5) and this binding diminished as time with excess competitor increased (Fig. 4-5C, Lanes 6-8). As expected, MyoD(NN)~E47 bound with reduced efficiency in the initial binding reaction (time=0; Fig. 4-5C, Lane 1). Interestingly, however, the reduction in the amount of bound heterodimer was faster for MyoD(NN~E47) (Fig. 4-5C, Lanes 2-4) than for wild type MyoD~E47 (Fig. 4-5C, lanes 6-8). Indeed, the initial off rate, as measured by the slope of the decrease in signal over the first ten minutes was two-fold faster for MyoD(NN) than MyoD (data not shown).

The MyoD myogenic code is required for noncanonical E box binding

The data presented above demonstrate that the myogenic code of MyoD is a critical determinant of DNA binding and that mutation of the myogenic code results in decreased DNA affinity. This decreased affinity is due in part to reduced dimerization affinity, a reduced affinity for E box binding, and an increased off rate for DNA binding. However, an intact myogenic code was not absolutely required for canonical E box binding (Fig. 4-3), and therefore, does not explain the lack of dominant myogenic induction by MyoD mutants lacking a myogenic code. Recently, the discovery of critical non-canonical E boxes in the *myogenin* promoter suggested that the DNA binding ability of MyoD must be optimal to bind stably to this critical locus in the muscle transcriptional program (Berkes, Bergstrom et al. 2004). Therefore, we tested the requirement of the myogenic

code for MyoD binding to these non-canonical E boxes (Fig. 4-6). Under conditions where we observed robust binding to *myogenin* non-canonical E boxes by wild type MyoD (Fig. 4-6, lane 2), we never observed any binding by MyoD(NN) (Fig. 4-6, lane 9). The binding by MyoD to the non-canonical E boxes was specific, as an unlabeled wild type E box was able to fully compete for binding to the non-canonical E boxes (Fig. 4-6, lanes 3-5), while an unlabeled mutant E box oligonucleotide was unable to compete for MyoD binding (Fig. 4-6, lanes 6-8). The lysate used in this experiment contained nearly equivalent binding activities for MyoD and MyoD(NN), as shown by the ability of each to bind a canonical E box (Fig. 4-6, lanes 14 and 15, respectively).

While myogenic code mutants are incapable of directly binding to the *myogenin* non-canonical E boxes, it is likely that MyoD binding to these non-canonical E boxes is aided *in vivo* by a resident Pbx/Meis heterodimer that is bound at a site adjacent to the noncanonical E boxes in the *myogenin* promoter (Fig. 4-1A) prior to myogenic induction (de la Serna, Ohkawa et al. 2005). Therefore, we compared the abilities of MyoD and MyoD(NN) to bind to the non-canonical E boxes when the adjacent Pbx/Meis binding site was occupied (Fig. 4-7). A radiolabeled probe representing both the Pbx/Meis and non-canonical E box binding sites was readily bound by Pbx1A/Meis1 heterodimers (Fig. 4-7, lane 5) and by MyoD/E12 heterodimers (Fig. 4-7, lane 2). As expected, MyoD(NN)/E12 heterodimers displayed no binding to the non-canonical E box in the absence of Pbx/Meis (Fig. 4-7, Lane 3). When all four proteins (Pbx1A, Meis1, MyoD, and E12) were added to the binding reaction, a higher order complex was formed that migrated slightly slower than the MyoD/E12 heterodimer (Fig. 4-7, lane 6). However,

the higher order complex containing Pbx1a/Meis1 was never observed when MyoD(NN) was included in the binding reaction (Fig. 4-7, lane 7). Intriguingly, in the presence of MRF and E12 we see a reduction in the strength of the Pbx/Meis alone shifted species, regardless of the presence of the myogenic code, suggesting that MRFs interact with Pbx/Meis in a complex that is not bound to DNA. This hypothesis is being further investigated. Thus, we conclude that myogenic code mutants are defective in transcriptional activation of the *myogenin* gene, a critical step in the up-regulation of the muscle transcriptional program, due to the combination of a deficit in dimerization and DNA binding which results in a complete inability to bind to essential non-canonical E boxes in the promoter.

III. Discussion

The myogenic code has long been established as the critical distinction between the muscle regulatory factor (MRF) family of bHLH transcription factors and all other bHLH family members. The two amino acids of the myogenic code, an alanine and threonine in the basic domain, are required for induction of the muscle transcriptional program.

Mutation of these amino acids results in a bHLH protein that is competent to activate transcription but that is no longer capable of converting non-muscle cells into muscle. It has remained unclear what properties these amino acids afford to the MRF family to confer myogenic-inducing ability. In the current study, we present work that establishes the myogenic code as a critical determinant that allows MyoD to bind DNA with high

affinity. Mutation of the myogenic code causes a decrease in affinity for E protein dimerization partners and also results in a profound decrease in the ability of the heterodimer to bind DNA. This defect is shown to be especially prominent at low affinity sites within the *myogenin* promoter, where the myogenic code is required for MyoD to bind directly to non-canonical E boxes and to form a tetrameric DNA bound complex with Pbx/Meis.

Previous studies have come to different conclusions about the function of the myogenic code in transcriptional activation and the induction of myogenesis (Weintraub, Dwarki et al. 1991; Schwarz, Chakraborty et al. 1992; Black, Molkentin et al. 1998; Huang, Weintraub et al. 1998). Some studies have suggested that the primary role of the myogenic code is for proper display of the transcriptional activation domains of the MRFs (Black, Molkentin et al. 1998; Huang, Weintraub et al. 1998). These models suggest that the activation domain of MyoD is masked or the signal to activate is not transmitted properly to the activation domain in the absence of an intact myogenic code. By contrast, the initial work on the myogenic code suggested that it functioned to recruit a “recognition factor” that was essential for myogenic activation (Weintraub, Dwarki et al. 1991; Schwarz, Chakraborty et al. 1992). The existence of this factor was based on the observation that myogenic code mutants for several of the MRFs activated transcription in certain cell types better than in others.

None of these earlier studies on the myogenic code have examined the requirement of this determinant for DNA binding in detail. Although it has been suggested that the

alanine of the myogenic code is important for DNA binding, the residues that comprise the myogenic code are not absolutely required for MRF binding to a canonical E box *in vitro* (Weintraub, Dwarki et al. 1991). The requirement for this essential myogenic determinant to bind to DNA when either the protein or DNA site is limiting has not been examined prior to the present study. Using a titration, we show that the myogenic code is critical for DNA binding (Figs. 4-3 and 4-6). The myogenic code mutant, MyoD(NN), exhibits substantially less binding to a canonical E box than wild type MyoD (Fig. 4-3). This requirement for efficient DNA binding is particularly pronounced on low affinity binding sites, as we never observed binding of MyoD(NN) to non-canonical E boxes, with or without a neighboring Pbx/Meis heterodimer (Figs. 4-6 and 4-7). This suggests that a primary requirement of the myogenic code is in DNA binding. Our data also show that the myogenic code affects MyoD heterodimerization (Fig. 4-4), which is mediated by a distinct portion of the protein. While our data suggest that the myogenic code is essential for DNA binding and dimerization, this does not preclude the possibility that an intact myogenic code may result in a conformation of MyoD that enables interaction with a factor that aids in activation, or perhaps more likely, a factor that helps to stabilize DNA binding.

Interestingly, mutations in MyoD that affect the ability of MyoD to induce chromatin remodeling, have also been shown to cause a diminished capacity to interact with Pbx/Meis at the *myogenin* promoter. MyoD mutants that lack a region that is enriched for cysteines and histidines, or a distinct region known as helix III, were originally shown to be defective in chromatin remodeling at the *myogenin* promoter (Gerber, Klesert et al.

1997). Subsequently, an additional defect of these mutants was shown to be a decrease in binding to non-canonical E boxes, suggesting that the original stabilization of binding to the promoter through interaction with Pbx/Meis is a critical step in the formation of a stably remodeled locus and transcriptional activation (Berkes, Bergstrom et al. 2004; de la Serna, Ohkawa et al. 2005). These mutants are distinct from myogenic code mutants in that they retain the ability to induce myogenesis, albeit less potently than wild type MyoD (Bergstrom and Tapscott 2001). We predict that this retained ability to induce myogenesis is the result of the residual capacity to bind non-canonical E boxes, which is in contrast to the complete inability of MyoD(NN) to bind to non-canonical E boxes and to induce myogenesis.

The existence of distinct mutations in diverse regions of the protein that affect the interaction of MyoD with Pbx/Meis, further supports the notion that there is a particular conformation that is critical to inducing the muscle transcriptional program. In addition, mutation of the critical alanine of the myogenic code in MyoD is known to cause the protein to have an altered conformation when bound to DNA, as shown by increased sensitivity to protease cleavage (Huang, Weintraub et al. 1998). A conformation role for the myogenic code is appealing since the MyoD crystal structure has shown that these two amino acids are buried in the molecule (Ma, Rould et al. 1994). The position of the myogenic code residues within MyoD suggests that they are inaccessible for protein/protein or protein/DNA interactions, and a critical role in bHLH conformation would explain how this seemingly subtle mutation has such drastic effects on numerous aspects of MyoD function.

The dramatic ability of MyoD to induce myogenesis in cell culture and to initiate muscle specification *in vivo* requires that MyoD bind to select immediate early targets. The ability to bind at critical muscle loci, such as *myogenin*, may require the ability to interact with Pbx/Meis and to bind to non-canonical E boxes (Berkes, Bergstrom et al. 2004; de la Serna, Ohkawa et al. 2005). We propose that the myogenic code is the critical determinant for optimal dimerization and DNA binding, which are required to stabilize MyoD on non-canonical binding sites in essential muscle loci to allow for subsequent chromatin remodeling and transcriptional activation. Examples such as this, of highly fine-tuned binding specificity, are likely to be a common mechanism by which individual members of large families of transcription factors are able to discriminate appropriate binding sites in the context of the genome and activate distinct transcriptional programs.

IV. Figure Legends

Figure 4-1. The myogenic code is necessary for maximal transcriptional activation of the *myogenin* promoter. (A) Schematic of the 184 proximal nucleotides of the *myogenin* promoter. The arrow indicates the transcriptional start site. Canonical E boxes 1 and 2 (E1,E2) flank a bipartite binding site composed of a binding site for a heterodimer of the HOX/TALE class of proteins Pbx/Meis, directly juxtaposed to two overlapping non-canonical E boxes (NC). (B) Plasmids expressing either MyoD or MyoD(NN) were co-transfected with a reporter plasmid that contained the wild type

myogenin promoter (WT 184) or a mutant form lacking canonical E boxes (mut E1/ E2) driving expression of *luciferase*. Neither protein, MyoD or MyoD(NN), significantly activated transcription of this plasmid when the *myogenin* promoter was removed (Lanes 2-3). MyoD significantly activated the wild type *myogenin* promoter, approximately 130-fold (Lane 5), while MyoD(NN) consistently gave 20-fold activation (Lane 6). Activation of the *myogenin* promoter by MyoD was marginally diminished to 90-fold if the canonical E boxes were mutated (Lane 8). Mutation of the canonical E boxes more dramatically affected the ability of MyoD(NN) to activate the Mut E1/E2 reporter, reducing the activation to less than 10-fold (Lane 9). pRK5 alone did not induce significant activation of any reporter plasmid (Lanes 1,4,7). The bars represent mean fold activation in three independent experiments. Error bars represent standard error of the mean. (C) Myogenic code mutants of MyoD do not utilize the non-canonical E boxes in the *myogenin* promoter to activate transcription. The bars represent activation of various reporters as a percent of activation by MyoD or MyoD(NN) on the wild type *myogenin* promoter, with error bars representing standard error of the mean. Fold activation exhibited on wild type myogenin was set to equal 100 percent for both activators as a way to compare the degree of deficit seen on each mutant reporter (Lanes 1,2). MyoD retains the majority of its activation ability on myogenin promoter plasmids that are mutant at both canonical E boxes (mE1/E2), as evidenced by the 64% of activation activity exhibited on this reporter (Lane 3). MyoD(NN), however, shows a greater percent decrease in activation when either E1 or both E1/E2 are mutated, retaining only 23% of its ability to activate wild type *myogenin* (Lane 4).

Figure 4-2. The myogenic code is not required for the transcriptional activation domain of MyoD to function. Myogenic code mutants activate transcription as well as wild type MyoD when tethered to the GAL4 DNA binding domain (DBD). Plasmids expressing fusion proteins of the GAL4 DBD and full length MyoD or MyoD(NN) were co-transfected into 10T1/2 cells with pG₅E1b, a UAS dependent reporter plasmid that has five binding sites for the GAL4 domain driving expression of *luciferase*. Approximately 300-fold activation was observed with either activator protein. The bars represent the mean fold activation from three independent experiments, with error bars representing the standard error of the means.

Figure 4-3. The myogenic code of MyoD is critical for optimized DNA binding to a canonical E box. (A) E12, MyoD and MyoD(NN) were used in EMSA analyses with double-stranded oligonucleotides representing the canonical E box from the skeletal muscle enhancer of the *mef2c* gene. E12 bound weakly to this E box as a homodimer in the absence of MRF protein (Lane 2). The addition of a titration of recombinant MyoD (Lanes 3-7) or MyoD(NN) protein (Lanes 8-12) shows that MyoD(NN) exhibits decreased binding affinity for the binding site compared to wild type MyoD. The MRF/E12 heterodimeric DNA bound species is labeled with an asterisk. When equivalent amounts of MRF are added, such as in lanes 3 and 8, MyoD(NN) exhibits less DNA binding, indicating a lower affinity for the E box probe. Lane 1 does not contain recombinant protein, however, an identical amount of reticulocyte lysate was included; lysate-derived non-specific mobility shifts are present where indicated. (B) A line graph

depicting the increase in MRF binding to the *mef2c*-Ebox seen in a typical experiment. Gels such as that seen in (A) were dried and exposed to a phosphorimager screen. The increase in counts of the lower species was counted and relative DNA binding was determined as pixel density as measured by phosphorimager analysis (Molecular Dynamics).

Figure 4-4. The myogenic code is important for optimizing dimerization

interactions between MyoD and E protein. Plasmids expressing a fusion of the bHLH domain of MyoD and the GAL4 DNA binding domain (GAL4-MyoDbHLH) were co-transfected into 10T1/2 cells with the reporter plasmid pG₅E1b. pG₅E1b is a UAS dependent reporter that has five binding sites for the GAL4 domain driving expression of the *luciferase* gene. GAL4, GAL4-MyoDbHLH, or GAL4-MyoD(NN)bHLH cannot activate this plasmid alone, as these proteins lack a transcriptional activation domain (Lanes 1-3). Co-transfection of GAL4-MRFBHLH with a plasmid that expresses the bHLH domain of E47 fused to the viral transcriptional activator protein VP16 (E47-VP16) allows for recruitment of the VP16 to the promoter through dimerization between the MRF and E protein bHLH domains. E47-VP16 did not activate this reporter on its own, as this protein does not bind to the UAS sequence (Lane 4). GAL4-MyoDbHLH dimerized with E47-VP16 and led to an approximately 80 fold activation of the reporter (Lane 5). MyoD(NN), however, dimerized slightly less efficiently, leading to an approximately 30-fold activation (Lane 6). The bars represent the average fold activation of 9 independent transfections, with error bars representing standard error of the mean.

Figure 4-5. Dimerization defects do not fully account for the transcriptional activation defect exhibited by myogenic code mutants. (A) Plasmids expressing MyoD, MyoD(NN) or these MRFs tethered through a flexible linker to E47 (MyoD~E47, MyoD(NN)~E47) (Neuhold and Wold 1993) were co-transfected into 10T1/2 cells with the plasmid reporter 4RTK-*luciferase*. This reporter contains four multimerized E boxes and the *thymidine kinase* promoter driving expression of the *luciferase* cDNA. MyoD activated this plasmid approximately 50-fold (Lane 2) and similar activation was observed when MyoD is tethered to E47 (Lane 3). An expression vector for MyoD(NN) activated the multimerized E box reporter only approximately 10-fold (Lane 4). This activation was slightly increased when a plasmid that expressed MyoD(NN) tethered to E47 (MyoD(NN)~E47) was co-transfected with 4RTK-*luciferase* (Lane 5), however, this plasmid was not able to induce transcription at the same level as wild type MyoD or MyoD~E47. (B) Tethering MyoD(NN) to E47 does not restore wild type binding affinity for the canonical E box from the *mef2c* gene. Recombinant MyoD~E47 or MyoD(NN)~E47 was used in EMSA with a radiolabeled double stranded oligonucleotide representing the E box from the *mef2c* gene. Lanes 2-8 show a titration of MyoD~E47 protein binding to the E box probe. There was significantly less DNA bound species when MyoD(NN)~E47 was used in EMSA (Lanes 9-15). Lane 1 contains reticulocyte lysate without recombinant MRF~E47 protein, represented by a minus sign. Non-specific lysate derived bands are present where indicated. (C) Kinetic analysis of recombinant MRF-E47 fusion protein bound to the canonical E box from the *mef2c* gene.

Recombinant MyoD~E47 or MyoD(NN)~E47 was used in EMSA with a radiolabeled double stranded oligonucleotide representing the E box from the *mef2c* gene. After MRF~E47 protein and radiolabeled oligonucleotide reached equilibrium at room temperature, unlabeled competitor oligonucleotides were added to the samples prior to loading the complex on a gel. Time in minutes indicates the length of competition. MyoD(NN) (Lanes 1-4), has a faster off rate from DNA than does MyoD (Lanes 5-8), as indicated by the rapid loss of binding to radiolabeled probe exhibited by the mutant (compare lanes 1 and 2).

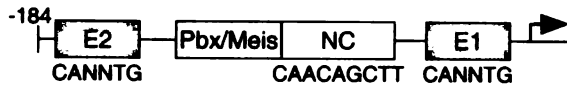
Figure 4-6. The myogenic code of MyoD is required for binding to non-canonical E boxes in the *myogenin* promoter. Recombinant MyoD, MyoD(NN) and E12 proteins were transcribed and translated *in vitro* and used in EMSA with a radiolabeled double stranded oligonucleotide representing the Pbx/Meis and non-canonical E box binding sites from the *myogenin* promoter (Pbx-Myg) (Berkes, Bergstrom et al. 2004). Lane 1 contains reticulocyte lysate without recombinant MRF or E12 protein, represented by a minus sign. Lane 2 shows that wild type MyoD bound to the two juxtaposed non-canonical E boxes in the *myogenin* promoter. This binding was specific and was efficiently competed away by an unlabeled competitor oligonucleotide containing the canonical E box from the *mef2c* gene (E, Lanes 3-5), but not with a mutant version of the oligo (mE, Lanes 6-8). A DNA bound species was never observed when MyoD(NN) was added to the binding reaction in place of MyoD (Lanes 9-13). This complete lack of binding was specific to non-canonical E boxes, as the same MyoD(NN) lysate used for the non-canonical EMSA was incubated with a radiolabeled oligonucleotide representing

the canonical *mef2c* E box (Lane 15) and exhibited binding similar to that of wild type MyoD (Lane 14).

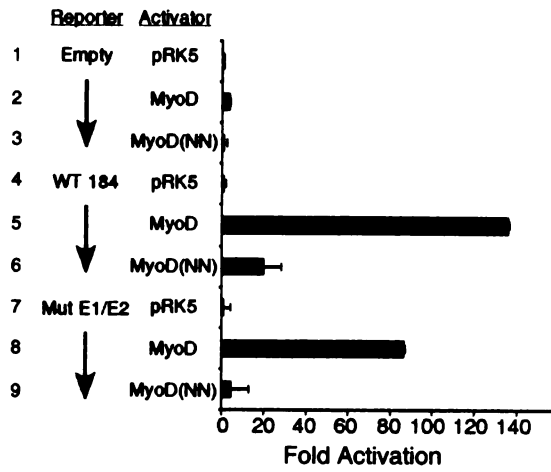
Figure 4-7. MyoD/E12 heterodimers form a tetrameric complex with Pbx/Meis heterodimers on juxtaposed binding sites in the *myogenin* promoter. This complex is not formed when the myogenic code of MyoD is mutated. Recombinant MyoD, MyoD(NN), E12, Pbx1A, and Meis1 proteins were used in EMSA with a radiolabeled double stranded oligonucleotide representing the Pbx/Meis and non-canonical E box binding sites from the *myogenin* promoter (Pbx-Myg) (Berkes, Bergstrom et al. 2004). Lane 1 contains reticulocyte lysate without recombinant protein, represented by a minus sign. Lane 2 shows that MyoD and E12 bound to the non-canonical E boxes in the Pbx-Myg oligonucleotide (*). This complex was not formed when MyoD was replaced with MyoD(NN) (Lane 3), or with E12 alone (Lane 4). Pbx1A/Meis1 heterodimers also bound efficiently to Pbx-Myg (Lane 5), and formed a higher order species representing a tetrameric complex with MyoD and E12 (Lane 6, **). MyoD(NN) did not form a tetrameric complex with Pbx1A and Meis1 (Lane 7). The lack of binding was not due to a lack of protein in the lysate used, as the MyoD and MyoD(NN) lysates were capable of binding with E12 to a double stranded radiolabeled oligonucleotide representing the canonical E box from the *mef2c* gene (data not shown).

Figure 4-1

A)



B)



C)

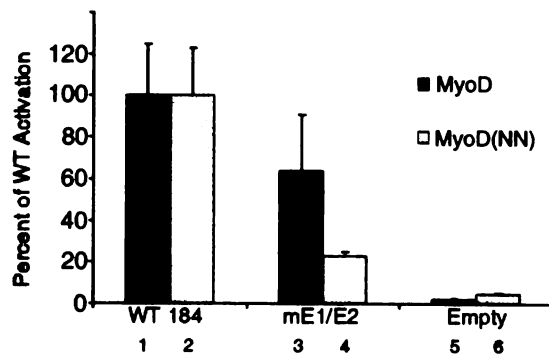


Figure 4-2

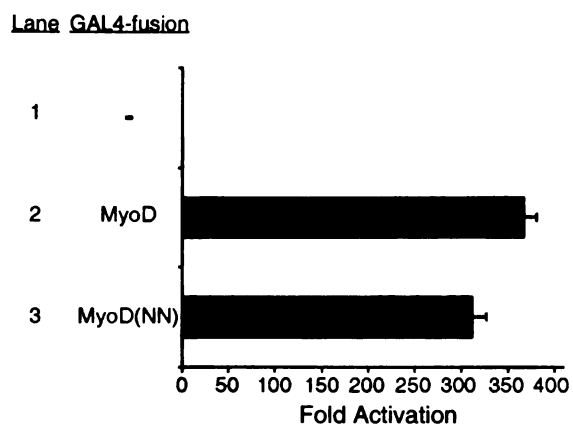
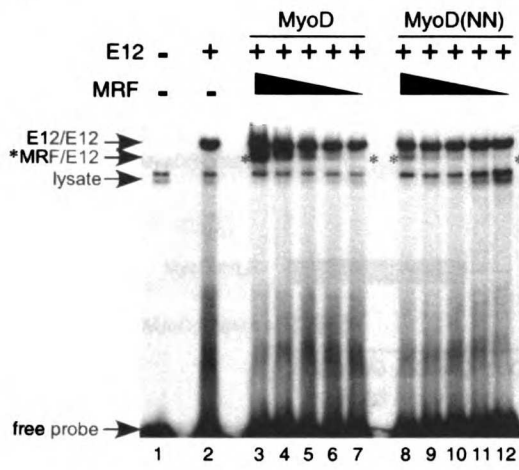


Figure 4-3

A)



B)

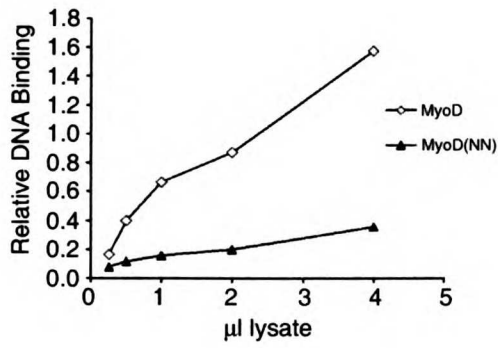


Figure 4-4

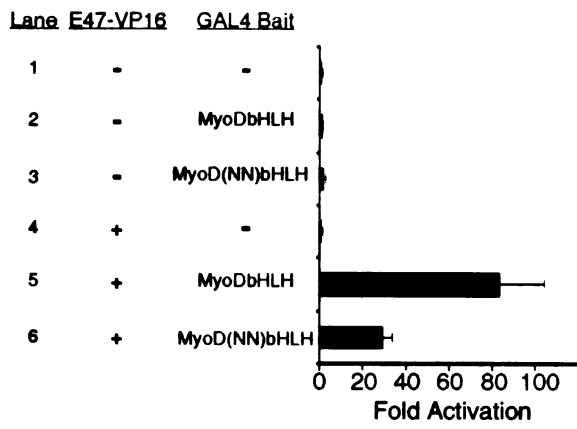
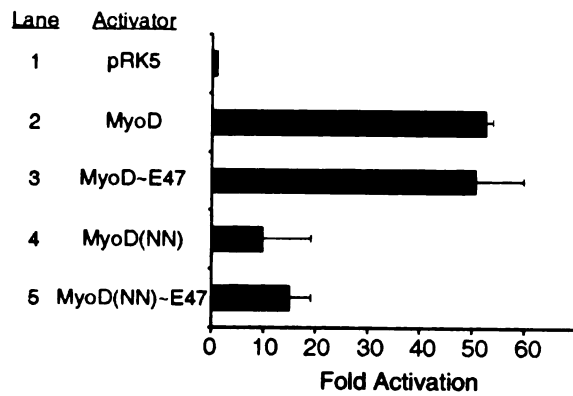
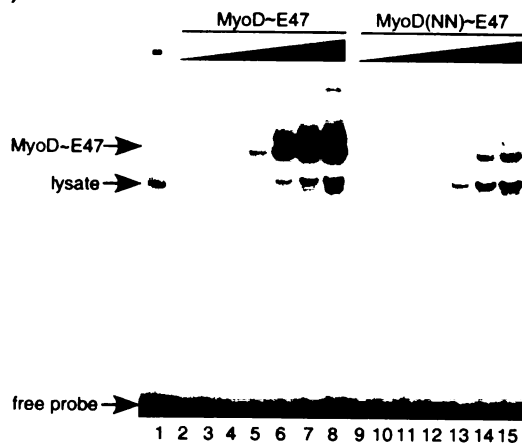


Figure 4-5

A)



B)



C)

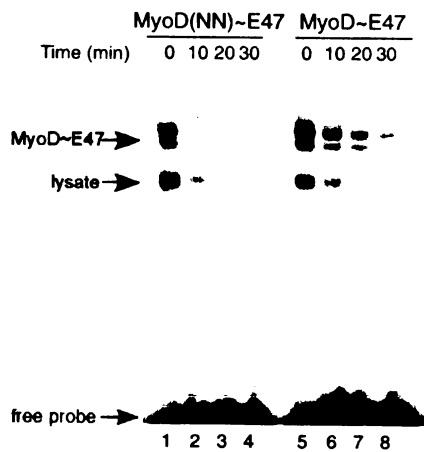


Figure 4-6

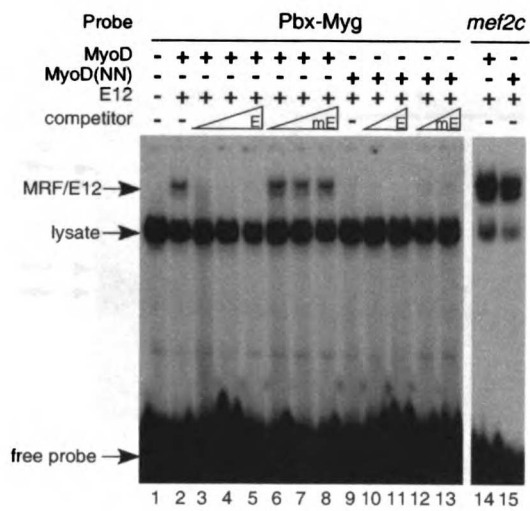
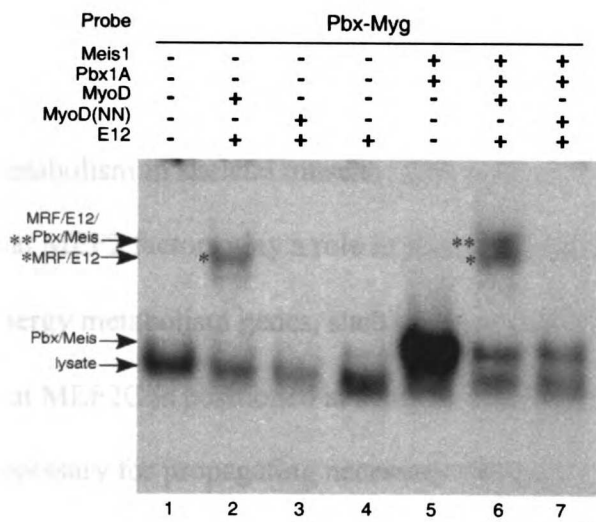


Figure 4-7



Conclusions

The role of *mef2c* in skeletal muscle has not been previously established due to the embryonic lethality of mice lacking *mef2c*. The conditional inactivation approach described herein highlights a role for MEF2 family members in the regulation of energy metabolism in skeletal muscle. This finding fits nicely with the known data that shows that MEF2 factors play a role in fiber type switching and also in the regulation of critical energy metabolism genes, such as *Pgc-1 α* and *Glut4*. These data also support the notion that MEF2C is positioned at a key step in the pathway and helps to turn on genes that are necessary for propagating necessary changes to increase cellular ATP. This data highlights the importance of determining what signals within the cell are critical for sensing energy depletion and more importantly, how these signals are relayed to critical transcription factors, such as MEF2C.

This is particularly important, as energy metabolism in skeletal muscle is a critical modulator of disease states. One of the primary symptoms of type II diabetes is the inability of skeletal muscle to undergo insulin stimulated glucose transport (Parish and Petersen 2005). There is also evidence that oxygen consumption in cardiac muscle is altered in diabetic patients leading to a decrease in cardiac efficiency (How, Aasum et al. 2006). Understanding the mechanisms that allow cells to sense energy demand and correctly utilize the energy supplied by the environment is a key step in understanding the progression of disease. As MEF2 proteins are significantly modified post-translationally, in response to numerous signals, the transcriptional program regulated by these events

may be a key to understanding the changes that skeletal muscle undergoes in response to energy demand. Further questions include determining what post-translational modifications are important for energy regulation and which modifying enzymes relay the signal for needed energy. It would be particularly interesting to identify a subtle mutation in *mef2c* that recapitulates the energy phenotype. We currently hypothesize that molecules such as AMP activated protein kinase $\alpha 2$, the catalytic subunit of a trimeric complex that is critical for sensing cellular energy demand will be directly responsible for the upregulation of MEF2C activation in times of energy demand. In addition, positive feedback loops are common features in the regulation of physiological outputs, and determining the activation of energy sensing molecules by MEF2C is another important challenge presented by the data herein. Mice with conditional inactivation of *mef2c* in skeletal muscle will provide a useful tool to further elucidate the pathways critical for skeletal muscle energy metabolism, and possibly the link between events early in development with adult physiology.

Due to the known role of MEF2 family members in muscle differentiation, our phenotype raises the interesting notion that adult physiological defects may be due both to defects in adult processes and also to contributions from misregulation of embryonic events. We have observed disorganization in the repeating pattern of the sarcomere in skeletal muscle specific knock out mice using electron microscopy. Inefficiency of contraction and force generation could certainly contribute to improper regulation of energy metabolism, as mice would utilize more energy per contraction. Models such as these have also been proposed as a mechanism leading to cardiac hypertrophy (Ashrafian, Redwood et al.

2003). More closely mapping the timing and characteristics of skeletal muscle development in embryos lacking *mef2c* in skeletal muscle will help distinguish the contribution of *mef2c* in the embryo to the observed adult phenotype. In addition, knocking out *mef2c* post-natally in skeletal muscle would be a clear method to isolate the events. Also, measuring the ability of muscle to contract and generate force *in vitro* would help to fill in a gap in our model, that is, the hypothesis that muscle in *mef2c* skeletal muscle specific mice is inefficient.

Critical for differentiation, *mef2* genes are direct and early targets of the MyoD family of transcription factors. It is MyoD and related molecules that initiate the skeletal muscle program in the embryo. MyoD is a member of the much larger bHLH transcription factor family. Members of this family have very similar biochemical characteristics, including heterodimerization with E proteins as a prerequisite step to DNA binding and binding to a highly degenerate binding site. *In vitro* studies have not detected a significant difference in affinity for the E box sequence between bHLH family members, and certainly not to a degree that would explain the exquisite specificity inherent in the different molecules. The myogenic code is unique in that it confers myogenic specificity to bHLH proteins, including non-myogenic regulatory factor family bHLH proteins. Understanding what the myogenic code confers to a protein may help lead to an understanding of the mechanisms by which specificity is achieved. Our results highlight the importance of low affinity DNA binding interactions and additional proteins, such as Pbx/Meis, as being critical for modulating the function of bHLH proteins. One interesting hypothesis based on the data presented is that the myogenic code may in fact only be required for

activation of critical genes, such as *myogenin*, that are capable of potentiating skeletal muscle differentiation. In addition, the ability of the myogenic code mutant version of MyoD to induce cell cycle withdrawal suggests that targets such as *Rb* or *P21*, inhibitors of progression through the cell cycle, may in fact be activated by MyoD(NN). Further studies to determine if myogenic code mutant proteins can activate transcription on a subset of endogenous genes will help to more closely identify the critical steps in myogenesis.

Methods

Plasmids

Cloning and Generation of skeletal muscle-specific Cre transgenic mice

A 954 bp fragment of the *mef2c* gene containing the skeletal muscle promoter and enhancer was isolated as a SacI/ClaI fragment from 73k-HSP68-*lacZ* (Dodou, Xu et al. 2003). This enhancer fragment was then cloned into a Cre expression plasmid containing the Cre cDNA and the SV40 splice and polyA signal sequence to create plasmid *mef2c*-73k-Cre. The approximately 2.5 kb *mef2c*-73k-Cre transgene fragment was purified as a NotI fragment and injected into the male pronuclei of fertilized oocytes as described previously (Dodou, Xu et al. 2003). MYO1565-Cre was created by excising a Acc65I/HindIII fragment from pMYO1565lacZ (Edmondson, Cheng et al. 1992), and cloning into HSP68-Cre cut with NarI, followed by blunting with Klenow, and digestion with HindIII to remove the HSP68 promoter. The approximately 3 kb MYO1565-Cre transgene was purified for injection as a Sall fragment following a double Sall/ScaI digest that cut the pBluescript backbone in half to allow for separation of the similarly sized pBluescript and MYO1565-Cre. Cre positive founder mice of both lines were identified by Southern blot using a Cre specific radiolabeled probe, which was a purified 400 bp fragment of an NcoI/BamHI digest of pBluescript-Cre, on genomic DNA isolated from tail biopsies. pBluescript-Cre was kindly provided by Shaun Coughlin. All experiments using animals complied with federal and institutional guidelines and were reviewed and approved by the UCSF Institutional Animal Care and Use Committee.

Expression vectors and pCITE clones used to analyze MEF2C regulation and function in skeletal muscle

The *mef2c* cDNA was amplified from the pCDNA1 expression vector using the following primers: 5'-gagaagaaacacggggaccatgg-3' and 5'-actatctagaaataatgtgatcatgt-3'. These primers generated a 5' NcoI restriction site that included the start codon of the *mef2c* cDNA and a 3' XbaI site that included the stop codon. These sites were used to clone the entire cDNA into the pCITE vector for protein translation to generate the plasmid pCITE-MEF2C. This cloning strategy was used to ensure that there would be no additional protein fused to the N-terminal end of MEF2C, as this has been shown previously to inhibit MEF2C DNA binding activity (Jefferey Molkentin, personal communication). pCDNA1-MEF2C has been described previously (Black, Martin et al. 1995). pRK5-MEF2-VP16 was generated by Mike Verzi. The expression vector pDP-NFATc1 was kindly provided by Jefferey Molkentin (Children's Hospital, Cincinnati, OH) and contains amino acids 241-1816 (Northrop, Ho et al. 1994). The Rel-DNA binding domain from NFATc1 was amplified using the following primers: 5'-tcccctacggatccgatgagcccgaccctg-3' and 5'-tgcgtctctagaaaaagcacc-3'. This fragment was cloned as a BamHI/XbaI fragment into pCITE2B to generate the plasmid pCITE2B-NFATc1rel. pSSR α -GATA2 was kindly provided by Walter Miller (UCSF). The GATA2 cDNA was excised from this plasmid as an NcoI fragment, blunted and cloned into pRK5 cut with XmaI. This plasmid uses the stop codon in the XbaI site of the polylinker, adding 4 amino acids to the C terminus of the protein. The human *DYSF* promoter was amplified from human DNA isolated from HEK cells and was amplified

using the following primers 5'-atgaatcaactcgagtccttg-3' and 5'-ccaatgacactcgagttgcaactg-3' and cloned by tailing with Taq polymerase and cloning into PCR2.1 using topoisomerase. A PstI/HindIII fragment was excised and cloned into pBluescript for subsequent mutagenesis. The MEF2 binding site was mutated using splicing by overlap extension (SOE) mutagenesis (Horton 1997) with the following mutagenic primers: 5'-aaattatggtgaattcttaaagaagt-3' and 5'-ctgtacttctttaagaattcaccata-3' and external primers T7x and T3x.

Expression vectors used to analyze numerous aspects of myogenic code function

A portion of the MyoD cDNA containing the entire coding region was excised from pEMSV-MyoD (Weintraub, Dwarki et al. 1991; Gerber, Klesert et al. 1997) with BspEI and HindIII and cloned into pBluescript SKII(+) to generate pBS-MyoD. Mutations of the alanine and threonine in the basic domain to asparagines were generated by the PCR mutagenesis technique of SOEing, using the mutagenic primers 5'-gctgatcgccgcaaggccaacaaca-3' and 5'-gcggcgcctcgcgcatgtgttg-3'. A PmlI/MluI fragment of the cDNA that contained the mutation was swapped into pBS-MyoD to generate the myogenic code mutant, pBS-MyoD(NN). Single mutations of the individual myogenic code amino acids separately were generated as above using the following mutagenic primers: MyoD(AmutN) – 5'-gccgcaaggccaacaccatgcgcga-3' and 5'-gcgctcgcgcatggtgttgcccttg-3'; MyoD(TmutN) – 5'-gccgcaaggccgccaacatgcgcga-3' and 5'-gcgctcgcgcatgttgccgccttg-3'. These cDNAs were subsequently cloned into the pRK5 expression vector, kindly provided by Rik Derynck (UCSF), as BamHI/XhoI [MyoD and MyoD(NN)] or BamHI/HindIII [MyoD(AmutN) and MyoD(TmutN)] to generate

plasmids pRK5-MyoD, pRK5-MyoD(NN), pRK5-MyoD(AmutN) and pRK5-MyoD(TmutN). pRK5-MyoD~E47, which contains a tethered heterodimer of MyoD and E47 (Neuhold and Wold 1993), was also provided by R. Derynck (UCSF). The myogenic code mutation was swapped into this tethered heterodimer construct as a PmlI/MluI fragment to generate plasmid pRK5-MyoD(NN)~E47. pCITE-E12 has been described previously (Black, Molkentin et al. 1998). pGEM-Pbx1A and pBluescript-Meis1 have also been described (Berkes, Bergstrom et al. 2004) and were kindly provided by Steve Tapscott (FHCRC, Seattle).

All MyoD fusions to the GAL4 DNA binding domain were generated in the expression vector pSG424, which contains the GAL4 DNA binding domain (DBD) downstream of the SV40 early promoter (Molkentin, Black et al. 1995). pSG424-MyoD-bHLH and pSG424-MyoD(NN)-bHLH were cloned as EcoRI fragments as described previously (Black, Molkentin et al. 1998). Fusions of the GAL4 DBD and full length versions of wild type or MyoD(NN) were generated by cloning the MRF cDNAs from pBS-MyoD and pBS-MyoD(NN) into the pSG424 expression vector as blunted BamHI/SalI fragments, to create plasmids pSG424-FL-MyoD and pSG424-FL-MyoD(NN) respectively. Reporter plasmid 4R-TK-luciferase has been described previously (Lassar, Davis et al. 1991). pG5E1b-*luciferase*, a GAL4 dependent reporter construct that contains 5 copies of the GAL4 binding consensus and the E1b promoter driving expression of the *luciferase* gene, was kindly provided by H. Bernstein (UCSF). The *mef2c* skeletal muscle specific promoter and enhancer was cloned as an XbaI-SpeI fragment from a previously described pBluescript parent (Dodou, Xu et al. 2003) into

pAUG-Bgal (McFadden, Charite et al. 2000) to create the reporter plasmid *mef2c-73K-lacZ*.

Mgn184-luciferase was generated by cloning a PstI/KpnI fragment from the previously described *myogenin* reporter plasmid pMyo184-*lacZ* (Cheng, Hanley et al. 1992) into HSP68-*lacZ* (McFadden, Charite et al. 2000), followed by excision of the fragment as a KpnI fragment and cloning into pG13-basic (BD Biosciences Clontech). Mutations in *Mgn184-luciferase* were generated by PCR mutagenesis with the following mutagenic primers: Noncanonical E box mutation (mutNC) -5'-gtgcaggaattccttagaggg-3' and 5'-ccctctaaggaattcctgcac-3'; Pbx/Meis binding site mutation (mutPbx) -5'-actggaacgtcggtcggtgcagc-3' and 5'-ctgttgctgcaccgaccgacgtt-3'; Canonical E1 E box mutation (mutE1)– 5'-aatggcaccagcagtcgacgtg-3' and 5'-acggggtgacgtcgactgctggg-3'. Deletion of canonical E box E2 was achieved by truncating the proximal end of the promoter by 40 base pairs, by cleaving with PciI, followed by Klenow treatment to fill in overhanging ends and re-ligating, such that the enhancer sequence ended just prior to the second E box (mutE1/E2).

Mouse work, histology, stains and immunohistochemistry

Analysis of Cre expression and recombination in *mef2c-73k-Cre* and *MYO1565-Cre* transgenic mice

Transgenic male founders or transgenic male offspring of female founders were crossed to female ROSA26R *lacZ* reporter mice (Soriano 1999). Embryos were collected at 11.5 dpc and stained with 5-bromo-4-chloro-3-indolyl Beta-D-galactopyranoside (X-Gal) to detect beta-galactosidase activity, as previously described (Anderson, Dodou et al. 2004). After establishing three transgenic lines that exhibited robust skeletal muscle specific expression, embryos or neonatal tissues were collected for X-gal staining. For analysis of sections, representative X-gal stained embryos or neonatal tissues were prepared and stained as described previously (Anderson, Dodou et al. 2004) and counterstained with Neutral Fast Red for better visualization of histology. Immunohistochemistry (IHC) was performed on paraffin sections of neonatal limbs, as described previously (Anderson, Dodou et al. 2004). Tissues were collected, fixed, and sectioned at a thickness of 5 μ m, and sections were blocked for 20 min in 3% normal goat serum diluted in PBS. Mouse monoclonal anti-skeletal muscle myosin (MY-32; Sigma) and rabbit anti-beta-galactosidase (ICN) were diluted 1:300 in 3% normal goat serum. Incubation in both primary antibodies was performed concurrently for 1 h at room temperature in a humid chamber. Following incubation with the primary antibodies, the sections were washed three times for 10 min each wash with PBS. The secondary antibodies, biotin-conjugated goat anti-rabbit (Molecular Probes) and tetramethyl rhodamine isocyanate (TRITC)-conjugated anti-mouse (Sigma), were diluted 1:300 into 3% normal goat serum, and slides were incubated in both for 1 h at room temperature in a humid chamber in the dark. Following incubation, the secondary antibody mix was removed and replaced by Streptavidin-Alexa Fluor (SA-488, Molecular Probes) diluted 1:500 in 3% normal goat serum in PBS for 1 h. After washing three times for 10 min in PBS, slides were mounted

using SlowFade Light antifade kit (Molecular Probes) and photographed on a fluorescence microscope.

Generation of *mef2c* skeletal muscle specific knockout mice

Conditional *mef2c* KO mice were obtained from John Schwarz (Vong, Ragusa et al. 2005). These mice have loxP sites flanking the second coding exon, which encodes the majority of the MADS and MEF2 domains of MEF2C. Thus, Cre recombinase creates an allele that lacks the DNA binding and dimerization domains of the protein, which creates a functional null. The skeletal muscle specific expression of Cre was provided by *mef2c*-73k-Cre or MYO1565-Cre expressing mice, as described in Chapter 2. These mice were crossed into a heterozygous *mef2c* background, *mef2c* +/- (Lin, Schwarz et al. 1997).

Once generated, male Cre Tg/0; *mef2c* +/- mice were crossed with female mice homozygous for the conditional allele of *mef2c*, *mef2c* Flox/Flox (Figure 4-1). This strategy was utilized for both 73k lines, 44k and 453G, and a MYO1565-Cre line, 641A. Genotyping of putative KOs was done using a Southern blot strategy. Cre was analyzed by Southern blot using an EcoRV digest of genomic tail DNA. The Cre probe used was an NcoI/BamHI fragment of the Cre cDNA, excised from pBS-Cre, kindly provided by Hiroshi Kataoka in the lab of Shaun Coughlin (UCSF). The *mef2c* genotype was determined on a PstI digest using a probe derived from the *mef2c* locus. The *mef2c* probe (Tm1) was generated by Dustin Khiem using the primers 5'-gctaaagcgcgatgctccagactg-3' and 5'-gagattatctgggtaatgtgggc-3'. The resulting 600bp fragment was gel purified following BglII/XmaI digestion. Both the Cre and Tm1 probes were hybridized at 1×10^6 cpm/ml in "Anker Hyb" (600mM NaCl, 8mM EDTA, 120mM Tris pH 7.4, 0.2%SDS,

0.1% tetrasodium pyrophosphate, 2% boiled and sheared Salmon Sperm DNA, 1% powdered milk, 10% Dextran Sulfate) at 58°C overnight. Blots were washed in the hybridization bottle with a 2x SSC/0.1%SDS solution, once quickly, followed by two ten minute washes. The EcoRV band indicating a mouse positive for the *mef2c*-73k-Cre transgene appears at approximately 700 bp for 73k lines and as a doublet migrating at approximately 4kb for MYO1565-Cre line 641A; the various alleles of *mef2c* run as follows on a PstI digest: WT 3.3kb, TM1 1.8kb, Flox 2.7kb, Recombined 1.3kb. All mice from litters intended to generate conditional knockout mice were weighted on the evening of the day of birth and this was designated P1. Overall body weight was also measured on P4, P7, P10, P14, P21 and P28 always in the late afternoon or early evening.

Skeletal muscle histology

Individual skeletal muscles were dissected out by identifying the tendons on either side of the muscle and severing to release intact muscles. Depending on the intended use of the muscle, it was processed for paraffin or frozen sections. Paraffin was used mainly for gross histology and the MY32 antibody, which recognizes all fast type muscle fibers, and works thus far exclusively on paraffin sections. For this process, muscles were dissected directly into 4% paraformaldehyde (PFA) in 1x PBS at approximately pH 7, as indicated by the salmon pink color of a phenol red indicator. After fixing overnight, muscles were quickly rinsed in 1x PBS, and then washed in 1x PBS for approximately 8 h. Muscles were then transferred to 70% methanol in 1x PBS until processed for embedding. All embedding was done in a pressurized tissue processor to allow for sufficient infiltration of the wax (Leica). Small muscles (Soleus, EDL, ECRL) were dehydrated by the

machine using the LacZ embryos program (60 min 80% ethanol, 120 min 95% ethanol, 240 min 100% Ethanol, 60 min xylene, 70 min embedding paraffin). Larger muscles were nutated in 100% methanol overnight at 4°C, followed by approximately 1 h in toluene at room temperature. When sufficiently cleared (only opaque tissue remaining is tendon) the muscles were placed in a wax only program in the tissue processor, which applied pressurized wax for four hours. All muscles were sectioned at 5 µm for histology and immunohistochemistry.

Tissue for frozen sections was attached to a piece of cork (a half circle of approximately 1/8 inch thick, sliced from a wine bottle cork) using OCT embedding medium (Tissue Tek 4583). The muscle was not put into PBS after dissection, and was sufficiently dried before freezing, as excess moisture causes disruptions in the muscle membrane when it expands upon freezing. The muscles were cut in half using two razor blades simultaneously, pulling in opposite directions to generate a clean cut. The halves were then either stood on end to generate transverse sections, or laid on the side to generate longitudinal sections. Once placed, the muscle was surrounded by OCT to stabilize the orientation and the whole cork was lowered into liquid nitrogen cooled isopentane. The alcohol was deemed to be the correct temperature for freezing when ice crystals formed around the inside of the glass, but then dissolved upon stirring. Tissues were agitated in the frozen alcohol for approximately 15 sec, followed by 2 min without agitation. The frozen samples were then placed on dry ice to allow the alcohol to evaporate. If necessary, more OCT was added at this time to allow for an even surface for sectioning. Frozen sections were used for gross histology, periodic acid and Schiff's base (PAS) stain

for glycogen, antibody staining, and myofibrillar ATPase staining that requires the enzymatic function of the muscle myosin to distinguish fiber type (See below).

Determination of fiber number/Area

In order to determine fiber area and number, paraffin sections of soleus, EDL and ECRL muscles were stained with 50 mg/ml Wheat Germ Agglutinin (WGA) conjugated to TRITC in 1x PBS. This protein intercalates into all membranes, including plasma and nuclear membranes, making the outline of the fibers easy to determine. For the staining protocol, paraffin sections were de-waxed for 3 min in xylene, followed by re-hydration in a series of ethanol washes for 1 min each. Once in water, slides were moved to PBS and incubated for 5 min. 50 μ l of 50 mg/ml WGA-TRITC was added to each slide and spread evenly by covering with a glass cover slip. Slides were incubated for 40 min at room temperature, followed by a 30 min wash in 1x PBS. Cover slips generally came off easily, but in some cases submerging in PBS was necessary for gentle removal, as forcing the cover slip off will damage the tissue. Slides were mounted in Slow Fade Gold (Molecular Probes, Invitrogen) for photographing on a fluorescent microscope at 10x magnification. Images were changed to grayscale and the brightness and contrast were increased in Photoshop (Adobe CS2). These images were printed and fiber number was counted manually. In addition, the altered images were saved as TIFF files and imported into ImageJ for area measurement (NIH). In ImageJ, the scale was set for each image (analysis menu >reset > check scale) to 1.684 pixels per μ m, as this is the conversion for 10x magnification on the microscope used (Nikon Microphot-FXA). In order to determine this conversion factor, a line of known length was drawn on a picture using the

Spot Advanced software. This picture was opened in ImageJ and the number of pixels in that line was determined using the calibrate menu. Using the trace tool (shaped like a kidney bean) the perimeter of 20 fibers per field were traced and measured (Analyze >Measure).

Fiber typing

Mouse monoclonal anti-skeletal muscle myosin (MY-32; sigma) was diluted 1:300 in 3% normal goat serum in 1x PBS. Incubation of the primary antibody was performed for 1 h at room temperature in a humid chamber. The sections were then washed in 35 ml of 1x PBS in a Coplin jar for 30 min. The secondary antibody, Alexa Fluor 498 anti-mouse (Molecular Probes, Invitrogen), was diluted 1:300 in 3% normal goat serum, and slides were incubated for 1 h at room temperature in a humid chamber in the dark. Following incubation, the secondary antibody was removed and slides were washed three times for 10 min in PBS. Slides were then mounted using SlowFade Light antifade kit (Molecular Probes) and photographed on a fluorescence microscope. Staining with this antibody indicates a fast twitch fiber type, but does not distinguish between types IIA/X/B. This stain is most useful when determining the number of type I fibers as a percentage of total fibers.

To determine the percentage of type IA and type IB fibers, we utilized the metachromatic staining method of Ogilvie and Feedback (Ogilvie and Feedback 1990). Fresh frozen sections were pre-incubated for 8 min in 0.025 M potassium acetate, 9 mM calcium chloride-dihydrate, pH to 4.5 with glacial acetic acid. Sections were then rinsed 3 times

in 0.1 M Trizma base (Sigma) and 0.018 M calcium chloride-dihydrate for 2 min each wash, followed by incubation for 25 min in 0.154 M ATP-disodium salt, 0.053 M glycine, 0.029 M calcium chloride, 0.065 M sodium chloride, 0.048 M sodium hydroxide, pH 9.4. Sections were then rinsed 3 times in 0.014 M calcium chloride-dihydrate. Staining was achieved by incubation for 1 min in Toluidine blue, followed by rinsing for 5 s in deionized water, and dehydration in a series of ethanol washes. Stained sections were cleared with xylene and mounted with Cytoseal 60 (Richard-Allan Scientific 8310-16). This method allows for the clear determination of type I (dark staining) and IIa fibers (intermediate staining), but distinguishing IIb from II d/x subpopulations is difficult and subjective as these stain with nearly the same intensity.

Exercise

mef2c skeletal muscle specific knockout mice and wild type (*mef2c* flox/+, No Cre) littermates were subjected to a voluntary running assay. Mice were housed in a normal mouse cage with the majority of the bedding removed, to prevent building of a nest that would impede the running wheel. 4.5 in diameter running wheels (Super Pet Mini Run Around) were purchased from www.healthypetstore.com, and were hung from the side of the cage. This required bending of the hooks that are intended for hanging to accommodate the thicker plastic of the mouse cages. A small bar magnet was attached to the running wheel using super glue. This magnet was placed in such a way that it traveled past the detector for a Sigma Sport BC600 or BC800 bicycle computer attached to the arm holding the wheel in place. The computers were purchased from REI (www.rei.com). A wheel size of 0359 was entered into the computer, which corresponds

to the circumference of the wheel in mm, and allows the computer to compute distance traveled from the number of revolutions turned by the wheel.

Mice were put into the exercise cages in the evening of day 0, and allowed to train for three days. The data generated in these three days was not included in the final averages of distance or time traveled per day. On day 4, time and distance was recorded at 10 am and the computers were reset. This continued for 7 or 42 days, depending on the experiment. When the values for running were exceedingly low (generally less than 10 min overall run time), the function of the wheel was double checked, prior to including that evening in the overall average. When wheel function was compromised due to misalignment or a dead battery in the computer, the data were not included. No run controls were moved into separate cages, similar to the running mice, with separate water bottles on a cart separate from the greater mouse colony.

Mice were sacrificed after running by injection of 10 mg/ml pentobarbital at 100 μ l/10g body weight. Blood was drawn through the vena cava with a 26 gauge needle on a 1ml luer-lok syringe containing 100 μ l of a 4% (w/v) sodium citrate solution (Sigma S5770) to prevent coagulation. Blood was spun at 5000 rpm for 5 min at 4°C to separate serum from cellular matter. Serum was transferred to a clean tube and stored at -80°C for further analysis of creatine kinase activity, and glucose levels (see below).

Individual muscles were dissected into 4% PFA or frozen (in liquid nitrogen cooled isopentane as described above) for histology. Muscles were added to TRIZOL

(Invitrogen 15596-018) for RNA extraction or flash frozen in liquid nitrogen for further protein extraction. These samples were stored at -80°C until further processing. In addition, the tibia was dissected out by cutting the tendons at both the proximal and distal joints and carefully cleaning away excess tissue. The tibia was measured using calipers for more accurate determination of length. In addition, the extensor digitorum longus (EDL) muscle from the left hindlimb was digested in tail buffer (10mM Tris pH 8.0, 25mM EDTA pH 8.0, 100mM NaCl, 1% SDS + 0.2 mg/ml Proteinase K) for DNA preparation. This DNA was used for Southern blot to measure the ratio of a mitochondrial gene to a nuclear gene, as a measure of the number of mitochondria per nucleus in a particular muscle. The DNA from one muscle was resuspended in 30 μL TE (10mM Tris pH 7.4, 0.1mM EDTA H 8.0) and 20 μl was digested with SpeI/EcoRI to yield a 1.1 kb band when hybridized with a probe that recognizes a region of the nuclear genome, exon 3 of the *myogenin* gene (Ex3). Two of the remaining 10 μl were digested with PstI/EcoRV to yield a 2.6 kb band when hybridized with a probe that recognizes a gene in the mitochondrial genome, *cytochrome b* (*Cytob*). The cytochrome b cDNA was kindly provided by Francisco Naya (Naya, Black et al. 2002). The Ex3 probe was excised from the vector pBS-Ex3 with SpeI and EcoRI, and was hybridized in Anker Hyb at 58°C , and was washed in the hybridization bottle once quickly with blot wash one (2x SSC, 0.1% SDS), then twice for 10 min with blot wash one. The *Cytob* probe was excised from the vector pCR4-TOPO with EcoRI, was hybridized at 65°C , and was washed in the hybridization bottle once quickly with blot wash one, for 10 min with blot wash one, followed by 10 min with blot wash two (0.2x SSC, 0.1% SDS). Both Southern blots were exposed to film overnight to visualize the bands. The blots were then exposed

to a phosphorimager screen to allow for quantitation of the ratio of nuclear gene signal to mitochondrial gene signals (Molecular Dynamics). For the calculation of pixel density in the scanned blots, the background values were set to local average to avoid differences in the normalization due to variation of the background over the length of the blot.

Creatine kinase activity of serum samples was measured using the protocol recommended by Sigma Aldrich. Briefly, muscle was homogenized on low speed using the Powergen 35 tissue homogenizer (Fisher) in ice cold protein extraction (PE) buffer (5mM HEPES pH 8.7, 1mM EGTA, 1mM DTT, 0.1% Triton x-100) at 50 mg/ml wet weight. Cellular proteins were extracted for 1 h at 4°C. The Reaction Cocktail (RC) for 60 samples was prepared as follows: 36 ml dH₂O; 10 ml 250 mM Glycylglycine buffer with 0.1% BSA, pH 7.4; 2 ml 400 mM phosphocreatine (dissolved in dH₂O); 2 ml 40 mM ADP (dissolved in dH₂O); 2 ml 1M D-glucose (β-D(+)) glucose dissolved in dH₂O); 1.2 ml 20 mM β-nicotinamide (dissolved in dH₂O); 800 μL 300 mM magnesium acetate. The pH of the RC was carefully adjusted to 7.4 with 1 M NaOH. 0.9 ml of RC was added to a cuvette suitable for monitoring absorbance at 340 nm. 30 μl of 300 units/ml hexokinase and 30 μl of 10 units/ml glucose-6-phosphate dehydrogenase (both diluted in dH₂O) were then added to the RC. This was inverted to mix and allowed to equilibrate until absorbance at 340 nm was constant. At this point, 30 μl of unused PE buffer or extracted muscle was added to the cuvette, immediately mixed and absorbance at 340 nm was recorded at 5 minutes. The Units/ml of enzyme in the extracted protein is equal to $(\Delta\text{Abs}_{340}/\text{min Sample} - \Delta\text{Abs}_{340}/\text{min Blank})(\text{dilution factor})/(6.22*0.03)$. The denominator is the

millimolar extinction coefficient of β -NADPH at 340 nm times the volume of sample added (0.03 ml).

Serum glucose was determined using the Therasense Freestyle brand diabetes meter (kindly provided by Jean Regard in the lab of Shaun Coughlin, UCSF, see below). 5 μ l of serum was pipetted onto parafilm to allow administration to the input area of the glucose reading strips used in the Freestyle meter.

Electron Microscopy

Mice were exercised for one week prior to collecting muscles for processing for electron microscopy. Mice were injected with 10 mg/ml pentobarbital at 100 μ l/10 g body weight, and perfused with saline through the left ventricle to remove blood from the circulatory system. The right atrium was cut away from the heart to provide an outlet for perfused fluid. When the solution coming from the heart was clear, the perfusion was switched to a solution of 2% glutaraldehyde (EM grade, Sigma G5882) in 0.1 M sodium cacodylate trihydrate pH 7.6 (Electron Microscopy Sciences 12310). Mice were perfused for 8 min, until quite rigid. These perfusions were kindly performed by Ivo Cornelissen in the lab of Shaun Coughlin (UCSF). Further processing of the tissue, including cutting 100 nm sections and shading for EM was kindly performed by Andrew Tauscher in the lab of Jennifer Lavail (UCSF). In addition 1 μ m sections were cut and stained with 1% Toluidine blue (Sigma 89640) in 1% sodium borate for gross histological analysis.

Glycogen

Glucose reading strips were purchased from www.AmericanDiabetesWholesale.com. These strips only require 0.3 μ l of blood and therefore blood glucose can be determined with a small drop of blood from the tail of the animal. We immobilized the mice in the largest apparatus possible to minimize the stress of the animal, as the release of epinephrine causes an increase in blood sugar. We then nicked the tail with a clean razor blade and squeezed slightly to generate a small drop of blood. Glucose tolerance tests (GTT) were performed after fasting for 16 hours (from 6 pm-10 am) in a clean cage. Changing the cage is crucial, as there is a significant amount of crumbled food in the bottom of a cage. Mice were injected intraperitoneally (IP) with 2 g glucose/kg body weight in LPS free saline (0.9% NaCl), and blood glucose levels were checked at 0, 30, 60, and 120 min post injection. Data were normalized by dividing all values by the starting blood glucose. Insulin tolerance tests (ITT) were performed between 9-10 am, to ensure similar time in the daily cycle of eating and glucose mobilization. No fasting was done prior to these experiments. Insulin from bovine pancreas was purchased as a resuspended stock from the UCSF cell culture facility at 24 U/ml (Sigma I5500). Mice were given one dose of insulin per day by IP injection of 1.5, 1.0, 0.75, or 0.5 Units of insulin/kg body weight. Insulin was diluted in LPS-free saline and data were normalized by dividing all readings by the blood sugar level at baseline. The rate of blood sugar decrease during a fast was analyzed at 0, 3, 6 hours post food withdrawal and the liver of fasted animals was harvested at 7 hours for PAS staining (see below).

PAS staining for glucose was done on fresh frozen sections of skeletal muscle and liver using the protocol described in *Muscle Pathology and Histochemistry*, Harvey B. Sarnat,

American Society of Clinical Pathologists Press (1983). All steps were done at room temperature in a fume hood. Sections were fixed in Carnoy's fixative (60% ethanol, 30% chloroform, 10% glacial acetic acid) for 5 min, followed by rinsing three times in deionized water. Sections were immersed in 0.5% periodic acid (Sigma P7875) for 5 min, followed by rinsing in deionized water four times. Sections were then transferred to Schiff's solution (Sigma 3952016) for 10 min, followed by rinsing in running tap water for 10 min. For mounting, sections were dehydrated in a series of Ethanol, cleared in xylene and mounted using Cytoseal 60 mounting medium (Richard-Allan Scientific 8310-16). PAS staining is evident as a pink/purple precipitate on the slides. To control for PAS staining of glycogen, we included a diastase control. This enzyme cleaves glycogen, but not the other polysaccharides that PAS staining will detect, thereby making evident the glycogen specific portion of the stain. An additional incubation in 0.5% α -amylase for 60 min at room temperature was included after the first set of rinses, prior to treatment in periodic acid to allow for glycogen digestion.

Total glycogen content in muscle and liver was quantitated using an adaptation of Hassid WZ and Abraham S, *Methods in Enzymology*, 1957 (Hassid WZ 1957). Briefly, 20-100 mg of frozen tissue was dissolved in 1 ml 5N KOH by boiling with occasional shaking until dissolved. 0.2 ml of saturated sodium sulfate and 1.5 ml ethanol was added and mixed by vortexing. This mixture was heated until bubbles formed in a boiling water bath, approximately 1-2 min. After cooling on ice, samples were spun at 2000g for 10 min at 4°C and the supernatant was discarded. The pelleted material was resuspended in 0.5 ml 2 M HCl, vortexed, and incubated in a boiling water bath for 2-2.5 hours. After

this incubation, samples were cooled and neutralized to pH 6-8 with 4 N KOH, 0.1 M triethanolamine. Glucose of this solution was measured using the hexokinase method glucose assay kit as recommended by the manufacturer (Sigma GAHK20). Briefly, the following mixtures were incubated for 15 min at room temperature: (1) 10-200 μ l extracted glycogen solution in 1 ml of glucose assay reagent, (2) 10-200 μ l extracted glycogen solution in 1 ml dH₂O and (3) 10-200 μ l dH₂O (same volume as glycogen solution above) in 1 ml of glucose assay reagent. The absorbance of these samples was measured at 340 nm versus a blank of deionized water. The total blank (A_{TB}) was calculated as the A_{340} of samples (2) + (3) above. The mg glucose/ml solution in the original sample was calculated as $(\Delta A)(TV)(F)(0.029)/(SV)$, where $\Delta A = A_{\text{sample}} - A_{TB}$, TV is the total assay volume (1 ml assay reagent plus μ l sample) in ml, F is the dilution factor of the added sample (dilution may be necessary to get the sample between 0.5 and 50 μ g of glycogen) and SV is the sample volume in ml.

RT-PCR

Total RNA from skeletal muscle was isolated using TRIZOL as recommended by the manufacturer (Invitrogen 15596-018, see microarray section below for more detail). cDNA was generated using the Omniscript kit from Qiagen, with slight modifications. Briefly, each reaction contained 2 μ l 10x buffer RT, 2 μ l 5 mM dNTP mix, 1 μ l RNase inhibitor diluted to 10 Units/ μ l, 1 μ l Reverse Transcriptase, 1 μ g of TRIZOL-extracted RNA and dH₂O up to 17 μ l for each sample. To this, 3 μ l of a 50 ng/ μ l Random Primer mix (Invitrogen 48190-011) was added per sample followed by incubation for 60 min at 37°C. Following the RT reaction, 1 μ l of cDNA was added to a 25 μ l PCR containing

1 μ l 10 mM dNTPs, 2.5 μ l 10x Taq buffer, 1 μ l 25 mM MgCl₂, 0.5 μ l Taq Polymerase (Promega), 1 μ l of each primer (25 or 100 ng/ μ l as indicated below) and 17 μ l dH₂O. Primer sequences used to analyze the transcript levels are described in Table 1.

Table 1. Sequence of RT-PCR primers used to measure levels of genes involved in glucose metabolism in *mef2c* skeletal muscle KO muscle

Gene	Forward Primer	Reverse Primer
GLUT4	5'- gggggaccgattccatccc -3'	5'- cccgaagatgagtgggggcg-3'
ERR1 α	5'-ggcctctggctaccactacgg-3'	5'-ctgggtcaggcatggcgtaca-3'
PGC-1 α	5'-cacgcagccctattcattgttcg-3'	5'-gcttctcgtctctttgcggat-3'
FABP	5'-gaagtcactcgggtggtggc-3'	5'-gtcaggatgagttcccgtc-3'
HIF-1 α	5'-gtggatatgtctgggtga-3'	5'-attcttcgcttctgtgtctt-3'
GAA	5'-cctgggggaacacctcagcc-3'	5'-atccagcgggaagtgtgtcc-3'
Insulin Receptor	5'-ccaggcaccgccaagggcaa-3'	5'- cagaccttagggcagggtcc-3'
PYGM	5'- ctggggctcgtgcctatgg-3'	5'-tcctggagggtggcagccac-3'
Glycogen Synthase 2	5'-gaggtgacagaccacgcaga-3'	5'-gcaaactctgtatcctggcc-3'
Glycogen Synthase 1	5'-ctggcgctgtggacttctac-3'	5'-tgtttgcgcacggcttggcc-3'
GanaB	5'-ccagagggccccagggtcc-3'	5'-cagaagatcccaggtctcg-3'
GSK3a	5'-tccgggggtggccccagcgg-3'	5'-agaaaaagtaccgcagcctc-3'
GSK3b	5'-ggccagggtcctgacaggcc-3'	5'-cattgggctctcctcggacc-3'
gapdH	5'-ccatggagaaggctgggg-3'	5'-caaagttgcatggatgacc-3'
α -actin	5'-aggtcatcaccatcggaatg-3'	5'-cgtcgtactcctgcttgggtg-3'

PCR conditions were as follows: 94°C for 5 min, varied number of cycles (typically 15, 25 or 30) of 94°C for 30 sec, 56°C for 1 min, 72°C for 1 min, 30 sec, with a final polish at 72°C for 10 min.

Microarray

Crural muscles from neonate mice were collected immediately after birth. This group of muscles is the superficial large complex in the lateral, dorsal portion of the hind limb, the gastrocnemius lateralis, gastrocnemius medialis, soleus and plantaris muscles. Muscle was dissected immediately into 500 μ l of TRIZOL RNA isolation reagent (Invitrogen 15596-018) on ice, and stored at -80°C . The litters dissected were generated by crossing a male *mef2c* +/-; MYO1565-Cre Tg/0 mouse with a female *mef2c* flox/flox mouse. Skeletal muscle knockout mice were generated at a frequency of $\frac{1}{4}$ using this breeding strategy. DNA extracted from the tails of these mice was genotyped for *mef2c* and Cre status as described above, but in addition, the sex of these animals was determined by PCR. This was critical, as differences between the sexes are known to have dramatic effects on metabolic disorders. Primers for ZFY, a locus present only on the Y chromosome, were kindly provided by Cecile de la Cruz in the lab of Barbara Panning (UCSF). The primer sequences are as follows: 5'-gataagcttacataatcacatgga-3' and 5'-cctatgaaatcctttgctgc-3'. A 20 μ l PCR reaction was prepared as follows: 15.5 μ l dH₂O, 0.5 μ l template DNA, 0.4 μ l 10 mM dNTPs, 0.4 μ l of each primer (20 μ M), 0.6 μ l 25 mM MgCl₂, 2 μ l 10X Taq polymerase buffer with 15mM MgCl₂, 0.2 μ l 5U/ μ l Taq polymerase. These reactions were subjected to the following PCR conditions: 95 $^{\circ}\text{C}$ for 5 min, 30 cycles of 95 $^{\circ}\text{C}$ for 30 sec, 55 $^{\circ}\text{C}$ for 1 min, 72 $^{\circ}\text{C}$ for 1 min, and a final polish at 72 $^{\circ}\text{C}$ for 10 min. A band, indicating possession of a Y chromosome, and therefore a male mouse, runs at approximately 600 bp.

Neonatal crural muscles were homogenized in TRIZOL by repeatedly pipetting with decreasing bore pipette tips to achieve dissociation of the tissue. All tissue but tendon was readily dissociated in this manner. Homogenized tissue was incubated in TRIZOL for 5 min at room temperature to facilitate disruption of protein/nucleic acid complexes. 100 μ l of chloroform was added, followed by vigorous shaking by hand for 15 seconds. 600 μ l was added to a Phase Lock Gel Tube and centrifuged for 10 min at 12,000 rpm at 4°C. The upper colorless phase was removed to a fresh tube and 250 μ l of isopropanol was added, followed by incubation at room temperature for 10 min. RNA was pelleted by centrifugation for 10 min at room temperature. The supernatant was removed and the pellet was washed by vortexing in 500 μ l of 75% ethanol. Washed RNA was re-pelleted at 9,000 rpm for 5 min in a microfuge at 4°C. The supernatant was removed and the pellet was air dried, with close attention paid to not over drying the pellet. This is critical, as the RNA will not go into solution readily if over dried. RNA was dissolved in 30 μ l RNase free water. One μ l was set aside for quantity and quality analyses, and 71 μ l was added to the remaining RNA to bring the total volume to 100 μ l. This volume was purified using the Qiagen RNeasy mini kit as recommended by the manufacturer. Briefly, 350 μ l of RLT buffer (plus β -ME) was added to the diluted RNA and mixed by hand followed by 250 μ l of 100% ethanol. This was mixed by pipetting and the sample was applied to an RNeasy column and spun at full speed for 15 seconds at room temperature. Flow through was discarded and 500 μ l RPE wash buffer (plus Ethanol) was added. The column was spun for 15 seconds in a microfuge at max speed, and the flow through was discarded. An additional 500 μ l was added and the column was spun for 2 min to dry the membrane. The column was carefully transferred to a new 1.5 ml

ependorf tube, and 30-50 μ l of RNase free water was added to the membrane. After a 4 min incubation at room temperature, the column was spun for 1 min to elute RNA. At this point, RNA was checked for quantity and purity by determining absorbance at 260 and 280 nm.

To generate amplified, biotin labeled RNA for microarray hybridization, the Ambion MessageAmp II-biotin kit (cat# 1761) was used as recommended by the manufacturer. Briefly, a mixture of 1 μ l of T7 Oligo(dT) primer and 1 μ g total RNA diluted with dH₂O to a total volume of 12 μ l, was incubated in a thermalcycler for 10 min at 70°C. Following this incubation, 2 μ l 10x first-strand buffer, 4 μ l dNTP mix, 1 μ l RNase inhibitor and 1 μ l ArrayScript reverse transcriptase were added and the mixture was then incubated for 2 h at 42°C. Second-strand cDNA was synthesized by adding 63 μ l nuclease free dH₂O, 10 μ l 10X second-strand buffer, 4 μ l dNTP mix, 2 μ l DNA polymerase and 1 μ l RNase H and incubating at 16°C for 2 h. 250 μ l of cDNA binding buffer was added to the cDNA, which was then purified using the columns provided with the kit and eluted with 2 x 12 μ l of 55°C dH₂O. 20 μ l of purified double stranded cDNA was mixed with 12 μ l biotin-NTP mix, 4 μ l T7 10x reaction buffer and 4 μ l T7 enzyme mix and incubated at 37°C for 15.5 hours. After purification over the provided columns, the final amplified RNA was quantitated by determining absorbance at 260 nm, and was fragmented using the Ambion fragmentation reagents (cat# 8740) as recommended. Briefly, 20 μ g of RNA was diluted to 18 μ l with dH₂O and 2 μ l of fragmentation reagent was added followed by incubation for 15 min at 70°C. 2 μ l of stop solution was added and fragmented, amplified, biotin-labeled RNA was stored at -80°C until further use.

***Mef2c* skeletal muscle conditional KO in a *mef2a* null background**

Mice harboring a null allele of *mef2a* were kindly provided by Francisco Naya (Naya, Black et al. 2002). PCR genotyping of the *mef2a* locus was done using the following primers: *mef2a*5'-5'-gctagccaacatttcaccttgagatct-3', *mef2a*3'-5'-caacgatatccgagttcgtcctgctttc-3' and neo5'-5'-ttggctaccctgatattgctgaagagc-3'. A mix of all three primers was made with the following concentrations: 12.5 μ M *mef2a*5', 25 μ M *mef2a*3', and 50 μ M neo5'. 1 μ l of the primer mix was added to 2.5 μ l 10x Taq buffer with 15mM MgCl₂, 1.5 μ l 25 mM MgCl₂, 2 μ l 2.5 mM dNTPs, 0.5 μ l Taq polymerase, 1 μ l DNA template and 16 μ l dH₂O to a final volume of 25 μ l. PCR conditions used were 94°C for 1 min, 30 cycles of 94°C for 30 sec, 60°C for 30 sec, 72°C for 30 sec, and a final polish at 72°C for 5 min. The resultant bands are 310 bp for the WT allele and 470 bp for the *mef2a* knockout allele. Heterozygous animals generated both bands after PCR analysis. Male mice harboring one null allele of *mef2a* were crossed with a *mef2c* flox/flox female to generate *mef2a* +/-; *mef2c* flox/+ animals. These were re-crossed to a flox/flox female to generate *mef2a* +/-; *mef2c* flox/flox animals. These mice were then crossed to animals of the genotype *mef2a* +/-; *mef2c* +/-; *mef2c*-73k-Cre Tg/0, which were generated by crossing *mef2a* heterozygous (*mef2a* +/-) mice to *mef2c* heterozygous Cre transgenic (*mef2c* +/-; *mef2c*-73k-Cre Tg/0) mice. The resultant offspring were sacrificed immediately after birth, skinned and placed into 4% PFA for at least 48 h. These animals were then rinsed extensively in 1x PBS by nutating at 4°C for 8 h with numerous PBS changes. The fixed neonates were then dehydrated by sequential washes in 70% and 100% methanol at 4°C on a nutator. Neonates were cleared by

nutating in glass vials of toluene until transparent, and embedded using a 4 h wax only program on the Leica tissue processor. Animals were sectioned at 5 μm for histological analyses of relevant tissues.

Electrophoretic Mobility Shift Assays (EMSA)

DNA binding assays were completed at room temperature using binding buffer conditions as described previously (Dodou, Xu et al. 2003). Proteins were generated by coupled in vitro transcription-translation reactions (TNT, Promega) and addition of protein to each EMSA was normalized by quantitation of [^{35}S]-methionine-labeled proteins generated in parallel reactions. Quantitation was conducted by phosphorimager analysis using ImageQuant v1.2 software (Molecular Dynamics). Radiolabeled double stranded oligonucleotide probes were generated using Klenow to fill in overhanging ends with α -[^{32}P]-dCTP. The sense strand sequences of the oligonucleotides used for EMSA are presented in Table 2. A total of 4 μl of lysate, consisting of 1 μl E12, and a combination of MRF and unprogrammed lysate totaling 3 μl , or 4 μl MEF2C or 4 μl NFATC1-rel was incubated in 1x binding buffer (40 mM KCl, 15 mM HEPES pH 7.9, 1 mM EDTA, 0.5 mM DTT, 5% glycerol), with 0.5 μl poly dI:dC (1 mg/ml) and 1 μl either of water or unlabeled oligonucleotide competitor at 500 $\mu\text{g}/\mu\text{l}$ for 10 min prior to addition of labeled probe (20,000 cpm total). After a 20 minute incubation with labeled probe, the entire reaction was loaded on a 6% nondenaturing polyacrylamide-TBE gel and run at 150V for 2 h at room temperature. Kinetic EMSA were performed as above, except after the addition of probe, the reactions were allowed to equilibrate at 25°C for 1 h. To check

that the system had reached equilibrium the experiment was repeated with 2 h and 4 h incubations to ensure comparable results. Unlabeled oligonucleotide competitor was

Table 2. Sequence of oligonucleotides used for EMSA analysis

Oligonucleotides for EMSA	Sequence of sense strand
Mef2c-E2-Ebox	5'-gagtgacatgaacaggtgcaccctggcctg-3'
Mef2c-E1-Ebox	5'-ggtataccatagaaagcc-3'
IL-4-NFAT	5'-gggtacattgaaaattttattacac-3'
mutIL-4-NFAT	5'-gggtacattccttaattttattacac-3'
73k-NFAT	5'-gggccgattggatattttccattgga-3'
mut-73k-NFAT	5'-gggccgattggatattaaggattgga-3'
myg-MEF2	5'-ggcgttgctatatttatctct-3'
RatGLUT4-MEF2	5'-ggcgtgggagctaaaaatagccat-3'
mutRatGLUT4-MEF2	5'-ggcgtgggaggggaaaatagccat-3'
PYGM-MEF2	5'-ggtggcagtttaatttagcagctctg-3'
mutPYGM-MEF2	5'-ggtggcagttggatttagcagctctg-3'
AMPK1-MEF2	5'-ggaaaccattttatttttagcatggtgc-3'
mutAMPK1-MEF2	5'-ggaaaccattttgggttagcatggtgc-3'
AMPK2-MEF2	5'-ggtatctctgctaataatagaaactttc-3'
mutAMPK2-MEF2	5'-ggtatctctgctgggaatagaaactttc-3'
hDysferlin-MEF2	5'-gggtacttcttaaaaaatagaccataat-3'
mut-hDysferlin-MEF2	5'-gggtacttctgggaaaatagaccataat-3'
hCaveolin3-MEF2	5'-ggctccagtcttaatttagcttgagg-3'
Nkx-ISL-WT1	5'-ggtctgggtcctaagcgggtggc-3'
Pbx/Meis-noncanonical	5'-cgtcttgatgtgcagcaacagcttaga-3'
canonicalEbox-Pbx	5'-gggttgattgacaggaacaggtg-3'

added at 100 fold excess at indicated times before loading the reaction on a 6% nondenaturing polyacrylamide-TBE gel. Percent binding over time was calculated by phosphorimager analysis. EMSA of non-canonical E boxes were conducted as previously described (Berkes, Bergstrom et al. 2004) with minor modifications. Briefly, each binding reaction contained a total of 12 μ l in vitro TNT lysate, consisting of various combinations of 2 μ l Pbx1a, 2 μ l Meis1, 2 μ l E12, 6 μ l MyoD or mutant MyoD. In reactions that omitted a member of the binding complex, unprogrammed lysate was used to adjust the reaction to a final lysate volume of 12 μ l. This mixture was then incubated at 37°C for 20 min. Labeled oligonucleotide probe was added (100,000 cpm / binding reaction) to the lysate mixture in 1x binding buffer [20 mM HEPES (pH 7.6), 5% glycerol, 1.5 mM MgCl₂, 50 mM KCl, 1 mM EDTA, 1 mM DTT, and 0.2 μ g poly dI:dC] to a total volume of 30 μ l and incubated at room temperature for 15 min. A MEF2 binding site from the *myogenin* gene (see myg-MEF2 sequence above) (Yee and Rigby 1993; Dodou, Xu et al. 2003) was added to every reaction as a non-specific competitor oligonucleotide. The probe/lysate mixture was run on a 6% nondenaturing polyacrylamide-TBE gel at 4°C for approximately 3 h. The sense strand sequence of the oligonucleotide used to assess binding to the non-canonical E box in the presence and absence of Pbx/Meis (Pbx/Meis-noncanonical) contains the Pbx/Meis binding consensus and two adjacent non-canonical E boxes and is presented in Table 2 (Berkes, Bergstrom et al. 2004). A control oligonucleotide (canonicalEbox-Pbx), containing a Pbx/Meis binding site next to a canonical E box, was used to show quaternary complex formation under the above conditions.

Cell Culture and Transfections

C3H10T1/2 cells were grown in 10% fetal bovine serum (FBS) in Dulbecco modified Eagle medium (DMEM). C2C12 cells were grown in 15% FBS in DMEM. A total of 2 μ g of plasmid DNA was transfected into 35 mm dishes at 50% confluency using FuGENE6 (Roche) as recommended by the manufacturer. Cells were allowed to recover for 18 hours and changed to differentiation medium [DMEM + 2% horse serum (HS)]. Transfections of the Mgn184 series of plasmids were conducted in 35 mm dishes using the Superfect transfection reagent (Qiagen) as recommended by the manufacturer. Following transfection, cells were cultured over night in growth medium (DMEM + 10% FBS), followed by 48 h in differentiation medium (DMEM + 2% HS + 1x insulin/transferrin/selenium). Cells were harvested by scraping the plates into 100 mM NaPO₄ following 48 h in differentiation medium. Cells were then lysed by 3 freeze-thaw cycles of 1 min in liquid nitrogen followed by 1 min in a 37°C water bath. Cell debris was removed by centrifugation and the supernatant was used to assess β -gal activity. Chemiluminescent β -galactosidase assays were performed using the Luminescent β -gal kit (Clontech) according to the manufacturer's recommendation and relative light units were determined using a Tropic TR717 microplate luminometer. All β -gal activity was normalized to the total protein in the cell lysates as determined by Bradford Assay (Biorad) and data are expressed as fold activation over the baseline activity of each reporter plasmid.

References

- Akimoto, T., S. C. Pohnert, et al. (2005). "Exercise stimulates Pgc-1alpha transcription in skeletal muscle through activation of the p38 MAPK pathway." J Biol Chem **280**(20): 19587-93.
- Akimoto, T., T. J. Ribar, et al. (2004). "Skeletal muscle adaptation in response to voluntary running in Ca²⁺/calmodulin-dependent protein kinase IV-deficient mice." Am J Physiol Cell Physiol **287**(5): C1311-9.
- Al-Khalili, L., A. V. Chibalin, et al. (2004). "MEF2 activation in differentiated primary human skeletal muscle cultures requires coordinated involvement of parallel pathways." Am J Physiol Cell Physiol **286**(6): C1410-6.
- Allen, D. L., J. N. Weber, et al. (2005). "Myocyte enhancer factor-2 and serum response factor binding elements regulate fast Myosin heavy chain transcription in vivo." J Biol Chem **280**(17): 17126-34.
- Amacher, S. L., J. N. Buskin, et al. (1993). "Multiple regulatory elements contribute differentially to muscle creatine kinase enhancer activity in skeletal and cardiac muscle." Mol Cell Biol **13**(5): 2753-64.
- Anderson, J. P., E. Dodou, et al. (2004). "HRC is a direct transcriptional target of MEF2 during cardiac, skeletal, and arterial smooth muscle development in vivo." Mol Cell Biol **24**(9): 3757-68.
- Andres, V., M. Cervera, et al. (1995). "Determination of the consensus binding site for MEF2 expressed in muscle and brain reveals tissue-specific sequence constraints." J Biol Chem **270**(40): 23246-9.
- Ashrafian, H., C. Redwood, et al. (2003). "Hypertrophic cardiomyopathy: a paradigm for myocardial energy depletion." Trends Genet **19**(5): 263-8.
- Bailey, P., M. Downes, et al. (1999). "The nuclear receptor corepressor N-CoR regulates differentiation: N-CoR directly interacts with MyoD." Mol Endocrinol **13**(7): 1155-68.
- Beals, C. R., N. A. Clipstone, et al. (1997). "Nuclear localization of NF-ATc by a calcineurin-dependent, cyclosporin-sensitive intramolecular interaction." Genes Dev **11**(7): 824-34.
- Benezra, R., R. L. Davis, et al. (1990). "Id: a negative regulator of helix-loop-helix DNA binding proteins. Control of terminal myogenic differentiation." Ann N Y Acad Sci **599**: 1-11.
- Benezra, R., R. L. Davis, et al. (1990). "The protein Id: a negative regulator of helix-loop-helix DNA binding proteins." Cell **61**(1): 49-59.
- Bengal, E., O. Flores, et al. (1994). "Positive control mutations in the MyoD basic region fail to show cooperative DNA binding and transcriptional activation in vitro." Proc Natl Acad Sci U S A **91**(13): 6221-5.
- Bergstrom, D. A., B. H. Penn, et al. (2002). "Promoter-specific regulation of MyoD binding and signal transduction cooperate to pattern gene expression." Mol Cell **9**(3): 587-600.

- Bergstrom, D. A. and S. J. Tapscott (2001). "Molecular distinction between specification and differentiation in the myogenic basic helix-loop-helix transcription factor family." Mol Cell Biol **21**(7): 2404-12.
- Berkes, C. A., D. A. Bergstrom, et al. (2004). "Pbx marks genes for activation by MyoD indicating a role for a homeodomain protein in establishing myogenic potential." Mol Cell **14**(4): 465-77.
- Bi, W., C. J. Drake, et al. (1999). "The transcription factor MEF2C-null mouse exhibits complex vascular malformations and reduced cardiac expression of angiopoietin 1 and VEGF." Dev Biol **211**(2): 255-67.
- Black, B. L., J. F. Martin, et al. (1995). "The mouse MRF4 promoter is trans-activated directly and indirectly by muscle-specific transcription factors." J Biol Chem **270**(7): 2889-92.
- Black, B. L., J. D. Molkentin, et al. (1998). "Multiple roles for the MyoD basic region in transmission of transcriptional activation signals and interaction with MEF2." Mol Cell Biol **18**(1): 69-77.
- Black, B. L. and E. N. Olson (1998). "Transcriptional control of muscle development by myocyte enhancer factor-2 (MEF2) proteins." Annu Rev Cell Dev Biol **14**: 167-96.
- Blackwell, T. K., J. Huang, et al. (1993). "Binding of myc proteins to canonical and noncanonical DNA sequences." Mol Cell Biol **13**(9): 5216-24.
- Blackwell, T. K. and H. Weintraub (1990). "Differences and similarities in DNA-binding preferences of MyoD and E2A protein complexes revealed by binding site selection." Science **250**(4984): 1104-10.
- Bothe, G. W., J. A. Haspel, et al. (2000). "Selective expression of Cre recombinase in skeletal muscle fibers." Genesis **26**(2): 165-6.
- Braun, T. and H. H. Arnold (1991). "The four human muscle regulatory helix-loop-helix proteins Myf3-Myf6 exhibit similar hetero-dimerization and DNA binding properties." Nucleic Acids Res **19**(20): 5645-51.
- Braun, T., E. Bober, et al. (1989). "Differential expression of myogenic determination genes in muscle cells: possible autoactivation by the Myf gene products." Embo J **8**(12): 3617-25.
- Braun, T., B. Winter, et al. (1990). "Transcriptional activation domain of the muscle-specific gene-regulatory protein myf5." Nature **346**(6285): 663-5.
- Brennan, T. J., T. Chakraborty, et al. (1991). "Mutagenesis of the myogenin basic region identifies an ancient protein motif critical for activation of myogenesis." Proc Natl Acad Sci U S A **88**(13): 5675-9.
- Brennan, T. J. and E. N. Olson (1990). "Myogenin resides in the nucleus and acquires high affinity for a conserved enhancer element on heterodimerization." Genes Dev **4**(4): 582-95.
- Buckingham, M., L. Bajard, et al. (2003). "The formation of skeletal muscle: from somite to limb." J Anat **202**(1): 59-68.
- Calvo, S., D. Vullhorst, et al. (2001). "Molecular dissection of DNA sequences and factors involved in slow muscle-specific transcription." Mol Cell Biol **21**(24): 8490-503.

- Chakraborty, T., T. J. Brennan, et al. (1991). "Inefficient homooligomerization contributes to the dependence of myogenin on E2A products for efficient DNA binding." *Mol Cell Biol* **11**(7): 3633-41.
- Chanoine, C., B. Della Gaspera, et al. (2004). "Myogenic regulatory factors: redundant or specific functions? Lessons from *Xenopus*." *Dev Dyn* **231**(4): 662-70.
- Charron, M. J., E. B. Katz, et al. (1999). "GLUT4 gene regulation and manipulation." *J Biol Chem* **274**(6): 3253-6.
- Chen, C. M., N. Kraut, et al. (1996). "I-mf, a novel myogenic repressor, interacts with members of the MyoD family." *Cell* **86**(5): 731-41.
- Chen, S. L., D. H. Dowhan, et al. (2000). "The steroid receptor coactivator, GRIP-1, is necessary for MEF-2C-dependent gene expression and skeletal muscle differentiation." *Genes Dev* **14**(10): 1209-28.
- Cheng, T. C., T. A. Hanley, et al. (1992). "Mapping of myogenin transcription during embryogenesis using transgenes linked to the myogenin control region." *J Cell Biol* **119**(6): 1649-56.
- Cheng, T. C., M. C. Wallace, et al. (1993). "Separable regulatory elements governing myogenin transcription in mouse embryogenesis." *Science* **261**(5118): 215-8.
- Chin, E. R., E. N. Olson, et al. (1998). "A calcineurin-dependent transcriptional pathway controls skeletal muscle fiber type." *Genes Dev* **12**(16): 2499-509.
- Cox, D. M., M. Du, et al. (2003). "Phosphorylation motifs regulating the stability and function of myocyte enhancer factor 2A." *J Biol Chem* **278**(17): 15297-303.
- Czernik, P. J., C. A. Peterson, et al. (1996). "Preferential binding of MyoD-E12 versus myogenin-E12 to the murine sarcoma virus enhancer in vitro." *J Biol Chem* **271**(15): 9141-9.
- Czubryt, M. P., J. McAnally, et al. (2003). "Regulation of peroxisome proliferator-activated receptor gamma coactivator 1 alpha (PGC-1 alpha) and mitochondrial function by MEF2 and HDAC5." *Proc Natl Acad Sci U S A* **100**(4): 1711-6.
- Davis, R. L., P. F. Cheng, et al. (1990). "The MyoD DNA binding domain contains a recognition code for muscle-specific gene activation." *Cell* **60**(5): 733-46.
- Davis, R. L. and H. Weintraub (1992). "Acquisition of myogenic specificity by replacement of three amino acid residues from MyoD into E12." *Science* **256**(5059): 1027-30.
- de la Serna, I. L., K. A. Carlson, et al. (2001). "Mammalian SWI/SNF complexes promote MyoD-mediated muscle differentiation." *Nat Genet* **27**(2): 187-90.
- de la Serna, I. L., Y. Ohkawa, et al. (2005). "MyoD targets chromatin remodeling complexes to the myogenin locus prior to forming a stable DNA-bound complex." *Mol Cell Biol* **25**(10): 3997-4009.
- Deng, X., D. Z. Ewton, et al. (2005). "Mirk/dyrk1B decreases the nuclear accumulation of class II histone deacetylases during skeletal muscle differentiation." *J Biol Chem* **280**(6): 4894-905.
- Deng, X., D. Z. Ewton, et al. (2003). "Mirk/dyrk1B is a Rho-induced kinase active in skeletal muscle differentiation." *J Biol Chem* **278**(42): 41347-54.
- Dezan, C., D. Meierhans, et al. (1999). "Acquisition of myogenic specificity through replacement of one amino acid of MASH-1 and introduction of an additional alpha-helical turn." *Biol Chem* **380**(6): 705-10.

- Dodou, E., S. M. Xu, et al. (2003). "mef2c is activated directly by myogenic basic helix-loop-helix proteins during skeletal muscle development in vivo." Mech Dev **120**(9): 1021-32.
- Dressel, U., P. J. Bailey, et al. (2001). "A dynamic role for HDAC7 in MEF2-mediated muscle differentiation." J Biol Chem **276**(20): 17007-13.
- Eckner, R., M. E. Ewen, et al. (1994). "Molecular cloning and functional analysis of the adenovirus E1A-associated 300-kD protein (p300) reveals a protein with properties of a transcriptional adaptor." Genes Dev **8**(8): 869-84.
- Edmondson, D. G., T. C. Cheng, et al. (1992). "Analysis of the myogenin promoter reveals an indirect pathway for positive autoregulation mediated by the muscle-specific enhancer factor MEF-2." Mol Cell Biol **12**(9): 3665-77.
- Edmondson, D. G., G. E. Lyons, et al. (1994). "Mef2 gene expression marks the cardiac and skeletal muscle lineages during mouse embryogenesis." Development **120**(5): 1251-63.
- Edmondson, D. G. and E. N. Olson (1989). "A gene with homology to the myc similarity region of MyoD1 is expressed during myogenesis and is sufficient to activate the muscle differentiation program." Genes Dev **3**(5): 628-40.
- Ferrari, S., S. Molinari, et al. (1997). "Absence of MEF2 binding to the A/T-rich element in the muscle creatine kinase (MCK) enhancer correlates with lack of early expression of the MCK gene in embryonic mammalian muscle." Cell Growth Differ **8**(1): 23-34.
- Fickett, J. W. (1996). "Coordinate positioning of MEF2 and myogenin binding sites." Gene **172**(1): GC19-32.
- Fitts, R. H. and J. J. Widrick (1996). "Muscle mechanics: adaptations with exercise-training." Exerc Sport Sci Rev **24**: 427-73.
- Gerber, A. N., T. R. Klesert, et al. (1997). "Two domains of MyoD mediate transcriptional activation of genes in repressive chromatin: a mechanism for lineage determination in myogenesis." Genes Dev **11**(4): 436-50.
- Gossett, L. A., D. J. Kelvin, et al. (1989). "A new myocyte-specific enhancer-binding factor that recognizes a conserved element associated with multiple muscle-specific genes." Mol Cell Biol **9**(11): 5022-33.
- Handschin, C., J. Rhee, et al. (2003). "An autoregulatory loop controls peroxisome proliferator-activated receptor gamma coactivator 1alpha expression in muscle." Proc Natl Acad Sci U S A **100**(12): 7111-6.
- Hassid WZ, A. S. (1957). "Chemical procedures for analysis of polysaccharide I. Determination of glycogen and starch — Determination of glycogen with the anthron reagent." Methods in Enzymology **3**: 35-36.
- Hasty, P., A. Bradley, et al. (1993). "Muscle deficiency and neonatal death in mice with a targeted mutation in the myogenin gene." Nature **364**(6437): 501-6.
- Hebrok, M., K. Wertz, et al. (1994). "M-twist is an inhibitor of muscle differentiation." Dev Biol **165**(2): 537-44.
- Heidt, A. B. and B. L. Black (2005). "Transgenic mice that express Cre recombinase under control of a skeletal muscle-specific promoter from mef2c." Genesis **42**(1): 28-32.
- Hesselink, R. P., M. Gorselink, et al. (2002). "Impaired performance of skeletal muscle in alpha-glucosidase knockout mice." Muscle Nerve **25**(6): 873-83.

- Holloszy, J. O. and P. A. Hansen (1996). "Regulation of glucose transport into skeletal muscle." Rev Physiol Biochem Pharmacol **128**: 99-193.
- Holmes, B. and G. L. Dohm (2004). "Regulation of GLUT4 gene expression during exercise." Med Sci Sports Exerc **36**(7): 1202-6.
- Holmes, B. F., D. P. Sparling, et al. (2005). "Regulation of muscle GLUT4 enhancer factor and myocyte enhancer factor 2 by AMP-activated protein kinase." Am J Physiol Endocrinol Metab **289**(6): E1071-6.
- Horton, R. M. (1997). "In vitro recombination and mutagenesis of DNA. SOEing together tailor-made genes." Methods Mol Biol **67**: 141-9.
- How, O. J., E. Aasum, et al. (2006). "Increased myocardial oxygen consumption reduces cardiac efficiency in diabetic mice." Diabetes **55**(2): 466-73.
- Howald, H. (1982). "Training-induced morphological and functional changes in skeletal muscle." Int J Sports Med **3**(1): 1-12.
- Hu, J. S., E. N. Olson, et al. (1992). "HEB, a helix-loop-helix protein related to E2A and ITF2 that can modulate the DNA-binding ability of myogenic regulatory factors." Mol Cell Biol **12**(3): 1031-42.
- Huang, J., H. Weintraub, et al. (1998). "Intramolecular regulation of MyoD activation domain conformation and function." Mol Cell Biol **18**(9): 5478-84.
- Hughes, S. M., K. Koishi, et al. (1997). "MyoD protein is differentially accumulated in fast and slow skeletal muscle fibres and required for normal fibre type balance in rodents." Mech Dev **61**(1-2): 151-63.
- Ishibashi, J., R. L. Perry, et al. (2005). "MyoD induces myogenic differentiation through cooperation of its NH₂- and COOH-terminal regions." J Cell Biol **171**(3): 471-82.
- Jansson, E. and L. Kaijser (1987). "Substrate utilization and enzymes in skeletal muscle of extremely endurance-trained men." J Appl Physiol **62**(3): 999-1005.
- Jen, Y., H. Weintraub, et al. (1992). "Overexpression of Id protein inhibits the muscle differentiation program: in vivo association of Id with E2A proteins." Genes Dev **6**(8): 1466-79.
- Jiang, P., J. Song, et al. (2002). "Targeted deletion of the MLC1f/3f downstream enhancer results in precocious MLC expression and mesoderm ablation." Dev Biol **243**(2): 281-93.
- Kablar, B., K. Krastel, et al. (2003). "Myf5 and MyoD activation define independent myogenic compartments during embryonic development." Dev Biol **258**(2): 307-18.
- Kahn, C. R., J. C. Bruning, et al. (2000). "Knockout mice challenge our concepts of glucose homeostasis and the pathogenesis of diabetes mellitus." J Pediatr Endocrinol Metab **13 Suppl 6**: 1377-84.
- Kang, J., C. B. Gocke, et al. (2006). "Phosphorylation-facilitated sumoylation of MEF2C negatively regulates its transcriptional activity." BMC Biochem **7**: 5.
- Kassar-Duchossoy, L., B. Gayraud-Morel, et al. (2004). "Mrf4 determines skeletal muscle identity in Myf5:MyoD double-mutant mice." Nature **431**(7007): 466-71.
- Katz, E. B., A. E. Stenbit, et al. (1995). "Cardiac and adipose tissue abnormalities but not diabetes in mice deficient in GLUT4." Nature **377**(6545): 151-5.
- Kern, M., E. B. Tapscott, et al. (1990). "Differences in glucose transport rates between perfused and in vitro incubated muscles." Horm Metab Res **22**(7): 366-8.

- Kim, Y. B., O. D. Peroni, et al. (2005). "Muscle-specific deletion of the Glut4 glucose transporter alters multiple regulatory steps in glycogen metabolism." Mol Cell Biol **25**(21): 9713-23.
- Kophengnavong, T., J. E. Michnowicz, et al. (2000). "Establishment of distinct MyoD, E2A, and twist DNA binding specificities by different basic region-DNA conformations." Mol Cell Biol **20**(1): 261-72.
- Kunne, A. G. and R. K. Allemann (1997). "Covalently linking BHLH subunits of MASH-1 increases specificity of DNA binding." Biochemistry **36**(5): 1085-91.
- Kunne, A. G., D. Meierhans, et al. (1996). "Basic helix-loop-helix protein MyoD displays modest DNA binding specificity." FEBS Lett **391**(1-2): 79-83.
- Lassar, A. B., J. N. Buskin, et al. (1989). "MyoD is a sequence-specific DNA binding protein requiring a region of myc homology to bind to the muscle creatine kinase enhancer." Cell **58**(5): 823-31.
- Lassar, A. B., R. L. Davis, et al. (1991). "Functional activity of myogenic HLH proteins requires hetero-oligomerization with E12/E47-like proteins in vivo." Cell **66**(2): 305-15.
- Lazaro, J. B., P. J. Bailey, et al. (2002). "Cyclin D-cdk4 activity modulates the subnuclear localization and interaction of MEF2 with SRC-family coactivators during skeletal muscle differentiation." Genes Dev **16**(14): 1792-805.
- Lemercier, C., R. Q. To, et al. (1998). "The basic helix-loop-helix transcription factor Mist1 functions as a transcriptional repressor of myoD." Embo J **17**(5): 1412-22.
- Lemercier, C., A. Verdel, et al. (2000). "mHDA1/HDAC5 histone deacetylase interacts with and represses MEF2A transcriptional activity." J Biol Chem **275**(20): 15594-9.
- Lilly, B., S. Galewsky, et al. (1994). "D-MEF2: a MADS box transcription factor expressed in differentiating mesoderm and muscle cell lineages during Drosophila embryogenesis." Proc Natl Acad Sci U S A **91**(12): 5662-6.
- Lilly, B., B. Zhao, et al. (1995). "Requirement of MADS domain transcription factor D-MEF2 for muscle formation in Drosophila." Science **267**(5198): 688-93.
- Lin, J., H. Wu, et al. (2002). "Transcriptional co-activator PGC-1 alpha drives the formation of slow-twitch muscle fibres." Nature **418**(6899): 797-801.
- Lin, Q., J. Lu, et al. (1998). "Requirement of the MADS-box transcription factor MEF2C for vascular development." Development **125**(22): 4565-74.
- Lin, Q., J. Schwarz, et al. (1997). "Control of mouse cardiac morphogenesis and myogenesis by transcription factor MEF2C." Science **276**(5317): 1404-7.
- Lin, Q., D. Srivastava, et al. (1997). "A transcriptional pathway for cardiac development." Cold Spring Harb Symp Quant Biol **62**: 405-11.
- Liu, D., B. L. Black, et al. (2001). "TGF-beta inhibits muscle differentiation through functional repression of myogenic transcription factors by Smad3." Genes Dev **15**(22): 2950-66.
- Liu, D., J. S. Kang, et al. (2004). "TGF-beta-activated Smad3 represses MEF2-dependent transcription in myogenic differentiation." Embo J **23**(7): 1557-66.
- Liu, S., P. Liu, et al. (1997). "Cyclosporin A-sensitive induction of the Epstein-Barr virus lytic switch is mediated via a novel pathway involving a MEF2 family member." Embo J **16**(1): 143-53.

- Liu, S., D. S. Spinner, et al. (2000). "Interaction of MyoD family proteins with enhancers of acetylcholine receptor subunit genes in vivo." *J Biol Chem* **275**(52): 41364-8.
- Lu, J., P. Chang, et al. (2000). "The basic helix-loop-helix transcription factor capsulin controls spleen organogenesis." *Proc Natl Acad Sci U S A* **97**(17): 9525-30.
- Lu, J., R. Webb, et al. (1999). "MyoR: a muscle-restricted basic helix-loop-helix transcription factor that antagonizes the actions of MyoD." *Proc Natl Acad Sci U S A* **96**(2): 552-7.
- Ma, K., J. K. Chan, et al. (2005). "Myocyte enhancer factor 2 acetylation by p300 enhances its DNA binding activity, transcriptional activity, and myogenic differentiation." *Mol Cell Biol* **25**(9): 3575-82.
- Ma, P. C., M. A. Rould, et al. (1994). "Crystal structure of MyoD bHLH domain-DNA complex: perspectives on DNA recognition and implications for transcriptional activation." *Cell* **77**(3): 451-9.
- Mak, K. L., R. Q. To, et al. (1992). "The MRF4 activation domain is required to induce muscle-specific gene expression." *Mol Cell Biol* **12**(10): 4334-46.
- Mal, A. and M. L. Harter (2003). "MyoD is functionally linked to the silencing of a muscle-specific regulatory gene prior to skeletal myogenesis." *Proc Natl Acad Sci U S A* **100**(4): 1735-9.
- Mal, A., M. Sturniolo, et al. (2001). "A role for histone deacetylase HDAC1 in modulating the transcriptional activity of MyoD: inhibition of the myogenic program." *Embo J* **20**(7): 1739-53.
- McFadden, D. G., J. Charite, et al. (2000). "A GATA-dependent right ventricular enhancer controls dHAND transcription in the developing heart." *Development* **127**(24): 5331-41.
- McGrew, M. J., N. Bogdanova, et al. (1996). "Distinct gene expression patterns in skeletal and cardiac muscle are dependent on common regulatory sequences in the MLC1/3 locus." *Mol Cell Biol* **16**(8): 4524-34.
- McKinsey, T. A., C. L. Zhang, et al. (2000). "Signal-dependent nuclear export of a histone deacetylase regulates muscle differentiation." *Nature* **408**(6808): 106-11.
- McKinsey, T. A., C. L. Zhang, et al. (2000). "Activation of the myocyte enhancer factor-2 transcription factor by calcium/calmodulin-dependent protein kinase-stimulated binding of 14-3-3 to histone deacetylase 5." *Proc Natl Acad Sci U S A* **97**(26): 14400-5.
- McKinsey, T. A., C. L. Zhang, et al. (2001). "Control of muscle development by dueling HATs and HDACs." *Curr Opin Genet Dev* **11**(5): 497-504.
- Meierhan, D., C. el-Ariss, et al. (1995). "DNA binding specificity of the basic-helix-loop-helix protein MASH-1." *Biochemistry* **34**(35): 11026-36.
- Michael, L. F., Z. Wu, et al. (2001). "Restoration of insulin-sensitive glucose transporter (GLUT4) gene expression in muscle cells by the transcriptional coactivator PGC-1." *Proc Natl Acad Sci U S A* **98**(7): 3820-5.
- Micheli, L., L. Leonardi, et al. (2005). "PC4 coactivates MyoD by relieving the histone deacetylase 4-mediated inhibition of myocyte enhancer factor 2C." *Mol Cell Biol* **25**(6): 2242-59.
- Miska, E. A., C. Karlsson, et al. (1999). "HDAC4 deacetylase associates with and represses the MEF2 transcription factor." *Embo J* **18**(18): 5099-107.

- Miwa, T., T. Koyama, et al. (2000). "Muscle specific expression of Cre recombinase under two actin promoters in transgenic mice." Genesis **26**(2): 136-8.
- Molkentin, J. D., B. L. Black, et al. (1995). "Cooperative activation of muscle gene expression by MEF2 and myogenic bHLH proteins." Cell **83**(7): 1125-36.
- Molkentin, J. D., A. B. Firulli, et al. (1996). "MEF2B is a potent transactivator expressed in early myogenic lineages." Mol Cell Biol **16**(7): 3814-24.
- Molkentin, J. D. and E. N. Olson (1996). "Combinatorial control of muscle development by basic helix-loop-helix and MADS-box transcription factors." Proc Natl Acad Sci U S A **93**(18): 9366-73.
- Momken, I., P. Lechene, et al. (2005). "Impaired voluntary running capacity of creatine kinase-deficient mice." J Physiol **565**(Pt 3): 951-64.
- Mora, S., C. Yang, et al. (2001). "The MEF2A and MEF2D isoforms are differentially regulated in muscle and adipose tissue during states of insulin deficiency." Endocrinology **142**(5): 1999-2004.
- Moreno, H., A. L. Serrano, et al. (2003). "Differential regulation of the muscle-specific GLUT4 enhancer in regenerating and adult skeletal muscle." J Biol Chem **278**(42): 40557-64.
- Murre, C., P. S. McCaw, et al. (1989). "A new DNA binding and dimerization motif in immunoglobulin enhancer binding, daughterless, MyoD, and myc proteins." Cell **56**(5): 777-83.
- Murre, C., P. S. McCaw, et al. (1989). "Interactions between heterologous helix-loop-helix proteins generate complexes that bind specifically to a common DNA sequence." Cell **58**(3): 537-44.
- Musaro, A., K. McCullagh, et al. (2001). "Localized Igf-1 transgene expression sustains hypertrophy and regeneration in senescent skeletal muscle." Nat Genet **27**(2): 195-200.
- Myer, A., E. N. Olson, et al. (2001). "MyoD cannot compensate for the absence of myogenin during skeletal muscle differentiation in murine embryonic stem cells." Dev Biol **229**(2): 340-50.
- Nabeshima, Y., K. Hanaoka, et al. (1993). "Myogenin gene disruption results in perinatal lethality because of severe muscle defect." Nature **364**(6437): 532-5.
- Naidu, P. S., D. C. Ludolph, et al. (1995). "Myogenin and MEF2 function synergistically to activate the MRF4 promoter during myogenesis." Mol Cell Biol **15**(5): 2707-18.
- Nakagawa, O., M. Arnold, et al. (2005). "Centronuclear myopathy in mice lacking a novel muscle-specific protein kinase transcriptionally regulated by MEF2." Genes Dev **19**(17): 2066-77.
- Naya, F. J., B. L. Black, et al. (2002). "Mitochondrial deficiency and cardiac sudden death in mice lacking the MEF2A transcription factor." Nat Med **8**(11): 1303-9.
- Neuhold, L. A. and B. Wold (1993). "HLH forced dimers: tethering MyoD to E47 generates a dominant positive myogenic factor insulated from negative regulation by Id." Cell **74**(6): 1033-42.
- Northrop, J. P., S. N. Ho, et al. (1994). "NF-AT components define a family of transcription factors targeted in T-cell activation." Nature **369**(6480): 497-502.

- Ogilvie, R. W. and D. L. Feedback (1990). "A metachromatic dye-ATPase method for the simultaneous identification of skeletal muscle fiber types I, IIA, IIB and IIC." Stain Technol **65**(5): 231-41.
- Oh, M., Rybkin, II, et al. (2005). "Calcineurin is necessary for the maintenance but not embryonic development of slow muscle fibers." Mol Cell Biol **25**(15): 6629-38.
- Ojuka, E. O., T. E. Jones, et al. (2002). "Regulation of GLUT4 biogenesis in muscle: evidence for involvement of AMPK and Ca(2+)." Am J Physiol Endocrinol Metab **282**(5): E1008-13.
- Olson, E. N. (1990). "MyoD family: a paradigm for development?" Genes Dev **4**(9): 1454-61.
- Olson, E. N. and W. H. Klein (1994). "bHLH factors in muscle development: dead lines and commitments, what to leave in and what to leave out." Genes Dev **8**(1): 1-8.
- Olson, E. N. and R. S. Williams (2000). "Remodeling muscles with calcineurin." Bioessays **22**(6): 510-9.
- Ornatsky, O. I., J. J. Andreucci, et al. (1997). "A dominant-negative form of transcription factor MEF2 inhibits myogenesis." J Biol Chem **272**(52): 33271-8.
- Ornatsky, O. I., D. M. Cox, et al. (1999). "Post-translational control of the MEF2A transcriptional regulatory protein." Nucleic Acids Res **27**(13): 2646-54.
- Ott, M. O., E. Bober, et al. (1991). "Early expression of the myogenic regulatory gene, myf-5, in precursor cells of skeletal muscle in the mouse embryo." Development **111**(4): 1097-107.
- Parish, R. and K. F. Petersen (2005). "Mitochondrial dysfunction and type 2 diabetes." Curr Diab Rep **5**(3): 177-83.
- Parsons, S. A., D. P. Millay, et al. (2004). "Genetic loss of calcineurin blocks mechanical overload-induced skeletal muscle fiber type switching but not hypertrophy." J Biol Chem **279**(25): 26192-200.
- Pette, D. (2002). "The adaptive potential of skeletal muscle fibers." Can J Appl Physiol **27**(4): 423-48.
- Pette, D. and R. S. Staron (2000). "Myosin isoforms, muscle fiber types, and transitions." Microsc Res Tech **50**(6): 500-9.
- Pinney, D. F., S. H. Pearson-White, et al. (1988). "Myogenic lineage determination and differentiation: evidence for a regulatory gene pathway." Cell **53**(5): 781-93.
- Polesskaya, A., A. Duquet, et al. (2000). "CREB-binding protein/p300 activates MyoD by acetylation." J Biol Chem **275**(44): 34359-64.
- Puigserver, P. (2005). "Tissue-specific regulation of metabolic pathways through the transcriptional coactivator PGC1-alpha." Int J Obes (Lond) **29** Suppl 1: S5-9.
- Puri, P. L., S. Iezzi, et al. (2001). "Class I histone deacetylases sequentially interact with MyoD and pRb during skeletal myogenesis." Mol Cell **8**(4): 885-97.
- Puri, P. L., V. Sartorelli, et al. (1997). "Differential roles of p300 and PCAF acetyltransferases in muscle differentiation." Mol Cell **1**(1): 35-45.
- Quinn, Z. A., C. C. Yang, et al. (2001). "Smad proteins function as co-modulators for MEF2 transcriptional regulatory proteins." Nucleic Acids Res **29**(3): 732-42.
- Rafael, J. A., E. R. Townsend, et al. (2000). "Dystrophin and utrophin influence fiber type composition and post-synaptic membrane structure." Hum Mol Genet **9**(9): 1357-67.

- Rao, M. V., M. J. Donoghue, et al. (1996). "Distinct regulatory elements control muscle-specific, fiber-type-selective, and axially graded expression of a myosin light-chain gene in transgenic mice." Mol Cell Biol 16(7): 3909-22.
- Rawls, A., J. H. Morris, et al. (1995). "Myogenin's functions do not overlap with those of MyoD or Myf-5 during mouse embryogenesis." Dev Biol 172(1): 37-50.
- Rawls, A., M. R. Valdez, et al. (1998). "Overlapping functions of the myogenic bHLH genes MRF4 and MyoD revealed in double mutant mice." Development 125(13): 2349-58.
- Rhodes, S. J. and S. F. Konieczny (1989). "Identification of MRF4: a new member of the muscle regulatory factor gene family." Genes Dev 3(12B): 2050-61.
- Rudnicki, M. A., T. Braun, et al. (1992). "Inactivation of MyoD in mice leads to up-regulation of the myogenic HLH gene Myf-5 and results in apparently normal muscle development." Cell 71(3): 383-90.
- Rudnicki, M. A., P. N. Schnegelsberg, et al. (1993). "MyoD or Myf-5 is required for the formation of skeletal muscle." Cell 75(7): 1351-9.
- Rutter, G. A., G. Da Silva Xavier, et al. (2003). "Roles of 5'-AMP-activated protein kinase (AMPK) in mammalian glucose homeostasis." Biochem J 375(Pt 1): 1-16.
- Ryder, J. W., Y. Kawano, et al. (1999). "Postexercise glucose uptake and glycogen synthesis in skeletal muscle from GLUT4-deficient mice." Faseb J 13(15): 2246-56.
- Sabourin, L. A. and M. A. Rudnicki (2000). "The molecular regulation of myogenesis." Clin Genet 57(1): 16-25.
- Sartorelli, V., J. Huang, et al. (1997). "Molecular mechanisms of myogenic coactivation by p300: direct interaction with the activation domain of MyoD and with the MADS box of MEF2C." Mol Cell Biol 17(2): 1010-26.
- Sartorelli, V., P. L. Puri, et al. (1999). "Acetylation of MyoD directed by PCAF is necessary for the execution of the muscle program." Mol Cell 4(5): 725-34.
- Sato, K., F. Imai, et al. (1977). "Characterization of glycogen phosphorylase isoenzymes present in cultured skeletal muscle from patients with McArdle's disease." Biochem Biophys Res Commun 78(2): 663-8.
- Schiaffino, S. and C. Reggiani (1994). "Myosin isoforms in mammalian skeletal muscle." J Appl Physiol 77(2): 493-501.
- Schwarz, J. J., T. Chakraborty, et al. (1992). "The basic region of myogenin cooperates with two transcription activation domains to induce muscle-specific transcription." Mol Cell Biol 12(1): 266-75.
- Sengers, R. C., A. M. Stadhouders, et al. (1980). "Muscle phosphorylase deficiency in childhood." Eur J Pediatr 134(2): 161-5.
- Silva, J. L., G. Giannocco, et al. (2005). "NF-kappaB, MEF2A, MEF2D and HIF1- α involvement on insulin- and contraction-induced regulation of GLUT4 gene expression in soleus muscle." Mol Cell Endocrinol 240(1-2): 82-93.
- Simone, C., S. V. Forcales, et al. (2004). "p38 pathway targets SWI-SNF chromatin-remodeling complex to muscle-specific loci." Nat Genet 36(7): 738-43.
- Soriano, P. (1999). "Generalized lacZ expression with the ROSA26 Cre reporter strain." Nat Genet 21(1): 70-1.

- Sparrow, D. B., E. A. Miska, et al. (1999). "MEF-2 function is modified by a novel co-repressor, MITR." Embo J **18**(18): 5085-98.
- Spicer, D. B., J. Rhee, et al. (1996). "Inhibition of myogenic bHLH and MEF2 transcription factors by the bHLH protein Twist." Science **272**(5267): 1476-80.
- Spinner, D. S., S. Liu, et al. (2002). "Interaction of the myogenic determination factor myogenin with E12 and a DNA target: mechanism and kinetics." J Mol Biol **317**(3): 431-45.
- Stein, T. P. and C. E. Wade (2005). "Metabolic consequences of muscle disuse atrophy." J Nutr **135**(7): 1824S-1828S.
- Stenbit, A. E., T. S. Tsao, et al. (1997). "GLUT4 heterozygous knockout mice develop muscle insulin resistance and diabetes." Nat Med **3**(10): 1096-101.
- Stewart, C. E. and P. Rotwein (1996). "Growth, differentiation, and survival: multiple physiological functions for insulin-like growth factors." Physiol Rev **76**(4): 1005-26.
- Stockdale, F. E., W. Nikovits, Jr., et al. (2002). "Slow myosins in muscle development." Results Probl Cell Differ **38**: 199-214.
- Streter, F. A., J. Gergely, et al. (1973). "Synthesis by fast muscle of myosin light chains characteristic of slow muscle in response to long-term stimulation." Nat New Biol **241**(105): 17-9.
- Sumariwalla, V. M. and W. H. Klein (2001). "Similar myogenic functions for myogenin and MRF4 but not MyoD in differentiated murine embryonic stem cells." Genesis **30**(4): 239-49.
- Summerbell, D., P. R. Ashby, et al. (2000). "The expression of Myf5 in the developing mouse embryo is controlled by discrete and dispersed enhancers specific for particular populations of skeletal muscle precursors." Development **127**(17): 3745-57.
- Tajbakhsh, S. (2003). "Stem cells to tissue: molecular, cellular and anatomical heterogeneity in skeletal muscle." Curr Opin Genet Dev **13**(4): 413-22.
- Tapscott, S. J., R. L. Davis, et al. (1988). "MyoD1: a nuclear phosphoprotein requiring a Myc homology region to convert fibroblasts to myoblasts." Science **242**(4877): 405-11.
- Thai, M. V., S. Guruswamy, et al. (1998). "Myocyte enhancer factor 2 (MEF2)-binding site is required for GLUT4 gene expression in transgenic mice. Regulation of MEF2 DNA binding activity in insulin-deficient diabetes." J Biol Chem **273**(23): 14285-92.
- Thayer, M. J., S. J. Tapscott, et al. (1989). "Positive autoregulation of the myogenic determination gene MyoD1." Cell **58**(2): 241-8.
- Tsai, F. Y., G. Keller, et al. (1994). "An early haematopoietic defect in mice lacking the transcription factor GATA-2." Nature **371**(6494): 221-6.
- Turner, E. C., C. H. Cureton, et al. (2004). "Controlling the DNA binding specificity of bHLH proteins through intramolecular interactions." Chem Biol **11**(1): 69-77.
- Vandromme, M., J. C. Cavadore, et al. (1995). "Two nuclear localization signals present in the basic-helix 1 domains of MyoD promote its active nuclear translocation and can function independently." Proc Natl Acad Sci U S A **92**(10): 4646-50.
- Vong, L. H., M. J. Ragusa, et al. (2005). "Generation of conditional Mef2loxP/loxP mice for temporal- and tissue-specific analyses." Genesis **43**(1): 43-8.

- Voronova, A. and D. Baltimore (1990). "Mutations that disrupt DNA binding and dimer formation in the E47 helix-loop-helix protein map to distinct domains." Proc Natl Acad Sci U S A **87**(12): 4722-6.
- Wang, D. Z., M. R. Valdez, et al. (2001). "The Mef2c gene is a direct transcriptional target of myogenic bHLH and MEF2 proteins during skeletal muscle development." Development **128**(22): 4623-33.
- Wang, J., H. Wilhelmsson, et al. (1999). "Dilated cardiomyopathy and atrioventricular conduction blocks induced by heart-specific inactivation of mitochondrial DNA gene expression." Nat Genet **21**(1): 133-7.
- Wang, Y. and R. Jaenisch (1997). "Myogenin can substitute for Myf5 in promoting myogenesis but less efficiently." Development **124**(13): 2507-13.
- Weintraub, H., R. Davis, et al. (1990). "MyoD binds cooperatively to two sites in a target enhancer sequence: occupancy of two sites is required for activation." Proc Natl Acad Sci U S A **87**(15): 5623-7.
- Weintraub, H., V. J. Dwarki, et al. (1991). "Muscle-specific transcriptional activation by MyoD." Genes Dev **5**(8): 1377-86.
- Weintraub, H., T. Genetta, et al. (1994). "Tissue-specific gene activation by MyoD: determination of specificity by cis-acting repression elements." Genes Dev **8**(18): 2203-11.
- Williams, R. S., S. Salmons, et al. (1986). "Regulation of nuclear and mitochondrial gene expression by contractile activity in skeletal muscle." J Biol Chem **261**(1): 376-80.
- Wright, W. E. (1992). "Muscle basic helix-loop-helix proteins and the regulation of myogenesis." Curr Opin Genet Dev **2**(2): 243-8.
- Wright, W. E., M. Binder, et al. (1991). "Cyclic amplification and selection of targets (CASTing) for the myogenin consensus binding site." Mol Cell Biol **11**(8): 4104-10.
- Wu, H., F. J. Naya, et al. (2000). "MEF2 responds to multiple calcium-regulated signals in the control of skeletal muscle fiber type." Embo J **19**(9): 1963-73.
- Wu, Z., P. Puigserver, et al. (1999). "Mechanisms controlling mitochondrial biogenesis and respiration through the thermogenic coactivator PGC-1." Cell **98**(1): 115-24.
- Yan, Z., S. Choi, et al. (2003). "Highly coordinated gene regulation in mouse skeletal muscle regeneration." J Biol Chem **278**(10): 8826-36.
- Yee, S. P. and P. W. Rigby (1993). "The regulation of myogenin gene expression during the embryonic development of the mouse." Genes Dev **7**(7A): 1277-89.
- Youn, H. D., T. A. Chatila, et al. (2000). "Integration of calcineurin and MEF2 signals by the coactivator p300 during T-cell apoptosis." Embo J **19**(16): 4323-31.
- Zhao, M., L. New, et al. (1999). "Regulation of the MEF2 family of transcription factors by p38." Mol Cell Biol **19**(1): 21-30.
- Zhu, Z. and J. B. Miller (1997). "MRF4 can substitute for myogenin during early stages of myogenesis." Dev Dyn **209**(2): 233-41.
- Zisman, A., O. D. Peroni, et al. (2000). "Targeted disruption of the glucose transporter 4 selectively in muscle causes insulin resistance and glucose intolerance." Nat Med **6**(8): 924-8.

Zorzano, A., M. Palacin, et al. (2005). "Mechanisms regulating GLUT4 glucose transporter expression and glucose transport in skeletal muscle." Acta Physiol Scand **183**(1): 43-58.

Handwritten text, possibly a list or index, with many entries starting with "L." and "M." and containing numbers and names. The text is very faint and difficult to read. Some legible fragments include:

- L. 100
- L. 101
- L. 102
- L. 103
- L. 104
- L. 105
- L. 106
- L. 107
- L. 108
- L. 109
- L. 110
- L. 111
- L. 112
- L. 113
- L. 114
- L. 115
- L. 116
- L. 117
- L. 118
- L. 119
- L. 120
- L. 121
- L. 122
- L. 123
- L. 124
- L. 125
- L. 126
- L. 127
- L. 128
- L. 129
- L. 130
- L. 131
- L. 132
- L. 133
- L. 134
- L. 135
- L. 136
- L. 137
- L. 138
- L. 139
- L. 140
- L. 141
- L. 142
- L. 143
- L. 144
- L. 145
- L. 146
- L. 147
- L. 148
- L. 149
- L. 150
- L. 151
- L. 152
- L. 153
- L. 154
- L. 155
- L. 156
- L. 157
- L. 158
- L. 159
- L. 160
- L. 161
- L. 162
- L. 163
- L. 164
- L. 165
- L. 166
- L. 167
- L. 168
- L. 169
- L. 170
- L. 171
- L. 172
- L. 173
- L. 174
- L. 175
- L. 176
- L. 177
- L. 178
- L. 179
- L. 180
- L. 181
- L. 182
- L. 183
- L. 184
- L. 185
- L. 186
- L. 187
- L. 188
- L. 189
- L. 190
- L. 191
- L. 192
- L. 193
- L. 194
- L. 195
- L. 196
- L. 197
- L. 198
- L. 199
- L. 200
- M. 100
- M. 101
- M. 102
- M. 103
- M. 104
- M. 105
- M. 106
- M. 107
- M. 108
- M. 109
- M. 110
- M. 111
- M. 112
- M. 113
- M. 114
- M. 115
- M. 116
- M. 117
- M. 118
- M. 119
- M. 120
- M. 121
- M. 122
- M. 123
- M. 124
- M. 125
- M. 126
- M. 127
- M. 128
- M. 129
- M. 130
- M. 131
- M. 132
- M. 133
- M. 134
- M. 135
- M. 136
- M. 137
- M. 138
- M. 139
- M. 140
- M. 141
- M. 142
- M. 143
- M. 144
- M. 145
- M. 146
- M. 147
- M. 148
- M. 149
- M. 150
- M. 151
- M. 152
- M. 153
- M. 154
- M. 155
- M. 156
- M. 157
- M. 158
- M. 159
- M. 160
- M. 161
- M. 162
- M. 163
- M. 164
- M. 165
- M. 166
- M. 167
- M. 168
- M. 169
- M. 170
- M. 171
- M. 172
- M. 173
- M. 174
- M. 175
- M. 176
- M. 177
- M. 178
- M. 179
- M. 180
- M. 181
- M. 182
- M. 183
- M. 184
- M. 185
- M. 186
- M. 187
- M. 188
- M. 189
- M. 190
- M. 191
- M. 192
- M. 193
- M. 194
- M. 195
- M. 196
- M. 197
- M. 198
- M. 199
- M. 200

LIBRARY

7537866



3 1378 00753 7866

For reference

Not to be taken from the room.

